UNIVERSITÀ DEGLI STUDI DI MESSINA

DIPARTIMENTO DI

SCIENZE CHIMICHE, BIOLOGICHE, FARMACEUTICHE ED AMBIENTALI

DOTTORATO DI RICERCA IN SCIENZE CHIMICHE

XXXII CICLO 2016-2019

Multimodal functionalization of PLA for biological applications

Serena Maria Torcasio

Supervisor
Prof. Angela SCALA

Coordinator
Prof. Paola DUGO

TABLE OF CONTENT

AIM OF THE WORK

Aliphatic polyesters, such as polyglycolide, polylactide, poly(ε-caprolactone), are an attractive class of polymers, which can be used for a broad range of practical applications from packaging to more sophisticated biomedical devices.

One of the main reasons for the growing interest in this type of degradable polymers is that their physical and chemical properties can be opportunely tuned by proper functionalization.

Due to the lack of functionalities along the polymer backbone, many efforts have been focused on the preparation of aliphatic polyesters with pendant functional groups. In general, two approaches have been used, to date: the first uses lactone derivatives bearing functional groups for the ring- opening polymerization; the second strategy consists in the post-polymerization modification of the polymer backbone, whose chain-ends can be tailored for specific applications, by direct grafting of functional groups.

Within the family of aliphatic polyesters, polylactide (PLA) is one of the most promising industrial products for plastics with the prospective to replace polymers such as PET, polystyrene and polycarbonate. Currently, the main applications of PLA are in short-term packaging, owing its biodegradability, and in biomedical applications (*drug delivery* and *tissue engineering*) owing to its biocompatibility. Besides these characteristics, PLA offers many advantages such as being produced from renewable resources, being FDA-approved for biomedical applications, and commercially available in different molecular weights. Moreover, PLA can be formulated in nanoparticles useful as biocompatible "nanocontainers" for gene and drug delivery. Various hydrophobic and hydrophilic drugs can be efficiently encapsulated into the PLA-based nanoparticles resulting in a sustained and controlled release of the payload over the time.

The great potentialities and versatility of *smart* polymeric nanomaterials render them one of the most exciting interfaces between chemistry and biology.

This thesis describes the synthesis and the characterization by complementary techniques (such as NMR spectroscopy, GPC, and MALDI-ToF analyses) of new PLA derivatives obtained by two main approaches (**Figure 1**). The CuAAC *click* reaction represents the common synthetic strategy exploited for the PLA functionalization under mild conditions. All the newly synthesized PLA derivatives are eventually formulated in nanoparticles or micelles loaded with selected antitumoral drugs (i.e., salinomycin and doxorubicin) and intended to biological assays on osteosarcoma cells. Osteosarcoma is the most common primary malignant tumor of bone, with an annual incidence worldwide of approximately 5.6 cases per million, typically diagnosed in children

and young adults and currently treated with surgery and intensive chemotherapy protocols based on the combination of cytotoxic drugs.

The present thesis is structured in three chapters.

The first chapter reports an overview of the main characteristics of PLA. It describes the currently available procedures for its production and functionalization, focusing on the characteristics of PLA-based block polymers and summarizing the main biological applications as *drug delivery system.*

The chapter II reports an innovative method for the functionalization of commercial PLA with terminal alkyne units and the subsequent *click* coupling with azido-derivatives (**Figure 1A**).

The application of the solvent-free technique to the PLA derivatization represents an innovation to produce alkyne-grafted PLA without use of solvents, catalysts and in mild conditions. The *"clickable"* PLA was obtained by an unprecedented solvent-free intra-chain amidation, using propargylamine as alkyne donor. Alkyne-grafted PLA derivatives have been exploited as building blocks for access to a variety of functionalized polymers by Cu(I)-catalyzed cycloaddition reaction (CuAAC) with three different azides. The commercial methoxypolyethylene glycol azide (m-PEG-N_3) and the azide-fluor 545 have been selected as models of hydrophilic polymer and fluorescent probe, respectively. Moreover, the CuAAC *click* coupling with a newly synthesized azide-folate (FA-N_3) has been also investigated. All the three PLA derivatives (PLA- PEG, PLA-Flu and PLA-FA) have been formulated in nanoparticles loaded with Salinomycin, by nanoprecipitation technique.

The chapter III reports a multistep synthetic procedure for the preparation of a three-arm star PLA-PEG, decorated with the integrin-targeting RGD peptide (**Figure 1B**), designed for antitumoral applications. Arginine-glycine-aspartic acid peptide (Arg-Gly-Asp or RGD peptide) is a cell recognition motif, specifically recognized by the αvβ3 integrin receptor, over-expressed in tumors and involved in the regulation of tumor angiogenesis.

The three-arm star PLA was prepared, in a typical *core-first* approach, by ring-opening polymerization (ROP) of lactide using glycerol as a trifunctional alcohol initiator. In this step, the setting of the correct reaction time was imperative to finely control the molecular weight of the product. The grafting of alkyne moieties on the terminal hydroxyl groups of the star PLA, carried out by esterification with pentynoic anhydride, was followed by CuAAC *click* reaction with polyethylene glycol monoazide (monoazide-PEG), to obtain an amphiphilic star PLA-PEG copolymer. To decorate the star polymer with the tumor-targeting ligand RGD peptide, the hydroxyl terminal groups of PEG have been esterified with pentynoic anhydride to finally coupled the RGD-azide. As the decoration of nanoparticles with RGD peptide has recently emerged as a useful strategy for targeting tumor cells, the final star PLA-PEG-RGD will be formulated in micelles incorporating a suitable anticancer drug (i.e., Doxorubicin) for biological assays on osteosarcoma cells.

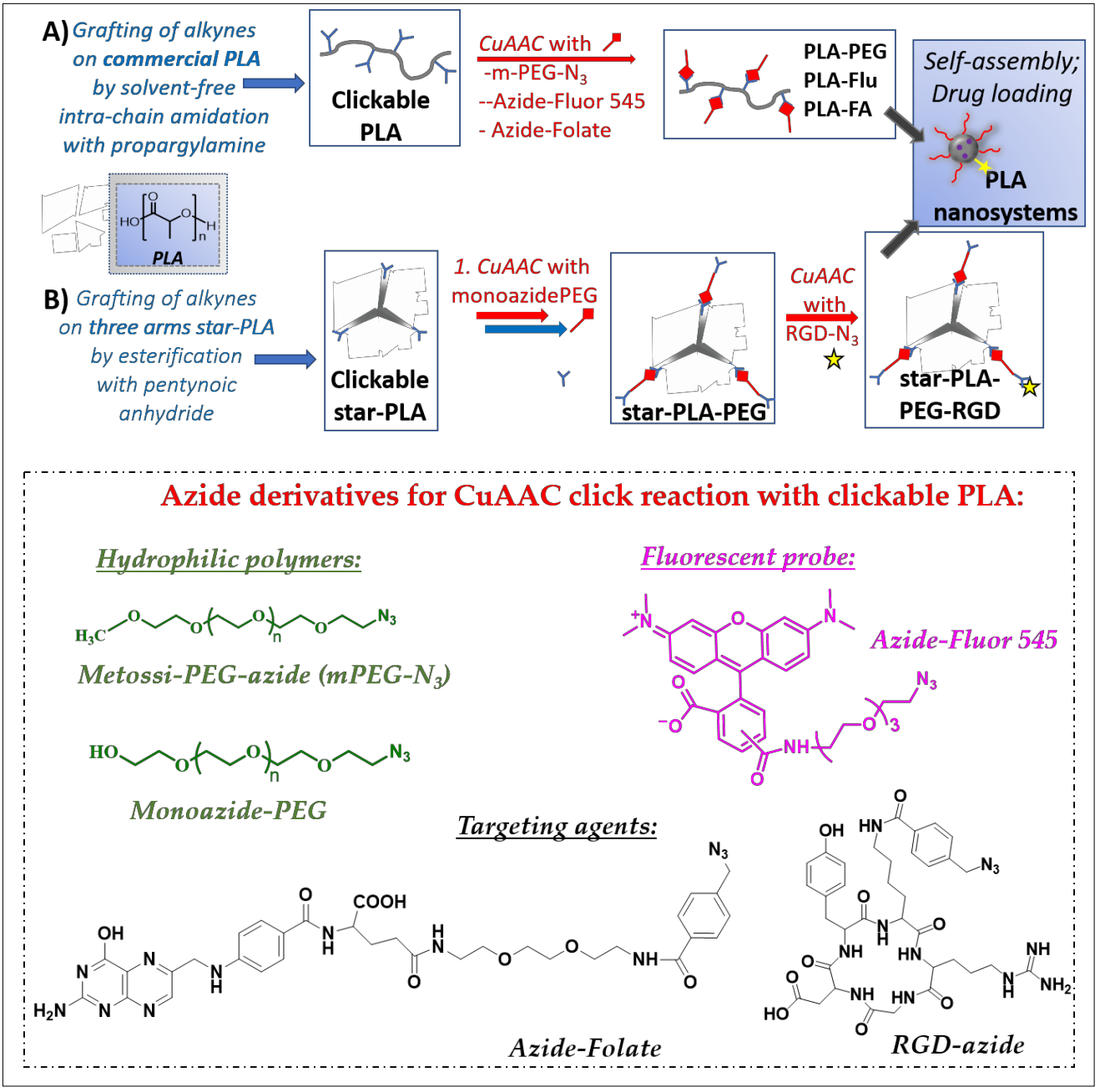
A) Grafting of alkynes on commercial PLA by solvent-free intra-chain amidation with propargylamine
Clickable PLA
CuAAC with -m-PEG-N3 --Azide-Fluor 545 - Azide-Folate
PLA-PEG
PLA-Flu
PLA-FA
Self-assembly; Drug loading
PLA nanosystems
PLA
B) Grafting of alkynes on three arms star-PLA by esterification with pentynoic anhydride
Clickable star-PLA
1. CuAAC with monoazidePEG
star-PLA-PEG
CuAAC with RGD-N3
star-PLA-PEG-RGD
Azide derivatives for CuAAC click reaction with clickable PLA:
Hydrophilic polymers:
Metossi-PEG-azide (mPEG-N3)
Monoazide-PEG
Fluorescent probe:
Azide-Fluor 545
Targeting agents:
Azide-Folate
RGD-azide

Figure 1

CHAPTER 1

Chapter 1

1.1 Polylactic Acid

Polylactic Acid (PLA) is an aliphatic polyester, biocompatible, biodegradable and widely used in several applications field, such as food packaging, production of fibers, in medical and pharmaceutical industries, as scaffolds, sutures, bone screws, wound dressings and drug delivery systems[1,2].

Since 1970's, PLA have been approved by the US food and drug administration (FDA) for food and pharmaceutical applications. The high interest for PLA is mainly due to its interesting physical and mechanical properties, recycling possibility and biodegradability, its large spectrum of applications and broad possibilities of functionalization.[3]

The recyclability of PLA is evident from **Figure 2**, that reports a closed loop system representing the "lifecycle" of PLA. PLA lifecycle starts with the bacterial fermentation of biomass to obtain lactic acid. Then two major routes can be applied to produce PLA from the lactic acid monomer: direct condensation polymerization of lactic acid or ring-opening polymerization (ROP) through the lactide intermediate. The biodegradation of PLA, which can be considered as a reverse polycondensation reaction, is a two-step process where polylactide first hydrolyzes into oligomers and then further breaks down into carbon dioxide and water by microorganisms. Finally, plants absorb carbon dioxide from the air, combine it with water and light, and make carbohydrates during photosynthesis, closing the cycle.

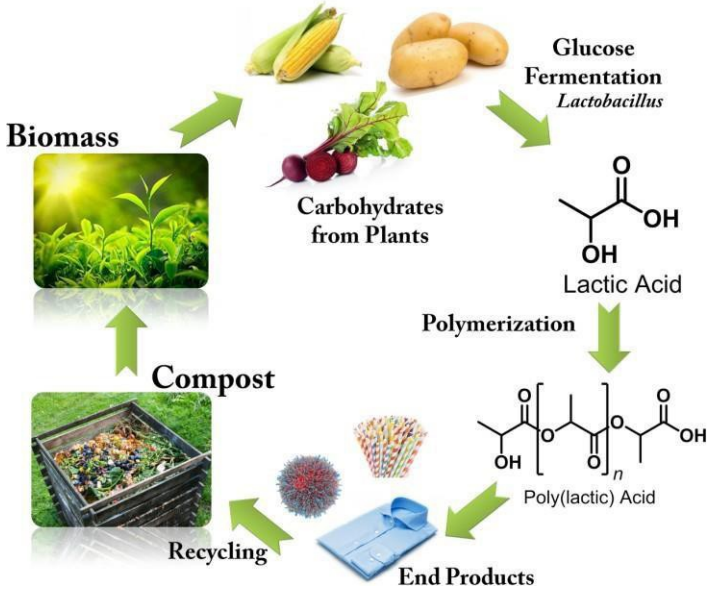

Figure 2: PLA life cycle

The economic convenience of PLA utilization depends on its production cost and on the possibility of after-use recycling using economically and environmentally friendly processes.[4]

PLA degradation was studied in animals and in human bodies since it has a great importance for biomedical applications of PLA derivatives (i.e. implants, surgical sutures, drug delivery). In these environments, PLA is initially degraded by hydrolysis, to reduce the molecular weight; then the soluble oligomers formed are metabolized by cells.[5] Albeit the complexity, the degradation of PLA matrices can be accounted for by two stages. The first stage of hydrolytic degradation occurs preferentially with the diffusion of water into the amorphous regions, which leads to an increase in the polymer crystallinity.[5] This phenomenon is known as "degradation inducedcrystallization".

In general, crystalline polymers tend to degrade slower than amorphous polymers because water cannot easily penetrate into the denser matrix. The hydrolytic cleavage of the ester bonds produces new carboxyl end-groups, and consequently acidification; the carboxyl end-groups of monomers and small oligomers further catalyze ester bonds cleavage (autocatalytic effect). Moreover, the rate of PLA degradation depends on molecular weight, stereochemical composition, pH and temperature of the media.

It is well known that the degradation of PLA is critical for the controlled release of drugs from delivery systems.[6] The drug release from degradable polymers can be considered as the result of different processes, such as (1) surface erosion of the polymer matrix, (2) cleavage of chemical bonds at the surface or within the bulk of the matrix, (3) diffusion of the physically entrapped drug. Although degradation and erosion are intrinsically connected, they correspond to different processes: degradation is the chemical process involving scission of polymer backbones, with formation of monomers and oligomers; erosion is a physical phenomenon consisting of the loss of material resulted from the monomers and oligomers leaving the polymer matrix.[7]

Ideally, a controlled release of drug from polymeric delivery systems can be achieved by regulation of the rate of polymer biodegradation and drug diffusion out of the polymer matrix.

1.2 Lactic Acid and Lactide Production

Lactic acid (2-hydroxy propanoic acid), the monomer utilized to produce PLA, is an optically active α-hydroxy acid with the chemical formula $C_3H_6O_3$ and it exists in two optically active enantiomeric forms: D-Lactic acid and L-Lactic acid (**Figure 3**).

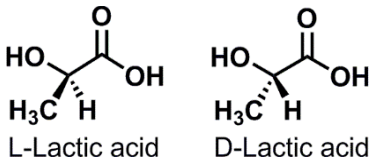

Figure 3: Stereoisomers of Lactic Acid

Humans produce the L-lactic acid enantiomer,[8] and it can be found in muscles after intense exercise and in mammary glands after the woman gives birth. The elected metabolic pathway is Krebs cycle, where lactate is transformed from pyruvate *via* lactate dehydrogenase in absence of oxygen[9]. Consequently, lactic acid and materials prepared starting by itself are naturally processed in human body, originating byproducts that are naturally present into our organism, not toxic, good tolerated and easily eliminated[10].

Lactic acid has two main production routes, such as chemical synthesis and bacterial fermentation. The chemical synthesis (**Figure 4**) is carried out by acidic hydrolysis of lactonitrile, leading to the production of a racemic mixture of L-and D-Lactic acid. Lactonitrile is producedfrom acetaldehyde and hydrogen cyanide as an intermediate in the production of acrylonitrile, and it is further hydrolyzed to lactic acid as described in Figure 4.

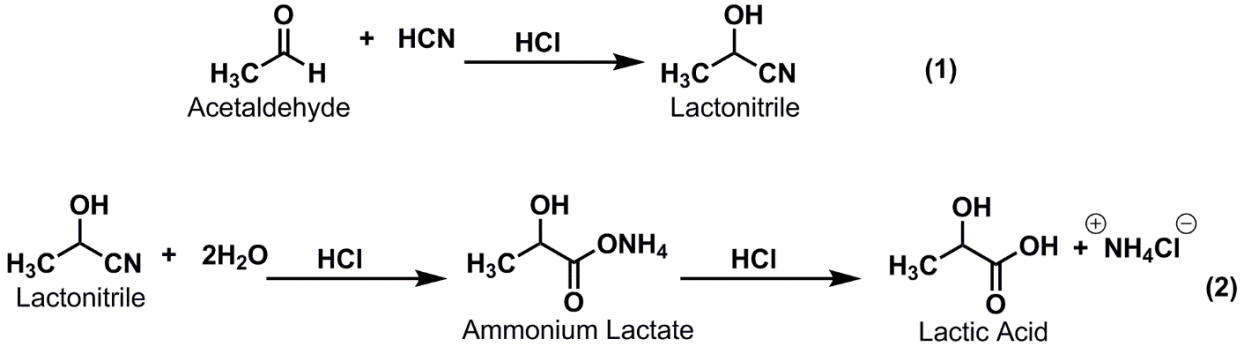

Figure 4: Stereoisomers of Lactic Acid

About 90% of the total lactic acid produced worldwide is made by bacterial fermentation[11] of carbohydrates (glucose, maltose, lactose and sucrose) obtained by biomass wastes of potatoes, corn, sugar cane and beets[12]. In the last years, lignin and cellulose are also utilized[13]. Fermentation process is the more interesting route of lactic acid production since optically pure L-lactic acid or D-lactic acid can be obtained by selecting a proper bacterial strain, with low production cost, high efficient and low environmental impact.

Elected bacteria are usually of *Lactobacillus* genus, since they are the most efficient in time and quantity of production. D-stereoform or the D/L-racemic mixture can be produced by *L.*

delbrueckii[14], *L. jensenii* and *L. acidophilusbatteri*, whereas *L. amylophilus*, *L. casei*, *L. maltaromicus*, *L. Bavaricus*, *L. Plantarum*[15] are able to produce the L-enantiomer. Actually, also other bacteria are going to be engineered to hyperproduce lactic acid, i.e. *Corynebacterium*.

Generally, industrial production[16] of lactic acid is conducted in batches, at pH ≈ 6, 40°C and low concentration in oxygen. To separate lactic acids from fermentation broth, calcium hydroxide or calcium carbonate are usually added. In this way calcium lactate, a soluble salt, is obtained and it can be separated by cells and other insoluble impurities through filtration. The filtrate is evaporated, crystallized and treated with sulfuric acid. Calcium sulfate is filtered and lactic acid is purified by nanofiltration, ultracentrifugation and electrodialysis[17]. The fermentation process can be classified according to the bacterial strains in:

- Heterofermentative, which produces 1.8 mol of lactic acid per mole of hexose, with several byproducts such as acetic acid, ethanol, glycerol, mannitol and carbon dioxide. *L. brevis*, *L. fermentum*, *L. parabuchneri* are obligatory *hetero*fermentative bacteria[18] that use phosphoketolase metabolic pathway to produce lactic acid, while *L. casei*, *L. rhamnosus*, *L. xylosus* are facultative *hetero*fermentative bacteria[19] that use both glycolysis and phosphoketolase metabolic pathway. Some of those bacterial strains are actually engineered to improve the yield of production.

- Homofermentative, which is the elected industrial method, allowing for a conversion of over 90%. *L. acidophilus*, *L. amilophilus*, *L. helveticus* are *homo*fermentative[20] bacteria using glycolysis metabolic pathway to convert glucose exclusively into lactic acid.

Lactic acid is used to prepare lactide (3,6-dimethyl-1,4-dioxane-2,-dione) which is the cyclic diester of lactic acid and the monomer used for the Ring Opening Polymerization (ROP) to synthesize PLA. The different stereoforms of lactide are shown in **Figure 5**. [21] From the combination of two molecules of L-lactic acid, L-lactide is obtained, while D-lactide is obtained from the combination of two molecules of D-lactic acid. From the combination of L-lactic acid and D-lactic acid molecules, a meso-lactide is obtained. The latter, unlike the L and D forms, is optically inactive.

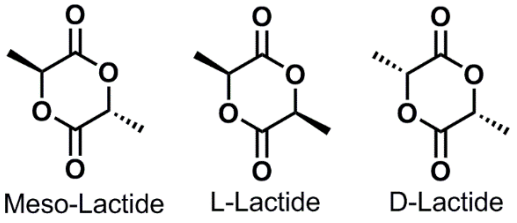

Figure 5: Stereoisomers of Lactide

Lactide can be obtained by depolymerization of PLA oligomers, through two consecutive steps: oligomerization of lactic acid and then depolymerization to lactide. The oligomers are formed

by traditional condensation polymerization but with short reaction times to limit the molecular weight. These pre-polymers are then heated above 180 °C at 2 mm Hg in the presence of an inorganic salt (Sb_2O_3) and the obtained lactide distilled and recrystallized from ethyl acetate[22].

Because of the chiral nature of lactic acid, lactide exists in various diastereomers from which PLA can be synthesized with controlled stereochemistry, since bonds to the chiral carbon are not broken during the polymerizations. The polymerization can yield poly(L-lactide) (PLLA), poly(D-lactide) (PDLA) and poly(DL-lactide) (PDLLA, the result of the polymerization of the racemic mixture formed by 50% L-stereoisomer and 50% D-stereoisomer).

The physical and chemical properties of PLA depend on the stereochemical composition and sequence of the polymer. In fact, the ratio of D and L isomers and their distribution along the polymer backbone influence the crystallinity and melting point of PLA. For example, optically active and isotactic PLLA and PDLA are semi crystalline polymers with a long degradation time due to the limited diffusion of water in crystal domains, whereas optically inactive PDLLA is amorphous and it has faster degradation time[23].

The L-isomer is a biological metabolite and constitutes the main fraction of PLA derived from renewable sources since the majority of lactic acid from biological sources exists in this form. PLLA has gained great interest due to its excellent biocompatibility and mechanical properties. As an example, PLLA fibers are the preferred material in applications that require high mechanical strength (e.g. ligament and tendon reconstruction; stents for vascular and urological surgery). However, its long degradation time and high crystallinity can generate inflammatory reactions in the body. In order to overcome this drawback, PLLA can be used as a material combination of L-lactic and D, L-lactic acid monomers.[24]

1.3 PLA synthesis

Lactic acid can be polymerized to PLA using different synthetic approaches,[25] including condensation (direct polycondensation, azeotropic condensation, solid phase polycondensation) and ring opening polymerization (**Figure 6**).

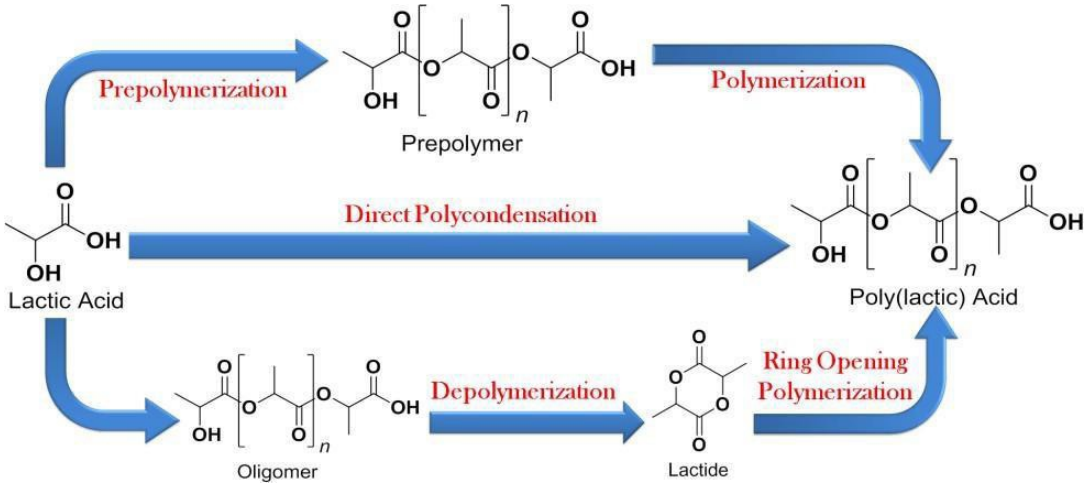

Figure 6: Pathways for PLA synthesis

1.3.1 Condensation

The polycondensation, also called step-growth polymerization, is the first method utilized for PLA synthesis and still represents the simplest and the cheapest way of production[26]. The presence of both hydroxyl and carboxyl groups in lactic acid enables it to undergo self-esterification[27] and to be converted into polyester via condensation reaction. This is a reversible step-growth polymerization with production of water as a byproduct that must be removed using high vacuum and high temperatures, to enhance monomer conversion and polymer molecular weight. However, the final PLA is a low molecular weight, glassy, fragile polymer (2.000-10.000 Da), which is useless for any applications, either in biomedical devices or in food packaging. Furthermore, intra-molecular transesterifications of the growing chains, also called *back-biting reactions*, lead to the formation of ring molecules as byproducts, i.e. lactide, the cyclic dimer of lactic acid, decreasing the average length of the polymer chains and affecting PLA purity (**Figure 7**).

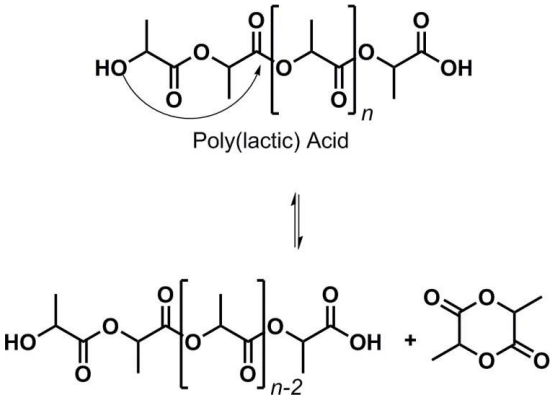

Figure 7: Back-biting reactions

Actually, coupling reagents, esterification-promoting additives (bis(trichloromethyl) carbonate, dicyclohexylcarbodiimide and carbonyl diimidazole) or chain extenders (isocyanates, acid chlorides, anhydrides, epoxides, thiirane and oxazoline) could be added to the reaction media to increase esterification rate and molecular weight of the final polymer, but they add complexity and costs to the polycondensation process.

In order to overcome these disadvantages, alternative polycondensation methods have been proposed, such as azeotropic polycondensation (AP) and solid state polymerization (SSP).

AP method represents an improvement of the above described process and doesn't require external adjuvants to increase the molecular weight of final polymer. Lactic acid and catalyst are azeotropically dehydrated in a refluxing, high-boiling, aprotic solvent under reduced pressure to obtain high-molecular weight PLA (greater than 300.000 Da)[28]. Typical experimental conditions are 130°C, 30-40 hours and a final purification step to remove the excess of catalyst used to avoid polymer degradation or hydrolysis. That purification is crucial for polymer utilized in biomedical field.

In the SSP (**Figure 8**), an aqueous solution of L-lactic acid is first dehydrated to obtain L-lactic acid oligomers and then melted and condensed in the presence of a catalyst to obtain a PLA prepolymer at low molecular weight. Prepolymer is crystallized at 105°C, then the temperature is increased at 150° C (but below the melting point) and it is polycondensed in solid phase to afford high molecular weight PLA.

The molecular weight of polymers obtained according to this method is exceptionally high (till 600.000 Da). Side reactions and byproducts formations are very limited in solid phase, resulting in a polymer formation yield of 100%.

This process is comparable to the ring opening polymerization (ROP) in product quality[29], but high temperature, long operating time and high pressures limit its industrial application.

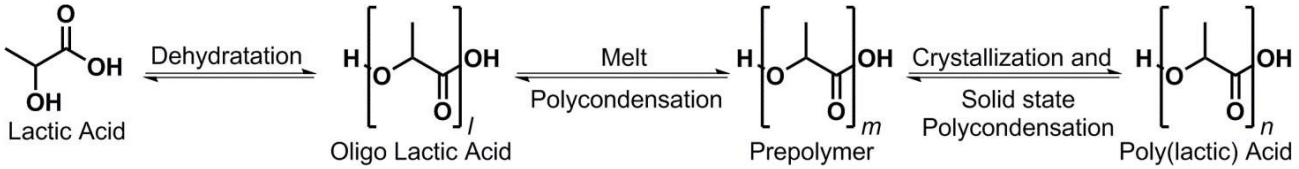

Figure 8: Synthesis of high molecular weight poly(lactic acid) via SSP

1.3.2 Ring Opening Polymerization (ROP)

The ring opening polymerization (ROP) of lactide, the cyclic dimer of lactic acid, is an alternative and very powerful way to produce PLA which avoids formation of water in the polymerization process[30]. Currently, it is the most largely used route in PLA industrial production.

In this synthetic process, lactic acid is first polymerized to a low molecular weight oligomer, which undergo catalytical depolymerization to lactide through internal transesterification, in the "back-biting" reaction. Then, the ring of lactide opens to form high molecular weight PLA.

The ROP of lactide was first demonstrated by Carothers in 1932,[31] but high molecular weights were not obtained until improved lactide purification techniques were developed by DuPont in 1954.[32]

The reaction is carried out using three basic components (**Figure 9**):

1) *lactide,* the cyclic lactone which represents the *monomer*. When the ring is opened, one extremity is linked to the initiator, and the other one, negatively charged, is essential for the propagation;

2) *initiator*, usually represented by alcohols or polyalcohols, which is activated by the catalyst, to open the monomer ring, starting the polymerization process;

3) *catalyst,* which can be of different nature (metal based, organo-catalysts), to activate the initiator.

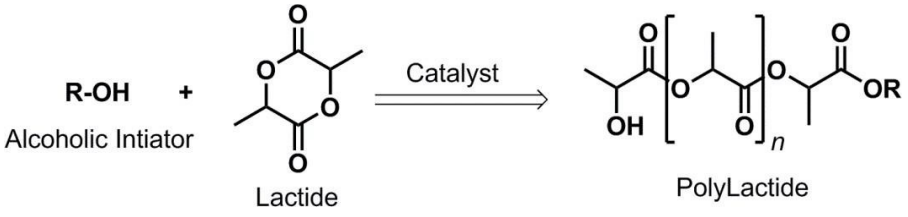

Figure 9: Ring Opening Polymerization (ROP) of Lactide

The absence of hydroxyl groups in the lactide avoids formation of water during propagation process. Propagation reaction of ROP consists into transesterifications between the monomer (lactide) and hydroxyl groups contained in the polymer chains, without byproducts formation. A fine control of molecular weight and polydispersity index can be achieved. High molecular weight PLA can be obtained without using external compounds such as chain extenders, coupling agents or high boiling solvents and avoiding high level of vacuum. The final polymer presents a high purity so that its biocompatibility is not affected by undesired compounds.

The process can be used not only for PLA production, since different type of cyclic monomers can undergo ring opening polymerization, such as glycolide, ε-caprolactone, ethylene oxide (**Figure 10**).

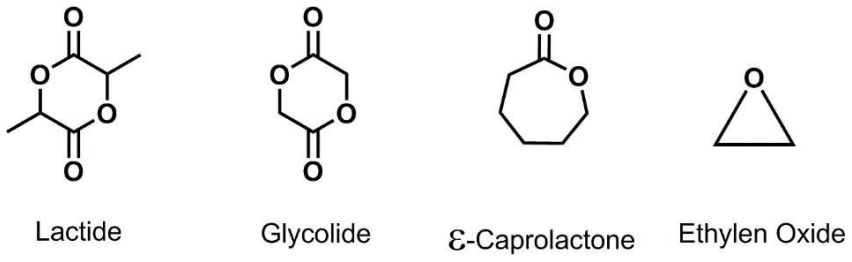

Figure 10: Different monomers for ROP

Different mechanisms for the ROP of lactide can be described: cationic, anionic or coordination-insertion[24].

Cationic ROP can be initiated by a very strong acid (triflic acid or methyl triflate). The propagation mechanism proceeds by nucleophilic attack of the oxygen atom of the triflate anion in the protonated ester-group on the positively charged lactide ring (**Figure 11**). The triflate end-group reacts again with a second molecule of lactide that is opened and the polymerization proceeds.

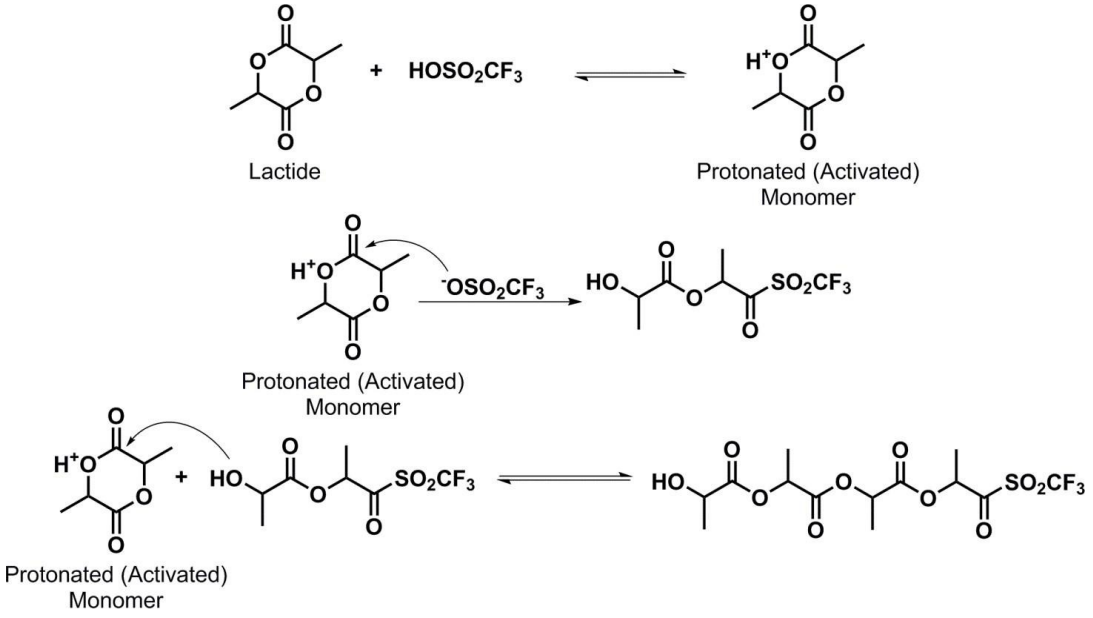

Figure 11: Propagation of Lactide by cationic mechanism with triflic acid (CF_3SO_3H) as the initiator

The anionic ring-opening polymerization of lactides proceeds by the nucleophilic reaction of the negatively charged initiator (an alkali metal alkoxide) with the lactide carbonyl, with the subsequent acyl-oxygen bond cleavage. This produces an alkoxide end-group which continues to propagate. (**Figure 12**).

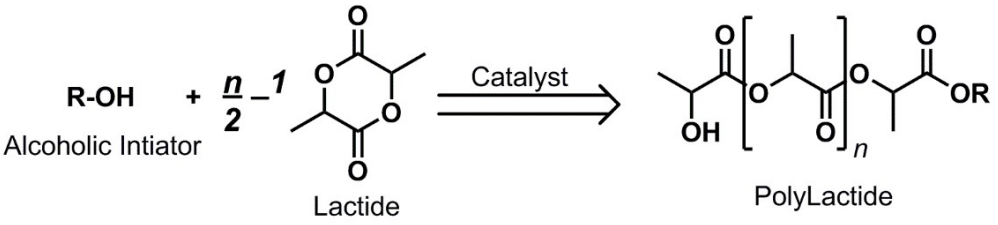

Figure 12: Anionic initiation of PLA

The coordination-insertion mechanism proceeds by the coordination of the carbonyl oxygen with the metal (the alkoxides of magnesium, aluminum, tin, zirconium or titanium) to enhance the electrophilicity of the carbonyl group as well as the nucleophilicity of the alkoxide part of the initiator (**Figure 13**). The cyclic structure of the lactide is then cleaved at the acyl-oxygen bond resulting in the structure RO-Lactide-ML_n. The propagation is then continued by an identical mechanism.

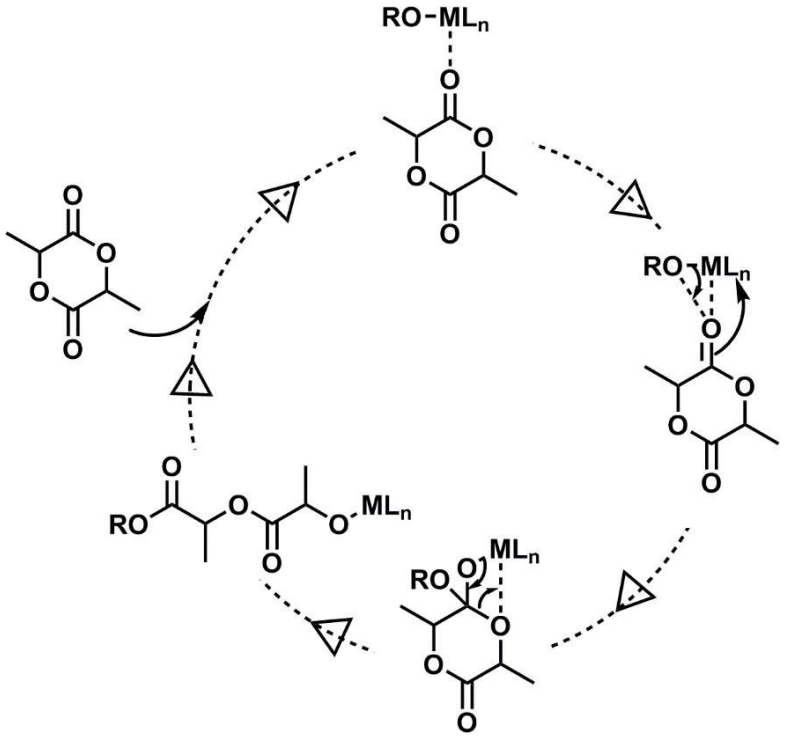

Figure 13: Coordination-insertion mechanism for ROP of lactones. R= growing polymeric chain

The catalysts used in the ROP can be of different nature, such as metal-based or organo-catalysts. Metal-based catalysts are metal alkoxides based on aluminum (Al), tin (Sn) and zinc (Zn). The most used are tin(II)bis-(2-ethylhexanoate) ($Sn(Oct)_2$), aluminum tri-isopropoxide ($Al(OiPr)_3$) and zinc lactate(II) ($Zn(lac)_2$) (**Figure 14**), which act through the 'coordination-insertion' mechanism. Tin(II) and zinc show the best performances as catalysts, as they lead to high molecular

weight PLA with high level of purity (almost complete monomer conversion), due to the presence of covalent metal-oxygen bonds and free *p* or d orbitals[33,34].

Interestingly, the stannous octoate ($Sn(Oct)_2$) is recognized as safe for use both in the medical field and in the food sector by the Food and Drug Administration (FDA).

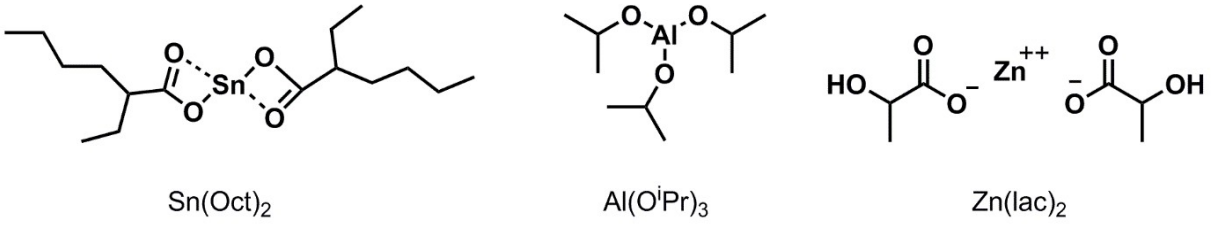

Figure 14: Metal-based catalysts for the ROP of lactones.

Two slightly different reaction pathways have been proposed for the $Sn(Oct)_2$ -mediated coordination-insertion mechanism. Kricheldorf and coworkers have proposed a mechanism,[35] where the monomer and the alcohol functionality are both coordinated to the $Sn(Oct)_2$ during propagation (**Figure 15**). Penczek and coworkers have reported a mechanism,[36] where the $Sn(Oct)_2$ - complex is converted into a tin-alkoxide before complexing the monomer and ring-opening it.

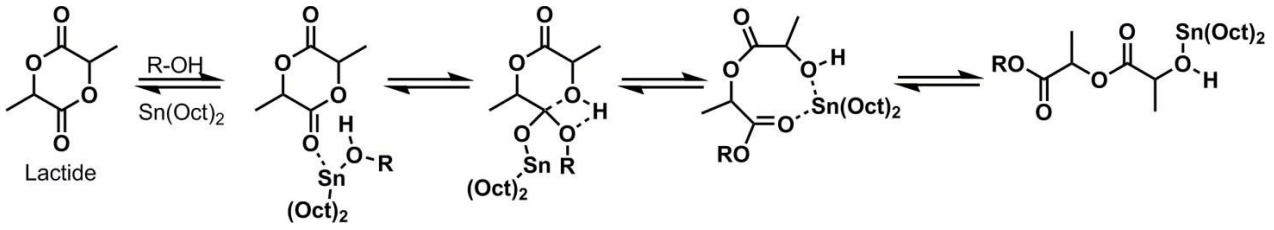

Figure 15: Generalized coordination–insertion mechanism of Lactide to PLA

Organocatalysts are generally amines (**Figure 16**). They are preferred when the PLA is destined to biological applications, since they can be easier removed, without toxic residues.

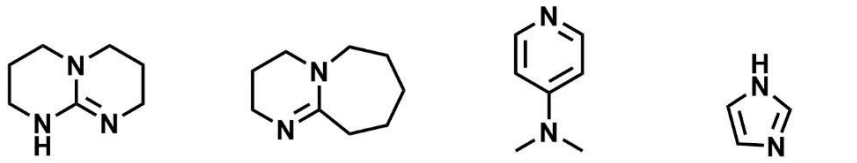

Figure 16: Organocatalysts used in ROP of lactones.

The mechanism of the organocatalysts is shown in **Figure 17**: the mild base activates the initiator through H-bond, de facto creating a negative charge on the initiator to promote the nucleophilic attack on the monomer.

Among them, DBU has been widely applied as valuable ROP catalyst, since it displays high catalytic activity with >98% monomer conversion being observed within 2 h for 500 equiv L-lactide (to initiator) with 1 mol % catalyst and [LA] = 0.7 M at ambient temperature.[37] Transesterification side reactions can occur with DBU at greatly extended reaction times, and the reaction is quenched by acid addition (.i.e. benzoic acid) leading to its deactivation.

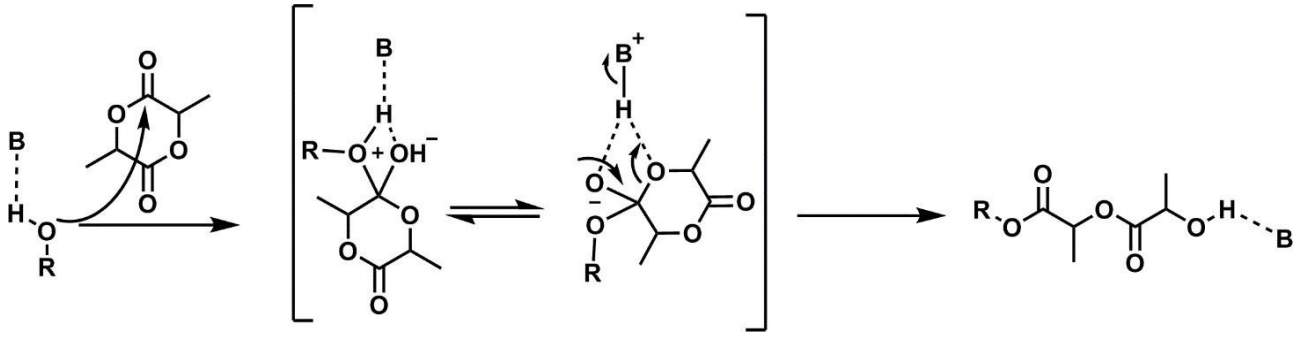

Figure 17: Initiator/chain-end activation mechanism. B is an organocatalyst (e.g. DBU).

It is noteworthy that, due to the structure of polyesters, the carbonyl groups on the linear chain could be also activated by the catalyst, starting intra- or inter-chain transesterification reactions. Intra-chain reactions produce cyclic polymers, whereas inter-chain reactions lead to the fragmentation of the polymer. In both cases, the result is the formation of different populations of polymers. To avoid those side reactions, it is important to choose a catalyst and an initiator that are not too much reactive, so the main mechanism of action becomes preponderant.

Although ROP currently represents the process of choice for industrial PLA production, alternative methods for PLA synthesis, like sonochemistry and microwave irradiation are under investigation as faster and more energy-efficient methods to synthesize PLA[38].

Both of these methods could reduce the need of high temperature and extremely low pressures and could be a potentially cheaper solution for production of PLA.

1.4 PLA-based block copolymers

PLA is widely used for various applications, ranging from biomedical, packaging, textile fibers to technological items.[3] Nonetheless, PLA suffers from some drawbacks, such as hydrophobicity and subsequently entrapment by macrophages through opsonization, long-term degradation time associated with microenvironment acidification (the latter causing inflammatory or allergic reactions), low loading for hydrophilic drugs and initial burst release.[39]

In this regard, numerous efforts have been devoted to overcome these downsides. Co-polymerization with other polymers can be helpful for resolving the problems of PLA homo-polymeric systems.

Thanks to the advancement of polymer synthetic strategies, PLA-based block co-polymers (BCPs) with defined architectures and precisely controlled molecular weights can be synthesized. The main synthetic strategies include: (1) the controlled polymerization of monomers; (2) the versatile post-polymerization end-functionalization by coupling reactions.[40]

Figure 18 illustrates a few examples of the many architectures of BCPs, which can be configured into linear, branched (graft and star), and cyclic polymers. Complex polymeric architectures can be synthesized either with the use of specially tailored starting compounds or by first synthesizing linear chains which undergo further reactions to become connected together.

In addition to the one-dimensional (linear BCPs) and two-dimensional (brush) polymers, also the three-dimensional polymers have gaining a great importance, represented by hyperbranched polymers and dendrimers.

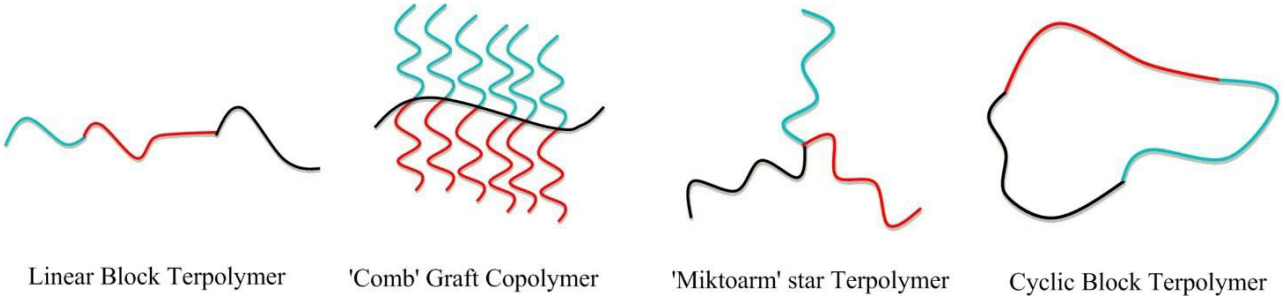

Figure 18: Representative architectures of linear block terpolymers, 'comb' graft copolymers, miktoarm star terpolymers and cyclic block terpolymers

Each polymeric architecture exerts a huge influence on the physical and chemical properties of the final material and, consequently, on the application field.[37]

In linear polymers the repeating units are joined together end to end in a single flexible chain. Copolymerization of different linear blocks leads to obtain a final product with tailored properties, e.g. amphiphilic block copolymers.

The introduction of branching to the PLA backbone is one highly effective approach to tailor the physical properties, to obtain more interesting rheological and mechanical properties, such as a lower viscosity or an increase of the polymer strength.[37]

Graft polymers are constituted by a linear polymer backbone on which side chains or branches of different nature are linked.[41]

Cyclic polymers are produced by ring-closure techniques involving the coupling of the reactive chain ends of a linear polymer to yield a cycle. Due to their shape and smaller hydrodynamic volume, cyclic polymers aggregates in smaller sized particles, compared to linear analogs.[42,45]

Star polymers present one multifunctional molecule centre (core) on which three or more polymeric arms are linked. Arms can be similar in length and chemical composition (regular star polymers), or different (miktoarm polymers). They can be prepared starting by the core (approach core-first) or starting by arms (approach arm-first).[43] One of the advantages of star polymer respect to linear analog with the same molecular weight is the reduced toxicity on human cells. In fact, the latter present not only more end-groups functionalizable but also shorter polymeric chains that are easier degraded and excreted., decreasing toxic effects on human body.[44]

One of the most common example of a PLA-based block copolymer is the poly(Lactic Acid)-co-(Glycolic Acid) (PLGA, **Figure 19**). PLGA has attracted considerable interest for biomedical applications due to its biocompatibility, approval for clinical use in humans by the FDA, tailored cristallinity and biodegradation rate, depending on the molecular weight and copolymer ratio, versatility by chemical functionalization.[45] Notably, the first FDA-approved drug delivery system (Lupron® Depot) based on a biodegradable polymer, released in 1989, consists of PLGA microspheres encapsulating leuprolide for the treatment of prostate cancer. The leuprolide release rate from the formulation is controlled by the biodegradation of PLGA, allowing a sustained drug release profile and minimizing toxic side effects and increase patient compliance.[46]

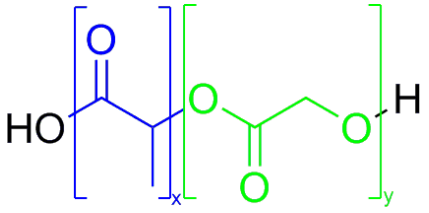

Figure 19: PLGA structure, where x represents number of Lactic Acid monomeric units and y represents number of Glycolic Acid monomeric units

The co-polymerization of PLA with hydrophilic polymers (i.e. polyethylene glycol, polysaccharides, polipeptides, etc...) produces powerful amphiphilic copolymers which are able to spontaneously self-assemble in an aqueous environment into different topological architectures, including micelles, vesicles, nanocapsules, nanospheres, depending on the polymer architecture, molar mass and chemical composition.[40]

The self-assembly is the process by which an organized structure spontaneously forms from individual components, as a result of specific, local interactions among the components. When amphiphilic BCPs self-assemble forming nanoparticles in water, the hydrophilic portion is freely exposed toward aqueous solution, whereas the hydrophobic moiety constitutes the *core* incorporating hydrophobic drugs (**Figure 20**). Consequently, such nanoparticles own a *core-shell* structure, in which the hydrophobic *core* serves as a compartment for the loading of hydrophobic biomolecules, and their subsequent sustained release; the hydrophilic *shell* formed by the hydrophilic block could stabilize nanoparticles in aqueous solution and prolong the blood circulation of nanoparticles.

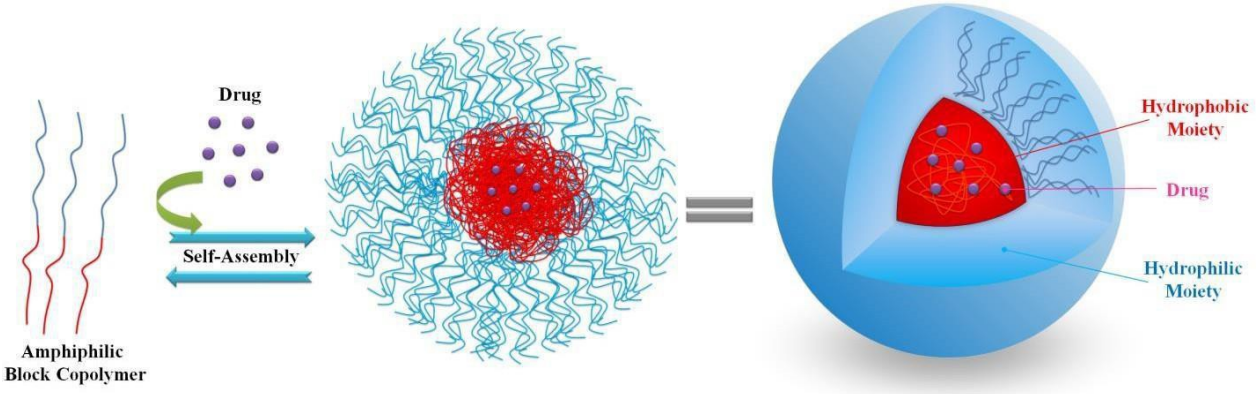

Figure 20: Nanoparticle formation and structure

The PLA-based amphiphilic block copolymers that are most used for biological applications are obtained by the covalent grafting of polyethylene glycol or hyaluronic acid onto PLA backbone.

Hyaluronic acid (HA) is a linear glycosaminoglycan composed of N-acetyl-D glucosamine and D-glucuronic acid units and it is a component of extracellular matrixes in human body. HA shows excellent potential for application in drug delivery, wound healing and tissue engineering due to its good biocompatibility, biodegradability and to the ability to improve tumor cell targeting of nanoparticles, owing to the specific binding with CD44 receptors highly expressed on the cancer cell surface.[47]

Polyethylene glycol (PEG) is a hydrophilic polymer, consisting of (OCH_2CH_2) repeating units, biocompatible, approved by the FDA for food, cosmetics and pharmaceutical purposes and by the European Agency for Medicaments (EMA).

PEG can be synthesized *via* anionic polymerization of ethylene oxide and a hydroxyl initiator. If the initiator is the hydroxyl ion, the diol is obtained, whereas the mono-methoxy polyethylene glycol (mPEG) is obtained when the initiator is the methoxy ion. Hydroxyl group could derive from water, ethylene glycol, or any diols or also from epoxyethane by ring-opening polymerization.[48]

Linear PEG bears only two hydroxyl functional groups. The ability to graft a variety of reactive groups to the terminal sites of PEG has greatly expanded its scope and applications. Therefore, commercial mono- and di-functionalized PEG are available with different activated functional groups and degrees of polymerization (**Figure 21**). Hetero- and homo-bifunctional PEG are especially suitable as cross-linking agents or spacers between two chemical entities, whereas mono-functional PEG prevent bridging reactions.[49]

The physico-chemical properties of PEG vary from viscous liquids to waxy solids according to their molecular weight, although all PEG -from oligomers up to those of a few million molecular weight- are totally and highly water soluble. Moreover, the solubility of PEG in organic solvents is affected by molecular weight. In particular, liquid PEGs (100-700 Da) are soluble in acetone, alcohols, benzene, glycerin, and glycols. Solid PEGs (>1000 Da) are soluble in acetone, dichloromethane, ethanol 95%, and methanol; and they are slightly soluble in aliphatic hydrocarbons and ether. Also the half-life and the fate of PEG is governed by the molecular weight.[50]

PEG fate in human body is strictly dependent on its molecular weight. Oligomers with a molar mass below 400 Da were found to be toxic in humans since they are processed by alcohol and aldehyde dehydrogenase enzymes to form oxidized products (i.e. hydroxyl acid and diacid metabolites). This metabolism is significantly reduced with increasing molar mass. On the other hand, the molecular weight should not exceed the renal clearance threshold to allow the complete excretion of the polymer: it seems that PEG with a molar mass below 20 kDa is easily excreted by renal filtration, while higher molar mass PEG is eliminated slowly and clearance through the liver becomes predominant. To overcome these drawbacks, branched, grafted and multiarm PEGs can be used to obtain systems more easily excreted.[51,52]

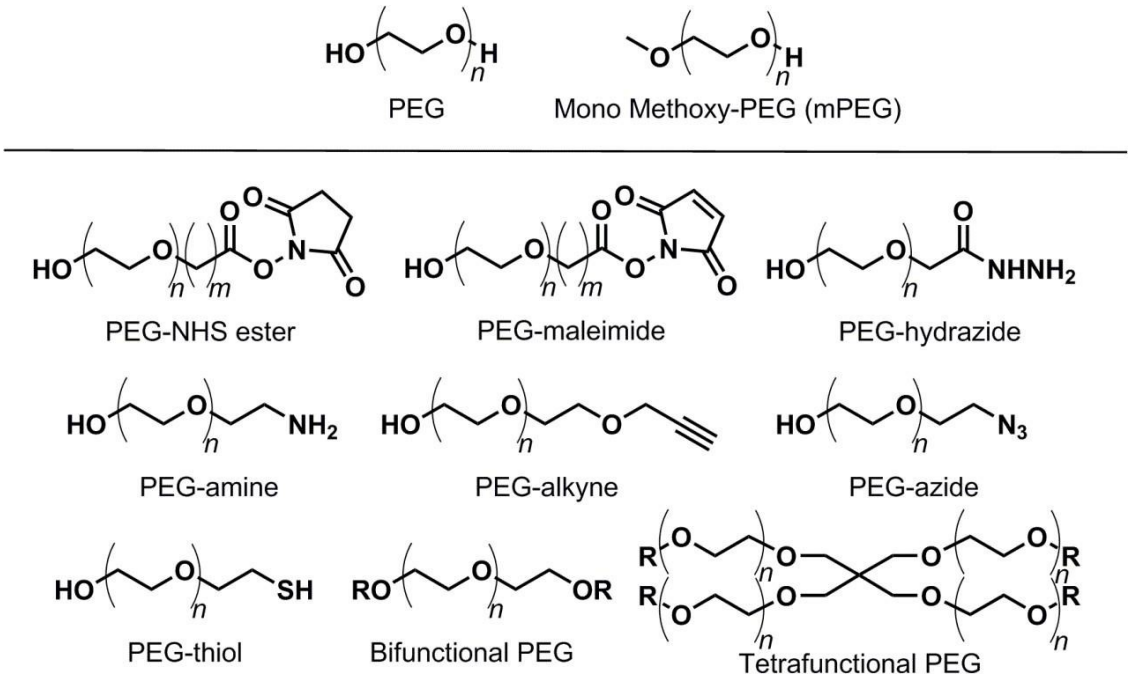

Figure 21: Structures of PEG, mPEG and some representative PEG derivatives.

The covalent grafting of PEG onto the PLA backbone, the so called *"PEGylation"*, improves the water solubility and biocompatibility, useful for drug delivery applications. Moreover, it increases the blood circulation half-life of the polymeric nanoparticles, avoiding the *opsonization.* Opsonization is the process by which a foreign organism or particle becomes covered with opsonin proteins, thereby making it more visible to phagocytic cells. Opsonins are proteins of the blood serum that quickly bind foreign nanoparticles, allowing macrophages of the mononuclear phagocytic system (MPS) to easily recognize and remove them, before they can perform their designed therapeutic function. PEGylation is one of the methods used for camouflaging or masking nanoparticles, conferring *"stealth properties"*, which allow them to temporarily bypass recognition by the MPS, increasing blood circulation half-life.[53]

The copolymer PLA-PEG is one of the most promising amphiphilic material very suitable for producing micelles as drug/gene delivery systems (**Figure 22**), owing to the excellent physicochemical and biological characteristics, namely nontoxicity, non-protein adsorption, and weakened uptake by the reticulo-endothelial system (RES) after intravenous injection.[54]

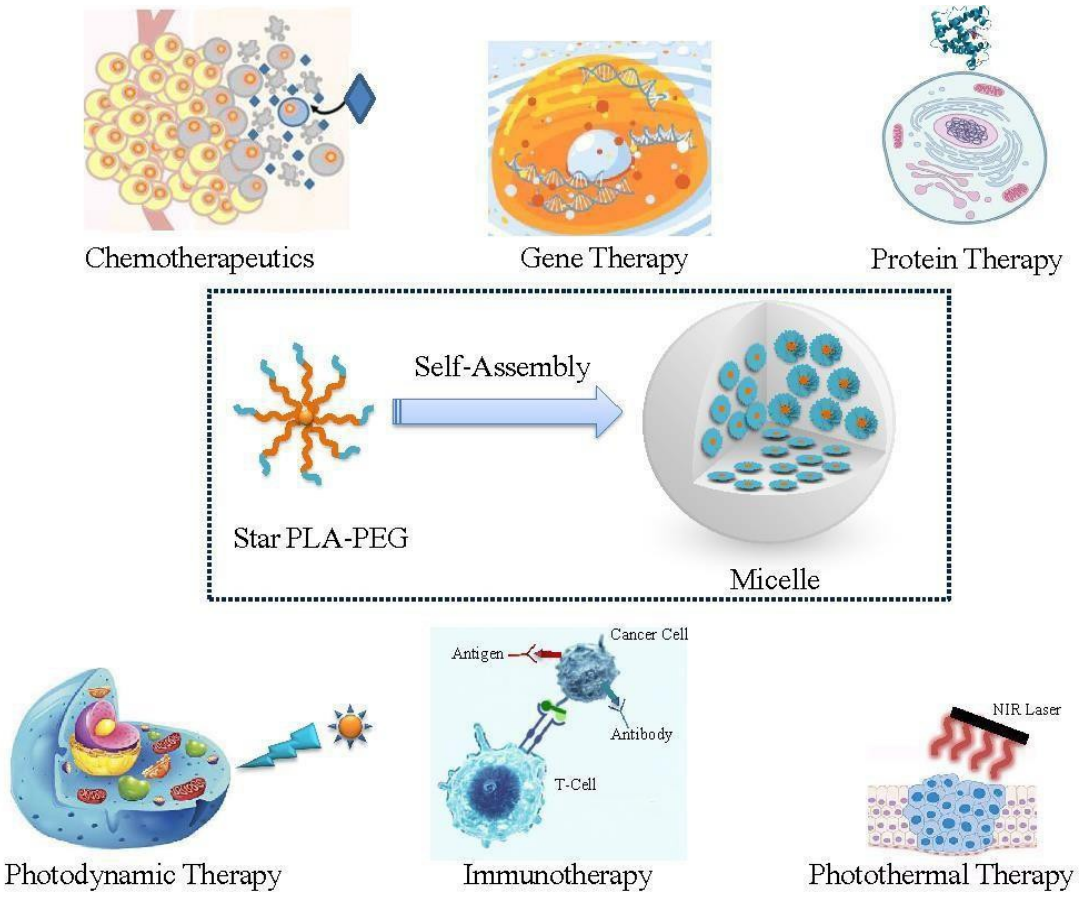

Figure 22: Schematic illustration of PLA-PEG micelles and their biological applications[54]

Notably, Genexol-PM (Samyang Co., Seoul, Korea) is a biodegradable polymeric micellar formulation of paclitaxel based on PEG–PLA copolymer, approved in Korea in 2007 for the treatment of breast, lung, and ovarian cancers[55]. In vivo, Genexol-PM shows greater antitumor activity and higher concentrations in tumor tissues compared to conventional paclitaxel. Moreover, it is currently under clinical development in the USA.[56]

1.5 Biological Applications

One of the main drawback of conventional chemotherapy is the non-specific distribution of the drug in the body which causes side effects to healthy cells and reduced therapeutic efficacy, as the drug concentration reaching the tumor target site is reduced.[57]

The emergence of polymer-based nanomaterials used as versatile *drug delivery systems* (DDS) has opened new perspectives in the modern chemotherapy. Currently, nanoscale DDS such as nanoparticles, nanoliposome, nanoemulsions, nanosuspensions, dendrimers, and nanosponge are believed to have the potential to revolutionize the drug delivery strategy.[58]

In this regard, amphiphilic block copolymers (e.g. PLA-PEG) able to form polymeric nanoconstructs, typically with dimensions below 200 nm, have gained increasing interest for the efficient delivery of biomolecules. These nanosystems possess unique characteristics for drug delivery applications, such as tailored size and design flexibility, improved stability, prolonged circulation life-time, enhanced drug solubility and bioavailability, reduced toxicity, controlled and sustained drug release.[57]

The drug(s) can be loaded in polymer-based DDS via physical encapsulation or via chemical conjugation, to form polymer-drug conjugates.

One of the main purposes of any DDS is to release the drug, selectively, to the target pathological site (*targeting*), reducing toxicity towards peripheral healthy tissues. Ideally, the DDS could act as a *"magic bullet"* recognizing cancer cells only. Two strategies of drug targeting can be applied to the site of action, *active* or *passive targeting* (**Figure 23**). The passive targeting is strictly related to the distinctive characteristics of the tumor microenvironment that facilitate accumulation of nanovectors, as a result of the enhanced permeability and retention (EPR) phenomenon, first described by Maeda and Matsumura.[59]

The EPR effect is based on the combination of factors inherent to the nanoparticle itself (size, shape, surface charge), with factors associated with the neoplastic tissues.[60] Solid tumors have an altered vascular pathophysiology[61]. In fact, tumor growth is generally accompanied by hypervascularization, that results in an abnormal blood flow and lack lymphatic drainage. Moreover, the characteristic defective endothelial cells with wide fenestrations cause enhanced permeability towards nanocarriers that could be easily entrapped and accumulated in tumor tissues.[62]

Active targeting requires cell-specific ligands, covalently linked to the surface of engineered polymeric nanoparticles, including antibodies, aptamers, sugar moieties, peptides and whole proteins (e.g., transferrin) and different receptor ligands (e.g., folic acid, RGD peptide).[63] Specific interactions between these ligands on the nanocarrier surface and receptors expressed on the tumor cells facilitate nanoparticle internalization by triggering receptor-mediated endocytosis.

Currently, the development of targeted-modified, stimuli-responsive, multifunctional PLA-based drug carriers attracts a great scientific interest as a promising frontier for biomedical science and nanotechnology.

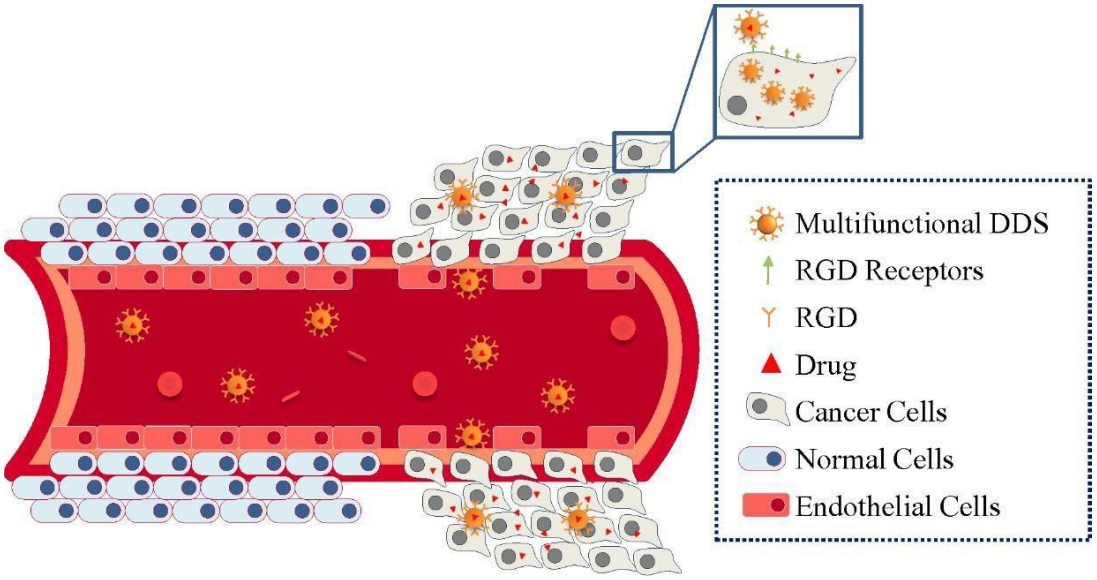

Figure 23: Representative internalization mechanism of nanoparticles: active targeting strategy.[64]

1.6 References

1. Tyler, B., Gullotti, D., Mangraviti, A., Utsuki, T., Brem, H. Polylactic acid (PLA) controlled delivery carriers for biomedical applications. *Adv. Drug Deliv. Rev.* 107, 163–175 (2016).
2. Tibbitt, M. W., Dahlman, J. E., Langer, R. Emerging Frontiers in Drug Delivery. *J. Am. Chem. Soc.* 138, 704–717 (2016).
3. Murariu, M., Dubois, P. PLA composites: From production to properties. *Adv. Drug Deliv. Rev.* 107, 17–46 (2016).
4. Annesini M. C., Frattari S., Gironi F., Piemonte V., Rocchina S., V. C. Degradation of Post-consumer PLA: Hydrolysis of Polymeric Matrix and Oligomers Stabilization in Aqueous Phase. *J. Polym. Environ.* 26, 4396–4404 (2018).
5. Elsawy, M. A., Kim, K.-H., Park, J.-W., Deep, A. Hydrolytic degradation of polylactic acid (PLA) and its composites. *Renew. Sustain. Energy Rev.* 79, 1346–1352 (2017).
6. Kamaly, N., Yameen, B., Wu, J., Farokhzad, O. C. Degradable Controlled-Release Polymers and Polymeric Nanoparticles: Mechanisms of Controlling Drug Release. *Chem. Rev.* 116, 2602–2663 (2016).
7. Zhu, X., Braatz, R. D. A mechanistic model for drug release in PLGA biodegradable stent coatings coupled with polymer degradation and erosion. *J. Biomed. Mater. Res. Part A* 103, 2269–2279 (2015).
8. Ferguson B.S., Rogatzki M. J., Goodwin M. L., Kane D. A., Rightmire Z., G. L. B. Lactate metabolism: historical context, prior misinterpretations, and current understanding. *Eur. J. Appl. Physiol.* 118, 691–728 (2018).
9. Stauffer, S., Gardner, A., Ungu, D. A. K., López-Córdoba, A., Heim, M. Cellular Respiration BT - Labster Virtual Lab Experiments: Basic Biology. in (eds. Stauffer, S., Gardner, A., Ungu, D. A. K., López-Córdoba, A., Heim, M.) 43–55 (Springer Berlin Heidelberg, 2018).
10. Vroman, I., Tighzert, L. Biodegradable polymers. *Materials* 2, 307–344 (2009).
11. Tsuge, Y., Kato, N., Yamamoto, S., Suda, M., Jojima, T., Inui, M. Metabolic engineering of Corynebacterium glutamicum for hyperproduction of polymer-grade l- and d-lactic acid. *Appl. Microbiol. Biotechnol.* 103, 3381–3391 (2019).
12. Wischral, D., Arias, J. M., Modesto, L. F., de França Passos, D., Pereira Jr, N. Lactic acid production from sugarcane bagasse hydrolysates by Lactobacillus pentosus: Integrating xylose and glucose fermentation. *Biotechnol. Prog.* 35, e2718 (2019).
13. Cubas-Cano, E., González-Fernández, C., Ballesteros, M., Tomás-Pejó, E. Biotechnological advances in lactic acid production by lactic acid bacteria: lignocellulose as novel substrate. *Biofuels, Bioprod. Biorefining* 12, 290–303 (2018).

14. de la Torre, I., Acedos, M. G., Ladero, M., Santos, V. E. On the use of resting L. delbrueckii spp. delbrueckii cells for D-lactic acid production from orange peel wastes hydrolysates. *Biochem. Eng. J.* 145, 162–169 (2019).
15. Okano, K., Uematsu, G., Hama, S., Tanaka, T., Noda, H., Kondo, A., Honda, K. Metabolic Engineering of Lactobacillus plantarum for Direct l-Lactic Acid Production From Raw Corn Starch. *Biotechnol. J.* 13, 1700517 (2018).
16. Komesu, A., Oliveira, J., Martins, L., Regina Wolf Maciel, M., Filho, R. *Lactic Acid Production to Purification: A Review*. *BioResources* 12, (2017).
17. Eş, I., Mousavi, K. A., Barba, F. J., Saraiva, J. A., Sant'Ana, A. S., Hashemi, S. M. B. Recent advancements in lactic acid production - a review. *Food Res. Int.* 107, 763–770 (2018).
18. Mayo, B., Aleksandrzak-Piekarczyk, T., Fernández, M., Kowalczyk, M., Álvarez-Martín, P., Bardowski, J. Updates in the Metabolism of Lactic Acid Bacteria, in: Biotechnology ofLactic Acid Bacteria, Mozzi, F., Raya, R. R., Vignolo, G. M., Eds., Blackwell publishing, Ames, USA, 2010, 1, 3-33.
19. Gao, C., Ma, C., Xu, P. Biotechnological routes based on lactic acid production from biomass. *Biotechnol. Adv.* 29, 930–939 (2011).
20. Castillo Martinez, F. A., Balciunasa, E. M., Salgadob, J. M., Domínguez González J. M., Converti, A., de Souza Oliveira, P. R., Lactic acid properties, applications and production: A review. *Trends Food Sci. Technol.* 30, 70–83 (2013).
21. Auras, R., Harte, B., Selke, S. An Overview of Polylactides as Packaging Materials. *Macromol. Biosci.* 4, 835–864 (2004).
22. Van Wouwe, P., Dusselier, M., Vanleeuw, E., Sels, B. Lactide Synthesis and Chirality Control for Polylactic acid Production. *ChemSusChem* 9, 907–921 (2016).
23. Jiang, X., Luo, Y., Tian, X., Huang, D., Reddy, N., Yang, Y. Chemical Structure of Poly(Lactic Acid), in: Poly(Lactic Acid): Synthesis, Structures, Properties, Processing, and Applications, Auras, R., Lim, L.-T., Selke, S. E. M., Tsuji, H., Eds., Wiley Publications, Hoboken, USA, 2010, 6, 67-82.
24. Lopes, M. S., Jardini, A. L., Filho, R. M. Poly (Lactic Acid) Production for Tissue Engineering Applications. *Procedia Eng.* 42, 1402–1413 (2012).
25. Hu, Y., Daoud, A. W., Cheuk, K. K., Lin, S. C. Newly Developed Techniques on Polycondensation, Ring-Opening Polymerization and Polymer Modification: Focus on Poly(Lactic Acid). *Materials* 9, (2016).
26. Ajioka, M., Enomoto, K., Suzuki, K., Yamaguchi, A. Basic Properties of Polylactic Acid Produced by the Direct Condensation Polymerization of Lactic Acid. *Bull. Chem. Soc. Jpn.* 68,

2125–2131 (1995).

27. Vink, E. T. H., Rábago, K. R., Glassner, D. A., Gruber, P. R. Applications of life cycle assessment to NatureWorks™ polylactide (PLA) production. *Polym. Degrad. Stab.* 80, 403–419 (2003).

28. Avérous, L., Polylactic Acid: Synthesis, Properties and Applications. in: Monomers, Polymers and Composites from Renewable Resources, Belgacem, M. N., Gandini, A., Oxford, UK, Elsevier, 2008, 21, 433–450.

29. Takenaka, M., Kimura, Y., Ohara, H. Molecular weight increase driven by evolution of crystal structure in the process of solid-state polycondensation of poly(l-lactic acid), *Polymer (Guildf).* 126, 133–140 (2017).

30. Josse, T., De Winter, J., Gerbaux, P., Coulembier, O. Cyclic Polymers by Ring-Closure Strategies. *Angew. Chemie Int. Ed.* 55, 13944–13958 (2016).

31. Carothers, W. H., Dorough, G. L., Natta, F. J. van. Studies of polymerization and ring formation. The reversible polymerization of six-membered cyclic esters. *J. Am. Chem. Soc.* 54, 761–772 (1932).

32. Lowe, C. E. No Title. U.S. Patent, 2, 668, 162 (1954).

33. Kricheldorf, H. R., Kreiser-Saunders, I. Polylactones, 19. Anionic polymerization ofL-lactide in solution. *Die Makromol. Chemie* 191, 1057–1066 (1990).

34. J. Dahlman, G. Rafler, K. Fechner, and B. M. British Polymer Journal. *Br. Polym. J.* 23, 235–240 (1990).

35. Kricheldorf, H., Kreiser-Saunders, I., Boettcher, C. Polylactones: 31. Sn(II)octoate-initiated polymerization of L-lactide: A mechanistic study. *Polymer* 36, (1995).

36. Kowalski, A., Duda, A., Penczek, S. Kinetics and mechanism of cyclic esters polymerization initiated with tin(II) octoate, 1. Polymerization of ε-caprolactone. *Macromol. Rapid Commun.* 19, 567–572 (1998).

37. Dove, A. P. Organic Catalysis for Ring-Opening Polymerization. *ACS Macro Lett.* 1, 1409–1412 (2012).

38. Dubey, S. P., Abhyankar, H. A., Marchante, V., Brighton, J. L., Bergmann, B., Trinh, G., David, C. Microwave energy assisted synthesis of poly lactic acid via continuous reactive extrusion: modelling of reaction kinetics. *RSC Adv.* 7, 18529–18538 (2017).

39. Ghasemi, R., Abdollahi, M., Emamgholi Zadeh, E., Khodabakhshi, K., Badeli, A., Bagheri,

H., Hosseinkhani, S. mPEG-PLA and PLA-PEG-PLA nanoparticles as new carriers for delivery of recombinant human Growth Hormone (rhGH). *Sci. Rep.* 8, 9854 (2018).

40. Feng, H., Lu, X., Wang, W., Kang, N.-G., Mays, W. J. Block Copolymers: Synthesis, Self-Assembly, and Applications. *Polymers* 9, (2017).

41. Feng, C., Li, Y., Yang, D., Hu, J., Zhang, X., Huang, X. Well-defined graft copolymers: from controlled synthesis to multipurpose applications. *Chem. Soc. Rev.* 40, 1282–1295 (2011).

42. Williams, R. J., Dove, A. P., O'Reilly, R. K. Self-assembly of cyclic polymers. *Polym.Chem.* 6, 2998–3008 (2015).

43. Hadjichristidis, N., Ratkanthwar, K., Pitsikalis, M., Iatrou, H. Synthesis of Star Polymers, in: Encyclopedia of Polymeric Nanomaterials, Kobayashi, S., Müllen, K., Eds., Springer Berlin Heidelberg, Berlin, Germany, 2015, Vol. 3, 2459–2484.

44. Ren, J. M., McKenzie, T. G., Fu, Q., Wong, E. H. H., Xu, J., An, Z., Shanmugam, S., Davis, T. P., Boyer, C., Qiao, G. G. Star Polymers. *Chem. Rev.* 116, 6743–6836 (2016).

45. Gentile, P., Chiono, V., Carmagnola, I., Hatton, V. P. An Overview of Poly(lactic-co-glycolic) Acid (PLGA)-Based Biomaterials for Bone Tissue Engineering. *Int. J. Mol. Sci.* 15, (2014).

46. Anderson, J. M., Shive, M. S. Biodegradation and biocompatibility of PLA and PLGA microspheres. *Adv. Drug Deliv. Rev.* 28, 5–24 (1997).

47. Deng, C., Xu, X., Tashi, D., Wu, Y., Su, B., Zhang, Q. Co-administration of biocompatible self-assembled polylactic acid–hyaluronic acid block copolymer nanoparticles with tumor-penetrating peptide-iRGD for metastatic breast cancer therapy. *J. Mater. Chem. B* 6, 3163–3180 (2018).

48. D'souza, A. A., Shegokar, R. Polyethylene glycol (PEG): a versatile polymer for pharmaceutical applications. *Expert Opin. Drug Deliv.* 13, 1257–1275 (2016).

49. Hutanu, D. Recent Applications of Polyethylene Glycols (PEGs) and PEG Derivatives. *Modern Chemistry & Applications* 02, (2014).

50. D'souza, A. A., Shegokar, R. Polyethylene glycol (PEG): a versatile polymer for pharmaceutical applications. *Expert Opin. Drug Deliv.* 13, 1257–1275 (2016).

51. Knop, K., Hoogenboom, R., Fischer, D., Schubert, U. S. Poly(ethylene glycol) in Drug Delivery: Pros and Cons as Well as Potential Alternatives. *Angew. Chemie Int. Ed.* 49, 6288–6308 (2010).

52. Garofalo, C., Capuano, G., Sottile, R., Tallerico, R., Adami, R., Reverchon, E., Carbone, E., Izzo, L., Pappalardo, D. Different Insight into Amphiphilic PEG-PLA Copolymers: Influence of Macromolecular Architecture on the Micelle Formation and Cellular Uptake. *Biomacromol.* 15, 403–415 (2014).

53. Pasut, G., Veronese, F. M. Polymer-drug conjugation, recent achievements and general strategies. *Prog. Polym. Sci. 32, 933-961*. *Progress in Polymer Science* 32, (2007).
54. Wang, J., Li, S., Han, Y., Guan, J., Chung, S., Wang, C., Li, D. Poly(Ethylene Glycol)–Polylactide Micelles for Cancer Therapy. *Frontiers in Pharmacology* 9, 202 (2018).
55. Luo, C.; Wang, Y.; Chen, Q.; Han, X.; Liu, X.; Sun, J.; He, Z. Advances of Paclitaxel Formulations Based on Nanosystem Delivery Technology. *Mini Rev. Med. Chem.* 12, 434–444 (2012).
56. Lee, S. W., Kim, Y. M., Cho, C. H., Kim, Y. T., Kim, S. M., Hur, S. Y., Kim, J. H., Kim, B. G., Kim, S. C., Ryu, H. S., Kang, S. B. An Open-Label, Randomized, Parallel, Phase II Trial to Evaluate the Efficacy and Safety of a Cremophor-Free Polymeric Micelle Formulation of Paclitaxel as First-Line Treatment for Ovarian Cancer: A Korean Gynecologic Oncology Group Study (KGOG-3021). *Cancer Res. Treat.* 50, 195–203 (2018).
57. Asem, H., Malmström, E. Polymeric Nanoparticles Explored for Drug-Delivery Applications. in *Gels and Other Soft Amorphous Solids* 1296, 16–315 (American Chemical Society, 2018).
58. Sen, R., Jyoti Das, P., Pachuau, L., Mazumder, B. Potential of Nanostructures for Drug Delivery: With a Special Reference to Polymeric Nanoparticles, in: 'Nanotechnology: Therapeutic, Nutraceutical, and Cosmetic Advances', Mazumder, B., Ray, S., Pal, P., Pathak, Y., Eds., CRC Press, Boca Raton, USA, 2019, 1, 1-24.
59. Matsumura, Y., Maeda, H. A New Concept for Macromolecular Therapeutics in Cancer Chemotherapy: Mechanism of Tumoritropic Accumulation of Proteins and the Antitumor Agent Smancs. *Cancer Res.* 46, 6387 LP – 6392 (1986).
60. Bazak, R., Houri, M., Achy, S. El, Hussein, W., Refaat, T. Passive targeting of nanoparticles to cancer: A comprehensive review of the literature. *Mol. Clin. Oncol.* 2, 904–908 (2014).
61. Brown, J. M., Giaccia, A. J. The Unique Physiology of Solid Tumors: Opportunities (and Problems) for Cancer Therapy. *Cancer Res.* 58, 1408 LP – 1416 (1998).
62. Golombek, S. K., May, J. N., Theek, B., Appold, L., Drude, N., Kiessling, F., Lammers, T. Tumor targeting via EPR: Strategies to enhance patient responses. *Adv. Drug Deliv. Rev.* 130, 17–38 (2018).
63. Bazak, R., Houri, M., El Achy, S., Kamel, S., Refaat, T. Cancer active targeting by nanoparticles: a comprehensive review of literature. *J. Cancer Res. Clin. Oncol.* 141, 769–784 (2015).
64. Muhamad, N., Plengsuriyakarn, T., Na-Bangchang, K. Application of active targeting nanoparticle delivery system for chemotherapeutic drugs and traditional/herbal medicines in cancer therapy: a systematic review. *Int. J. Nanomed.* 13, 3921–3935 (2018).

CHAPTER 2

Chapter 2

2.1 Alkyne-functionalized PLA

End-functionalization (*"end-capping")* is a feasible way to introduce into PLA backbone a variety of functional groups that can be conjugated with hydrophilic polymers (i.e. polyethylene glycol, polysaccharides, polipeptides…), targeting agents, fluorescent probes, etc…

The recent developments of click chemistry and its combination with controlled polymerization techniques have provided powerful tools in polymer chemistry.[1] Among the *click* chemistry reactions, the copper(I)-catalyzed azide-alkyne 1,3-dipolar cycloaddition (CuAAC) is widely used for the synthesis of functional polymeric architectures[2,3] due to the mild reaction conditions, high yield, simple work-up and good tolerance to a variety of functional groups. In fact, the selectivity of this approach allows to perform coupling reactions in the presence of various functional groups without cross-linking, branching or other side reactions.

Moreover, the application of *click* chemistry to aliphatic polyesters is a valid way to overcome the sensitivity of the polyester backbone to the conditions required for many conventional organic reactions.[1,4]

The functionalization of PLA via *click* chemistry is a powerful synthetic tool for the generation of novel biodegradable PLA derivatives with favorable physical properties, i.e. amphiphilicity,[5] or with stimuli-responsive or fluorescence properties.[5,6] Moreover, click chemistry can be exploited for the preparation of polymer-drug conjugates, in which the drug is covalently bounded to the polymer scaffold through linkages that may be cleaved *in vivo*, under desirable circumstances, for drug release.

The drug conjugation strategy is a good alternative to the physical incorporation of the biomolecule into the polymeric nanovector.[7]

Generally, the *click* post-modification of PLA is realized starting from a *clickable* alkyne-functionalized PLA. To date, the introduction of alkyne groups in the PLA backbone has been achieved by two main ways: (i) (organo)catalyzed ROP of native lactide with propargyl alcohol[8] or, more generally, with ethynyl-functionalized initiators;[8] alternatively, ROP of acetylene functionalized lactide,[2] (ii) esterification of hydroxyl end-groups of PLA with pentynoic acid catalyzed by 4-dimethylaminopyridine.[9] Moreover, recently, an intra-chain transesterification with propargyl alcohol catalyzed by dibutyltindilaurate (DBTDL) has been reported by Volet and coworkers, for the introduction of alkynyl moieties in the PLA backbone.[10,11] The transesterification was carried out with a large excess of alkyne donor (0.25 equivalents of propargyl alcohol for

monomeric unit of PLA) yielding an impressive cleaving of the high molecular weight PLA chain (from Mn=8.72×10^4 g mol^{-1} to 1.6×10^3 g mol^{-1}), depending on reaction time and catalyst concentration. A series of alkynyl-terminated PLA with various molecular weights was obtained to be used for the preparation of amphiphilic graft copolymers.[10,11]

2.2 *"Clickable"* PLA by intra-chain solvent-free amidation

We have recently proposed an innovative solvent- and catalyst-free method for the grafting of alkyne end-groups in the PLA backbone.[5] Propargylamine has been selected as alkyne donor, due to its ability to react in solvent-free reactions[12,13] and its high reactivity towards intra-chain ester groups of PLA.

The reaction (**Scheme 1**) was performed at 75 °C, under vacuum, into a Kugelrohr apparatus in the presence of phosphorus pentoxide (P_2O_5) as dehydrating agent. First, the mixing of PLA (**1**) and propargylamine (**2**) in dichloromethane, followed by solvent evaporation under argon flow, allowed the formation of an amorphous organic film that guaranteed the homogeneity of the reaction mixture and the reactivity of propargylamine under vacuum/heating/solvent-free conditions.

According to general solvent-free procedures, an initial excess of propargylamine must be guaranteed: it will be partially "stripped-off" (b.p. 83 °C) and lost under vacuum during the reaction, avoiding tedious workup to eventually remove unreacted traces.

Two different polymeric populations (**PLA-Prg 3a+3b**) were obtained by the intra-chain amidation, as the hydroxyl groups previously engaged into the intrachain ester linkages were released as soon as the propargylamide groups were formed (**Scheme 1**). In particular, the polymeric population **3a** resulted from the intrachain amidation, whereas *3b* is the "formal" leaving group of the reaction.

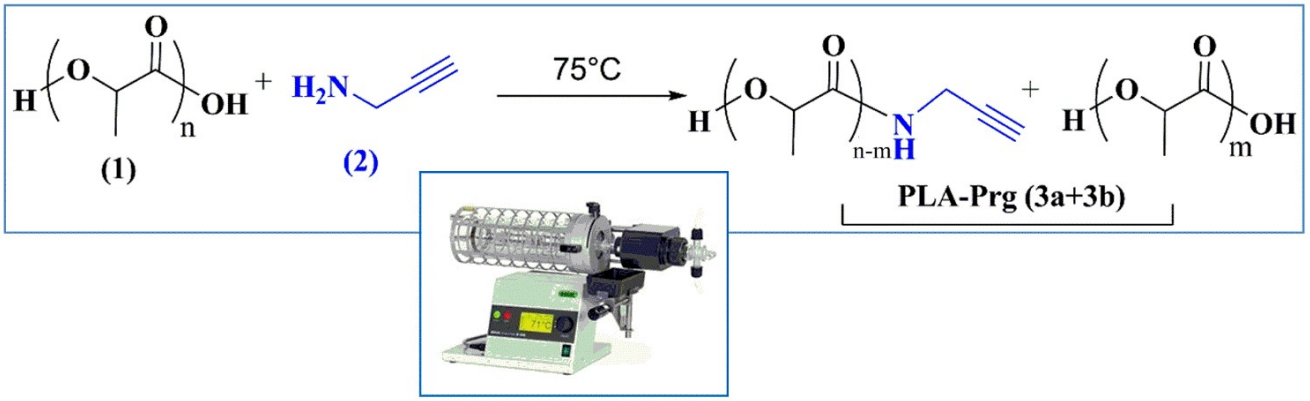

Scheme 1. Solvent-free intra-chain amidation reaction between PLA and propargylamine

The reaction was monitored by ^{1}H NMR spectroscopy (**Figure 1**). At the time t=0, the characteristic signals of PLA monomeric units at δ 5.2 and 1.5 ppm (CH and CH_3, respectively), together with the signals of propargylamine at δ 3.5 (CH_2) and 2.3 ppm (≡CH), can be clearly observed (Fig. 1, blue trace). The ^{1}H NMR spectra of the crude reaction mixture was recorded after 8 h and 16 h (Fig. 1, green and red traces, respectively), showing a novel signal at δ 4.1 ppm due to the CH_2 protons of the new propargylamide moiety downfield shifted from 3.5 ppm. Moreover, as the intra-chain amidation generated free hydroxyl groups, the peak at δ 4.3 ppm relative to the CH protons of the hydroxyl end-groups of both populations, became evident, together with amidic NH signals at δ 6.4, 6.5, 6.6 ppm. The new signals grew up to 16 h, whereupon the reaction was left under vacuum for an additional hour to remove unreacted traces of propargylamine.

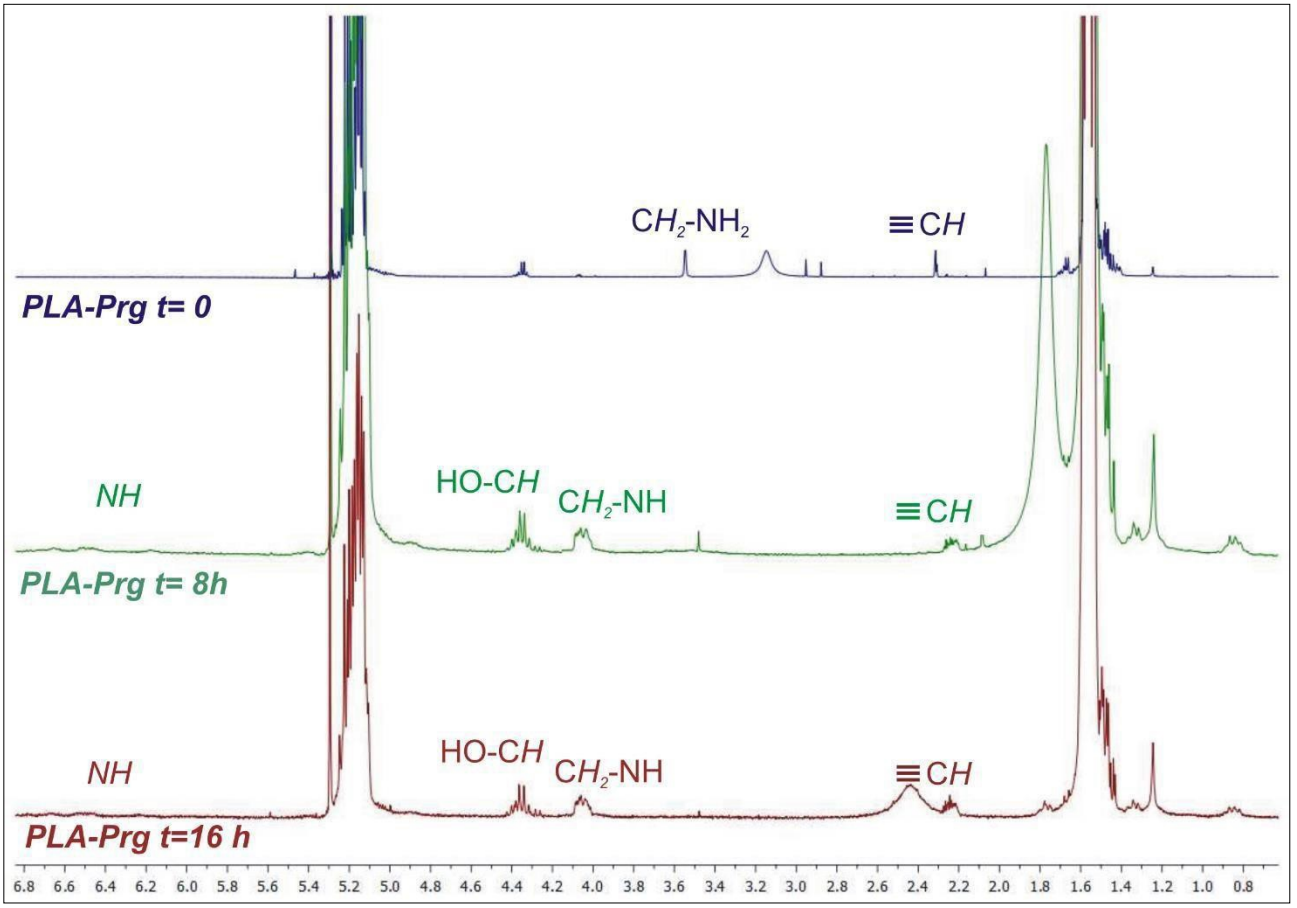

Figure 1. Monitoring of the progress of PLA functionalization with propargylamine, by ^{1}H NMR spectroscopy. All the spectra were recorded in $CDCl_3$ at r.t.

MALDI-TOF MS analyses confirmed the successful insertion of propargylamide moiety in the PLA backbone (**Figure 2**): two series of peaks (revealed as MNa^{+}) were mainly detected in the

spectrum of **PLA-Prg** at m/z 1087+n72, "*", and at m/z 1121+n72, "#", corresponding to **3a** and **3b** populations, respectively.

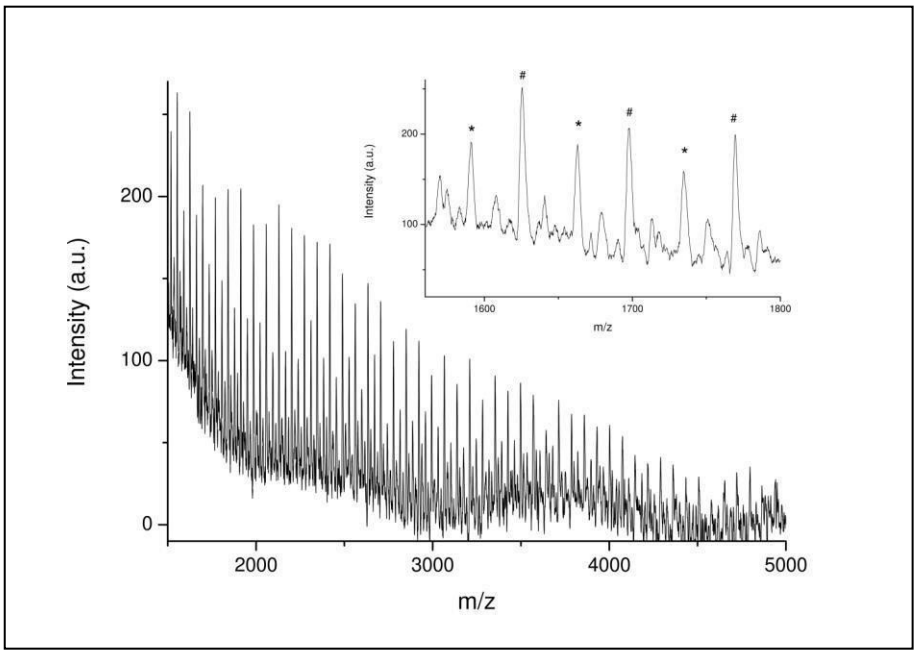

Figure 2. MALDI TOF mass spectrum of PLA-Prg

The synthetic procedure was tested at two different PLA/propargylamine molar ratio (1:10; 1:20) and the efficiency was determined in terms of functionalization degree and molecular weights. The average molecular weights of **PLA-Prg** were determined by GPC-MALS on the crude solvent-free reaction mixture. With respect to the commercial PLA (Mw 13960, Mn 10470), lower molecular weights were expected for **PLA-Prg**, as a consequence of the intra-chain amidation. In fact, the molecular weight values were slightly decreased for the 1:10 ratio (Mw 8460, Mn 5600) and almost halved for the 1:20 ratio (Mw 6210, Mn 4990) (**Figure 3**).

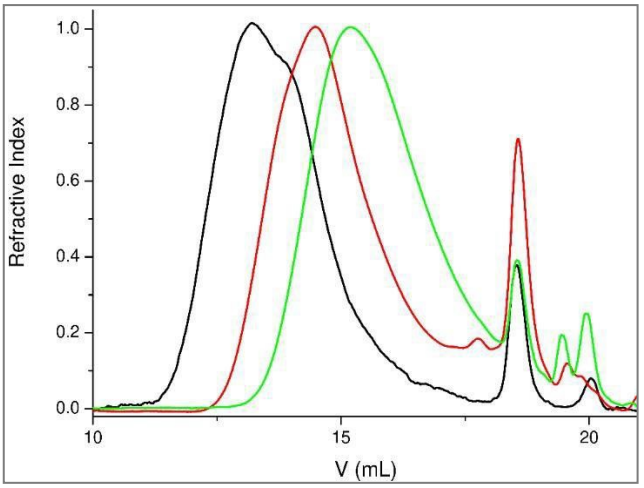

Figure 3. GPC traces of PLA (black), PLA-Prg 1:10 (red), PLA-Prg 1:20 (green)

Comparing the results of our solvent-free amidation with the transesterification proposed by Volet and coworkers,[10,11] our strategy showed several advantages such as one-step reaction, mild conditions, absence of catalyst, solvent, and tedious workup. Moreover, a restrained cleaving of PLA chain was observed, since only ≈2 ester bonds have been broken under our experimental conditions, as determined by ^{1}H NMR spectroscopy which allowed to calculate a functionalization of PLA in terms of grafted alkynes of 0.9 w/w% (0.016 mmol/100 mg) and 1.1% w/w (0.020 mmol/100 mg), using 1:10 and 1:20 ratio, respectively, corresponding to ≈2 broken ester bonds.

2.3 Esterification of PLA hydroxyl groups with pentynoic anhydride

Furthermore, the free hydroxyl end-groups of both polymeric populations (**PLA-Prg 3a+3b**) obtained by solvent-free amidation have been further derivatized by esterification with pentynoic anhydride, with the aim to increase the alkyne functionalities on the polymer backbone.

Interestingly, the association of the two synthetic procedures (solvent-free amidation followed by esterification) allowed the derivatization of both carbonyl and hydroxyl groups of PLA, leading to an overall amount of alkynyl functionalities suitable for *click* chemistry exploitation.

The pent-4-ynoic anhydride (**4**) was prepared from the commercial pent-4-ynoic acid using EDC as dehydrating agent. The esterification of **PLA-Prg 3a+3b** was carried out in anhydrous dichloromethane in the presence of dry pyridine and dimethylaminopyridine (DMAP), leading to **PLA-Prg-Pent (5a+ 5b)** (**Scheme 2**).

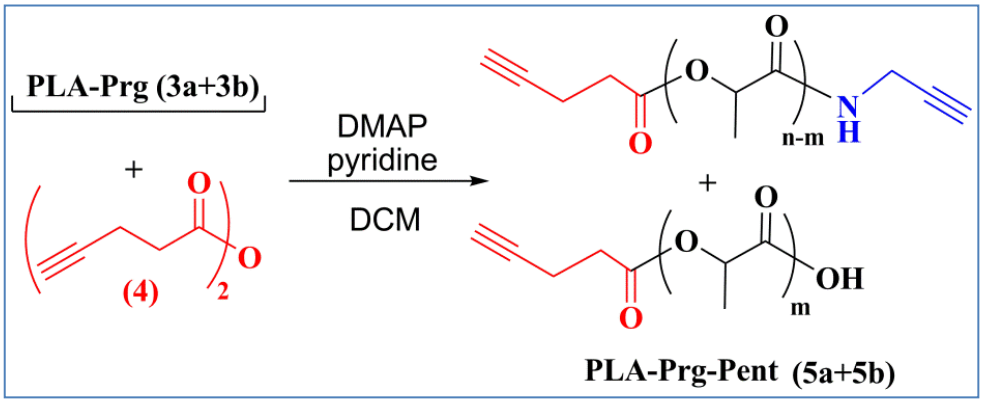

Scheme 2. Esterification of PLA hydroxyl groups with pentynoic anhydride

The ^{1}H NMR spectrum of **PLA-Prg-Pent** (**Figure 4**) showed a novel set of signals related to the pentynoic end-group protons ($CH_2CH_2C{\equiv}CH$) at δ 2.6, 2.5, 1.9 ppm, together with the disappearance of the peak at δ 4.3 ppm, confirming the quantitative esterification of the terminal hydroxyl groups of PLA.

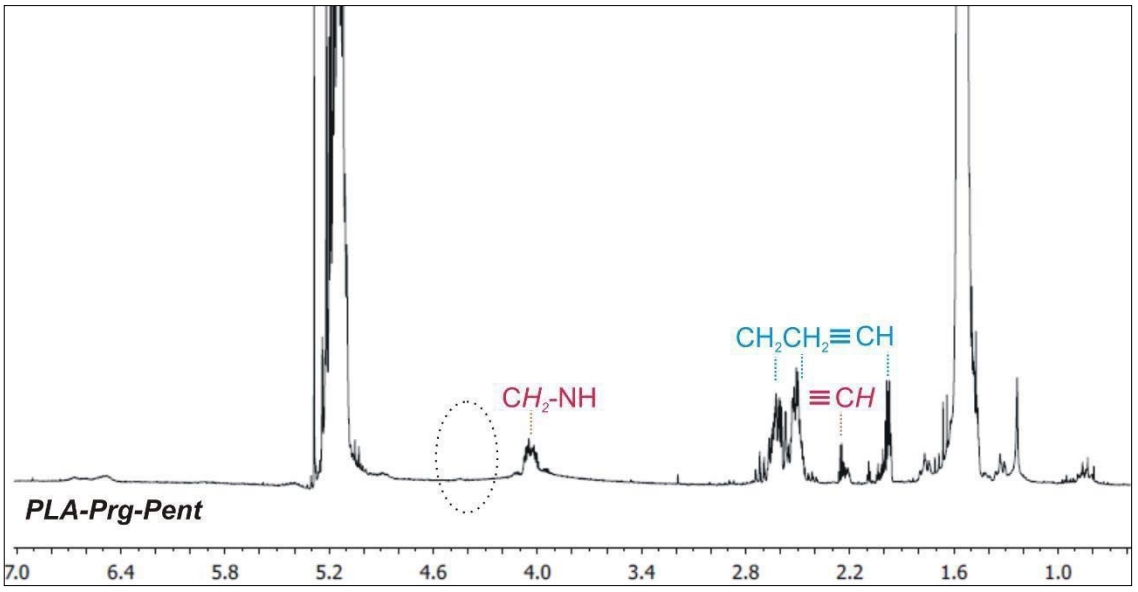

Figure 4. ^{1}H NMR spectrum of PLA-Prg-Pent recorded in $CDCl_3$ at r.t.

MALDI-TOF MS analysis further confirmed the complete transformation, as two series of peaks (revealed as MNa^+) were mainly detected at *m/z* 1022+n72, "*", and at *m/z* 985+n72, "#", corresponding to the expected species **5a** and **5b** (**Figure 5**).

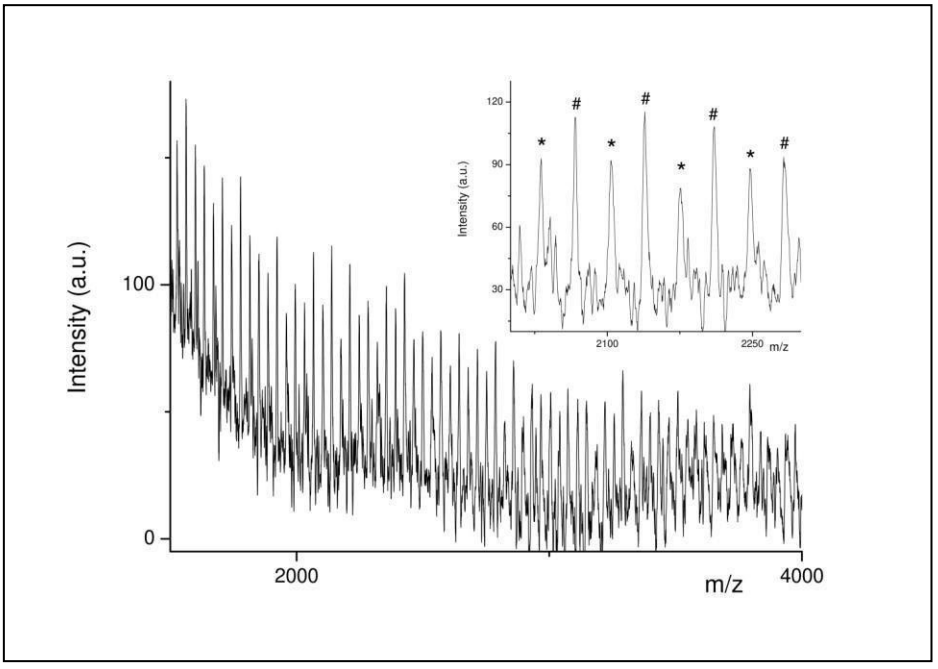

Figure 5. MALDI TOF mass spectrum of PLA-Prg-Pent.

GPC-MALS analysis showed Mw 8990, Mn 7340 and Mw 6680, Mn 5630 for **PLA-Prg- Pent** obtained from the 1:10 and 1:20 samples, respectively. A slight decrease of the PDI was observed for **PLA-Prg-Pent** respect to **PLA-Prg**, since the low-molecular weight oligomers were removed during workup by washing with water.

The weight average molecular weight (Mw), number average molecular weight (Mn), and polydispersity index (PDI) of the different PLA derivatives are summarized in Table 1.

Table 1

	Mw (g/mol)[a]	Mn (g/mol) [a]	PDI
Native PLA	13960	10470	1.33
PLA-Prg 1:10	8460	5600	1.51
PLA-Prg 1:20	6210	4990	1.24
PLA-Prg (1:10)-Pent	8990	7340	1.22
PLA-Prg (1:20)-Pent	6680	5630	1.18

[a]Calculated by GPC.

The overall amount of alkynyl functionalities, calculated by ^{1}H NMR spectroscopy, resulted 5.0 w/w % for PLA-Prg (1:10)-Pent and 6.4 w/w % for PLA-Prg (1:20)-Pent.

On the basis of the molecular weight values and the functionalization degree, we can state out that both 1:10 and 1:20 ratio have proved to be good conditions for the grafting of terminal alkyne groups in the PLA scaffold, with the 1:10 ratio giving the best compromise between an adequate functionalization and the control of the molecular weight.

2.4 *Click* coupling of alkyne-functionalized PLA

It's well known that *"clickable"* alkyne-grafted PLA are useful building blocks for the synthesis of a variety of functionalized polymers by Cu(I)-catalyzed cycloaddition reaction (CuAAC) with azide derivatives.[5,6]

In order to determine the feasibility of the CuAAC reaction and to test the *"clickable"* properties of **PLA-Prg-Pent (5a+5b)**, we selected methoxypolyethylene glycol azide (**mPEG-N$_3$**), azide-fluor 545 (**Flu-N$_3$**) and folate-azide (**FA-N$_3$**) as models of hydrophilic polymer, fluorescent probe, and targeting ligand, respectively.

The azide derivatives **mPEG-N$_3$** and **Flu-N$_3$** were commercially available, whereas **FA-N$_3$** was synthesized in our laboratories by amide coupling protocol (**Scheme 3**), according to a

previously reported procedure,[14] with slight modifications. To ensure the high affinity for the folate FR-α receptor, the γ-carboxyl moiety of folic acid was covalently linked to the free amine group of N-(2-(2-(2-aminoethoxy)ethoxy)ethyl)-4-(azidomethyl)benzamide.

The structure of **FA-N$_3$** was confirmed by NMR spectroscopy and MALDI-ToF analysis, that unambiguously confirmed the expected mass values exhibiting the value of the sodiated specie at m/z 753.62 Da (MNa^+) (Experimental).

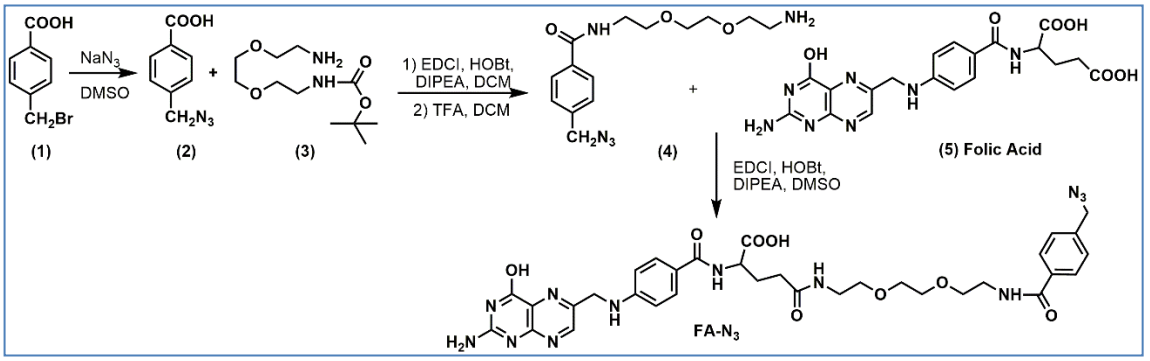

Scheme 3. Multi-step synthesis of FA-N$_3$

The *click* couplings of **PLA-Prg-Pent (5a+5b)** with **mPEG-N$_3$**, **Flu-N$_3$**, and **FA-N$_3$** (**Scheme 1)** were performed in mild conditions, at room temperature, under inert atmosphere, in anhydrous dimethylformamide (DMF) and in the presence of $CuSO_4$/sodium ascorbate as a source of Cu(I).

The reactions yielded the amphiphilic **PLA-PEG** copolymer, the fluorescence-labeled **PLA-Flu**, and the folate receptor-targeted **PLA-FA**, respectively. All the functionalized PLA derivatives were characterized by complementary techniques, such as ^{1}H NMR spectroscopy, GPC/SEC-MALS measurements.

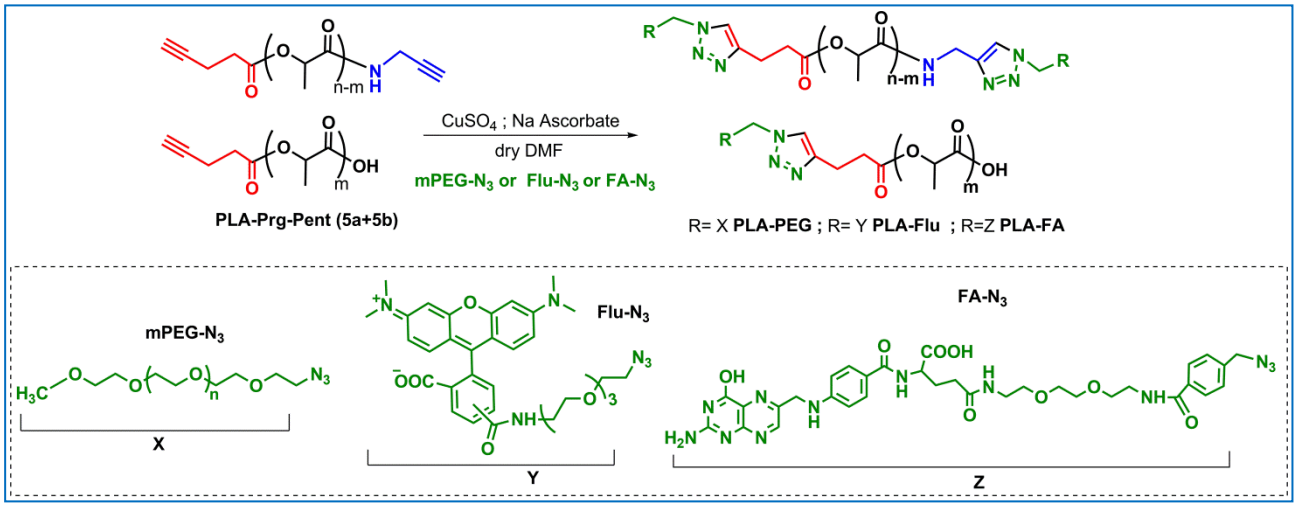

Scheme 4. CuAAC *click* coupling of PLA-Prg-Pent with mPEG-N$_3$, Flu-N$_3$ and FA-N$_3$

^{1}H NMR spectroscopy confirmed the formation of the expected triazole unit, with the typical H-5 proton signal in the aromatic region. According to literature data,[9] the two signals at δ 7.5 and 7.7 ppm can be attributed to the triazole rings originated by the pentynoic moieties, while the resonance at δ 8.0 ppm can be related to the triazole ring originated by the propargyl fragment.

The GPC analysis of **PLA-Flu** (**Figure 6**) was carried out by connecting in parallel a differential refractometer (DR) detector, revealing all the compounds eluted from the column, and a UV–visible spectrophotometer (UV) set at the λ_{max} of Flu-N_3 (545 nm), that revealed only the eluted compounds containing the fluorophore units. The analysis obtained by the two detectors (black and red lines, Figure 6) yielded superimposable traces that confirmed the successful synthesis of **PLA-Flu**.

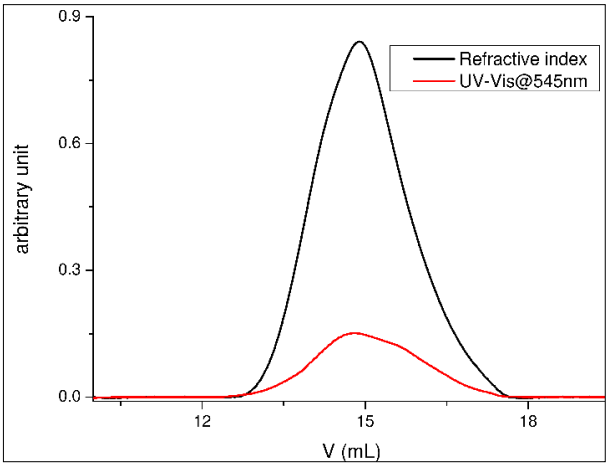

Figure 6. GPC traces of PLA-Flu obtained using two detectors connected in parallel (red line: UV–visible @545 nm detector; black line: differential refractometer detector)

2.5 Biological applications

All the three PLA derivatives (**PLA-PEG, PLA-Flu** and **PLA-FA**) are endowed with interesting properties and could be further exploited for biological applications.

Currently, our attention was focused on the preparation of PLA-Flu and PLA-FA nanoparticles (NPs) loaded with Salinomycin (Sal, **Figure 7**), to evaluate their biological activityon osteosarcoma cancer stem cells.

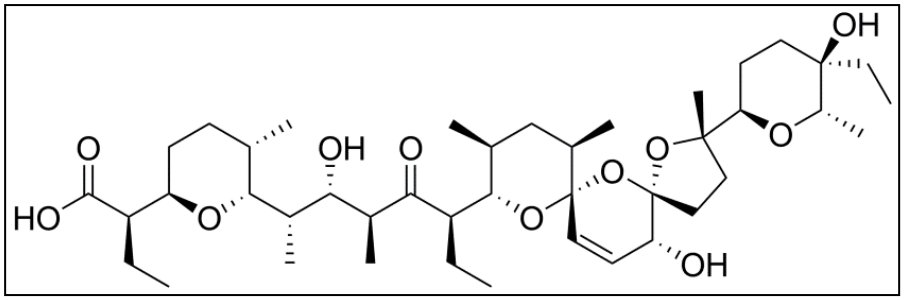

Figure 7. Chemical formula of Salinomycin

Osteosarcoma (OS) is the most common primary malignant tumor of bone, with an annual incidence worldwide of approximately 5.6 cases per million, typically diagnosed in children and young adults.[15] The current care combines surgery and intensive chemotherapy protocols based on the combination of cytotoxic drugs (e.g. doxorubicin, methotrexate, cisplatin, etc.).[16]

In this scenario, a special attention was recently paid to Sal, as an alternative to traditional anticancer drug due to its potent activity against OS cancer stem cells (CSCs). CSCs represent the primary tumor initiator cells, responsible for metastasis, recurrences and multi-drug resistance. They are more resistant than the normal cancer cells to conventional therapies[17], representing a novel target for cancer treatment.

Actually, Sal is widely used as ionophoric coccidiostat antibiotic in poultry and growth promoter in livestock. Its potentiality as a human drug candidate was discovered by Gupta in 2009 within a high-throughput screening over 16000 chemicals to select the ones targeting CSCs.[18] Within that screening, SAL resulted nearly 100-fold more effective towards the breast CSCs than paclitaxel (Taxol®), commonly used for breast cancer treatment.

However, the clinic application of Sal for cancer treatment is greatly hindered by the poor pharmacokinetics and systemic toxicity[19].

In this context, the development of novel drug delivery systems incorporating Sal could represent a promising strategy to overcome these drawbacks, increasing the solubility, the bioavailability, the selective accumulation into the target site, enhancing the therapeutic efficacy.

To date, only few papers reported Sal-loaded polymeric nanoparticles to treat drug-resistant cancer cells or CSCs.[20-22]

For the preparation of PLA-Flu nanoparticles loaded with Sal (**PLA-Flu/Sal NPs)**, the *nanoprecipitation* method was adopted. The *nanoprecipitation* is one of the most commonly used methods for the preparation of polymeric NPs, also known as *solvent displacement method*, developed by Fessi and coworkers.[23] Briefly, this technique requires two solvents that are miscible in each other. Typically, a solution of drug and polymer in organic solvent (i.e. acetone, methanol) was added dropwise to an aqueous solution under vigorous stirring; the suspension was stirred at room

temperature until the organic solvent evaporated. The NPs were recovered by centrifugation and lyophilization (**Figure 8**).

Acetone was used for **PLA-Flu/Sal NPs** preparation, whereas a modified nanoprecipitation method, using dimethylsulfoxide was adopted for **PLA-FA/Sal NPs**, due to the poor solubility of PLA-FA in acetone (see Experimental).

For comparison, unloaded NPs (blank NPs) were prepared by the same method, starting from an organic solution of polymer in acetone or DMSO, without drug. Also, empty PLA NPs and PLA/Sal NPs were prepared and used for antitumoral assays.

Preliminary DLS analysis evidenced an average size of 50-100 nm.

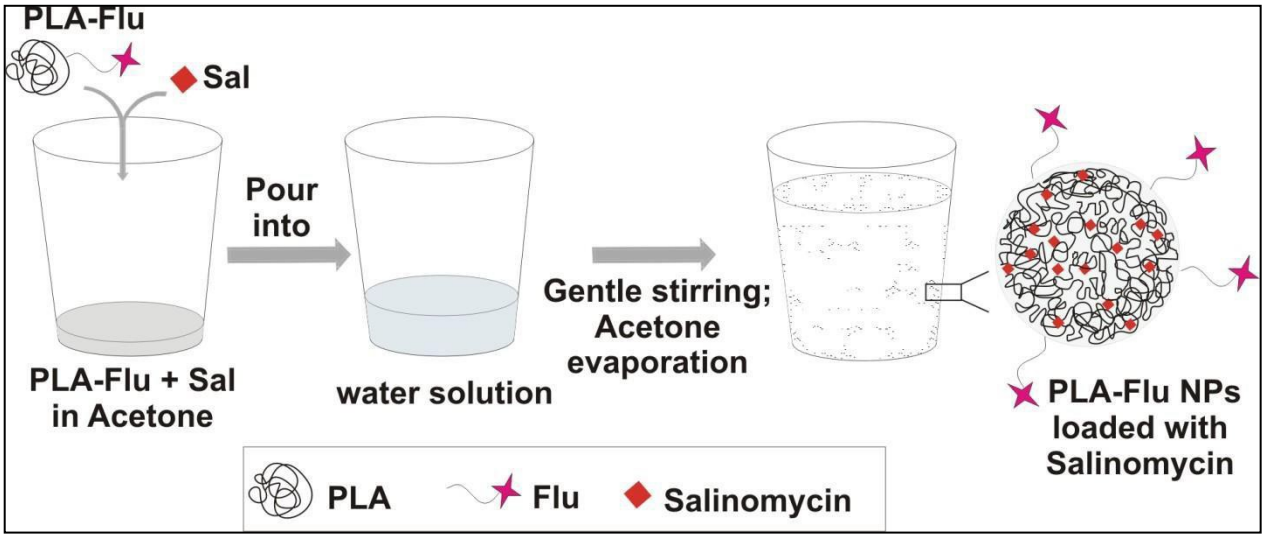

Figure 8. Schematic representation of PLA-Flu/Sal NPs preparation by nanoprecipitation

The biological investigation on the antitumoral effect of Sal loaded into the PLA-based NPs towards OS CSCs is currently in progress at ISTEC (Institute of Science and Technology for Ceramics) belonging to the CNR Department of Chemical Science and Materials Technology (Faenza (RA), Italy).

The presence of a fluorophore in **PLA-Flu NPs** will allow to investigate the cellular internalization, intracellular trafficking and accumulation into organelles of the polymeric NPs. The presence of an active targeting ligand (i.e. folate) on the surface of **PLA-FA NPs** could enable specific interactions between folate and specific receptor expressed on tumoral cells, enhancing NPs internalization by receptor-mediated endocytosis.

First, the cytotoxicity of the polymeric NPs will be assessed, without drug, on human mesenchymal stem cells (MSCs) through the evaluation of the induction of apoptosis, autophagy and production of reactive oxidative species. The cellular uptake, intracellular localization and degradation of

fluoroprobe-loaded NPs will be evaluated. The anticancer activity will be evaluated by investigating the ability of Sal-loaded NPs to suppressed the sphere-forming capacity and chemoresistance in OS CSCs without severe side effects on MSCs.

2.6 Experimental section

2.6.1 Materials and Methods

Poly(lactic acid) (Mw 7000-17000), propargylamine, *N*-(3-dimethylaminopropyl)-*N*′-ethylcarbodiimide hydrochloride (EDC), pent-4-ynoic acid, 4-dimethylaminopyridine (DMAP), anhydrous pyridine, methoxypolyethylene glycol azide (mPEG-N_3), azide-fluor 545 (Flu-N_3), anhydrous dimethylformamide (DMF) anhydrous dichloromethane (DCM), Salinomycin sodium salt and other solvents and reagents were purchased from Sigma-Aldrich.

^{1}H NMR spectra were recorded on a Varian 500 and 300 MHz spectrometer at room temperature (25 °C). MALDI-TOF mass spectra were collected by a Voyager DE (PerSeptive Biosystem) using a delay extraction procedure (25 kV applied after 2600 ns with a potential gradient of454 V mm^{-1} and a wire voltage of 25 V) and detecting the ions in linear mode. The instrument was equipped with a nitrogen laser (emission at 337 nm for 3 ns) and a flash AD converter (time base 2 ns). In order to avoid the polymer fragmentation, laser irradiance was maintained slightly above threshold. Each spectrum was an average of 32 laser shots. The analyses were performed by loading on the sample plate 0.1 mmol of sample and 40 mmol of *trans*-2-[3-(4-*tert*-butylphenyl)-2- methyl-2 propenylidene]-malononitrile (DCTB) as a matrix, using THF as a solvent. 5,10-di(p-dodecanoxyphenyl)-15,20-di(p-hydroxyphenyl) porphyrin (C68H78N4O4, 1014 Da), tetrakis(p-dodecanoxyphenyl)porphyrin (C92H126N4O4, 1350 Da) and a PEG sample of known molecular structure were used as external standards for *m*/*z* calibration. Molecular weight and molecular weight distribution were determined by a PL-GPC 110 (Polymer Laboratories) thermostated system, equipped with two mixed-D and one mixed-E PL-gel 5 μm columns joined in series. A differential refractometer (Polymer Laboratories) and a multi-angle laser light scattering detector DAWN HELEOS (Wyatt Technology Corporation), connected in parallel, were used as detectors. THF was used as the mobile phase (flow rate of 1 mL/min). Ultraviolet-visible spectrophotometry (UV‑Vis) Shimadzu 1601 was used to quantify the amount of conjugated azide-fluor 545, by dissolving 0.5 mg of PLA-Flu in 2 mL of water. On the basis of optical absorbance data and molar extinction coefficient (92000 cm^{-1}M^{-1}), the dye content was estimated using the following equation: dye content = (dye weight in the conjugate/weight of the conjugate) × 100. NPs sizes were determined by means of a miniDAWN Treos (Wyatt Technology) multi-angle light scattering detector, equipped with a Wyatt QELS DLS Module. The measurements were performed at 25°C using the ASTRA 6.0.1.10 software (Wyatt) to analyzing the data. The drug loading was determined by means of a PL-GPC 110 (Polymer Laboratories) thermostated system, equipped with three PL-gel 5 mm columns (two Mixed-D and

one Mixed-E) attached in series. The analyses were performed at 35 ± 0.1°C using THF as eluent at a flow rate of 1 mL/min. A differential refractometer (Polymer Laboratories) was used as detector.

2.6.2 Synthesis of PLA-Prg (3a+3b)

In a small glass vial, PLA (200 mg, 0.019 mmol; 3 mmol monomeric units) was dissolved into 2 mL of anhydrous DCM. Then propargylamine (molar ratio 1:10 and 1:20 PLA/Propargylamine) was added and the solution was sonicated for 5 min, till complete dissolution of reagents. Solvent was evaporated under argon flow to obtain a thin layer on vial wall. Finally, the vial was put in Kugelrohr apparatus at 75°C, under vacuum, in presence of P_2O_5. Samples were taken at regular times to monitor the reaction by ^{1}H NMR analysis. The new signals of the product PLA-Prg grew up to 16 h. The reaction was left an hour more under vacuum to remove excess of propargylamine. The final product was used without further purification in the next synthetic step. A blank experiment was carried out in the same experimental conditions without propargylamine, demonstrating no changes on polymer molecular weight.

^{1}H NMR (500 MHz, $CDCl_3$, δ): 6.6 (br s, NH), 6.5 (br s, NH), 6.4 (br s, NH), 5.2 (m, CH PLA), 4.3 (m, C*H*-OH), 4.1 (m, C*H2*N), 2.3 (m, C≡C*H*), 1.5 (m, CH_3 PLA).

2.6.3 Synthesis of PLA-Prg-Pent (5a+5b)

PLA-Prg (0.04 mmol) was dissolved in 3 mL of anhydrous DCM into a round bottom flask under inert atmosphere, followed by the addition of dry pyridine (0.2 mmol) and DMAP (0.2 mmol). Pent-4-ynoic anhydride (0.64 mmol) previously dissolved in 8 mL of anhydrous DCM was added and the solution was stirred overnight at room temperature. The crude reaction was extracted with distilled water, dried over Na_2SO_4 and evaporated under vacuum, leading to PLA-Prg-Pent as pale yellow oil.

^{1}H NMR (500 MHz, $CDCl_3$, δ): 6.6 (br s, NH), 6.5 (br s, NH), 6.4 (br s, NH), 5.2 (m, CH PLA), 4.1 (m, CH_2N_{prg}), 2.6 (m, CH_{2pent}), 2.5 (m, CH_{2pent}), 2.3 (m, C≡CH_{prg}), 1.9 (m, C≡CH_{pent}), 1.5 (m, CH_3 PLA).

2.6.4 Synthesis of FA-N_3

2.6.4.1 Synthesis of N-(2-(2-(2-aminoethoxy)ethoxy)ethyl)-4-(azidomethyl)benzamide (4)

A solution of 4-bromomethyl benzoic acid (**1**) (2.23 g, 13 mmol) and sodium azide (2.55 g, 39.2 mmol) in DMSO (10 mL) was stirred for 48h at 80 °C. After cooling to room temperature, 10 mL of deionized water and 20 mL of Et_2O were added. The organic phase was extracted with water and

dried over $MgSO_4$; the solvent was removed under reduced pressure to obtain the pure 4-azomethyl benzoic acid (**2**) (2.1 g, yield 95%). A solution of (**2**) (100 mg, 0.56 mmol) and EDCI (161 mg, 0.85 mmol) in anhydrous DCM (20 mL) was stirred at room temperature for 20 min, followed by the addition of tert-butyl 2-(2-(2-aminoethoxy)ethoxy)ethylcarbamate (**3**) (139 mg, 0.56 mmol), HOBt (114 mg, 0.85 mmol) and DIPEA (86 mg, 0.67 mmol). The reaction mixture was stirred for 24 h at room temperature. The organic phase was washed with citric acid 10%, saturated sodium bicarbonate solution, water and eventually dried over Na_2SO_4. The solvent was removed under vacuum to obtain the Boc-protected product (194 mg, yield 85%). For the Boc-deprotection, the product (194 mg, 0.48 mmol) was dissolved in DCM (10 mL) and TFA (1.18 g, 9.6 mmol,) was added dropwise. The mixture was stirred for 2 h. After addition of 2 mL of toluene, the solvent was removed under vacuum. The residue was dissolved in 4 mL of methanol, Amberlite resin was added and the mixture was stirred for 30 min. The solution was filtered, washed with methanol and the organic phase was concentrated under reduced pressure, to obtain (**4**) (167 mg, yield 88%). ^{1}H NMR (CD_3OD, 300 MHz): δ 3.08 (t, 2H, J=6 Hz), 3.59 (t, 2H, J=6 Hz), 3.63-3.70 (m, 8H), 7.44 (d, 2H, J=9 Hz), 7.86 (d, 2H, J=9 Hz). ^{13}C NMR (CD_3OD, 75 MHz): δ 39.6, 39.8, 54.0, 66.5, 69.7, 69.8, 70.0, 127.8, 128.0, 139.0, 156.5, 167.7.

2.6.4.2 Synthesis of FA-N_3

FA (**5**) (259 mg, 0.543 mmol) and EDCI (156 mg, 0.814 mmol) were solubilised in anhydrous DMF (15 mL) under sonication (5 min). To the stirring solution, HOBt (110 mg, 0.814 mmol) was added and the reaction mixture was stirred in the dark for 1 h. A solution of (**4**) (167 mg, 0.543 mmol) in 2.5 mL of anhydrous DMF, dry pyridine (4.5 mL) and DIPEA (84 mg, 0.651 mmol) were added and the reaction mixture was stirred in the dark for 24 h at room temperature. The solvent was removed under vacuum and the residue was washed several times with diethylether and acetone. The solid material was dried to give an orange powder (**FA-N_3**, 304 mg, 76 % yield) as inseparable mixture of γ-regioisomer and α-regioisomer. The ^{1}H NMR spectrum indicated an almost exclusive γ-conjugation of FA whereas the amount of the α-regioisomer was negligible (≈1%).

^{1}H NMR (DMSO-d_6, 300 MHz): δ 2.02-1.99 (m, 2H), 2.20-2.15 (m, 2H), 3.04-2.96 (m, 2H), 3.18-3.12 (m, 2H), 3.48-3.38 (m, 8H), 4.31-4.21 (m, 1H), 4.47-4.45 (m, 2H), 4.50 (s, 2H), 5.94 (bs, 1H), 6.60 (d, 2H, J= 9 Hz), 6.94 (bs, 1H), 7.42 (d, 2H, J= 9 Hz), 7.62 (d, 2H, J= 9 Hz), 7.85 (d, 2H, J= 9 Hz), 8.54 (bs, 1H), 8.63 (s, 1H), 11.41 (bs, 1H).

MALDI-TOF: (m/z 753.62 Da [detected as MNa^+] cld for $C_{33}H_{38}N_{12}O_8$ 730.29 Da

^{13}C NMR (DMSO-d_6, 300 MHz): δ 25.6, 30.58, 42.7, 53.5, 55.12, 69.06, 69.11, 69.2, 69.83, 113.58, 121.29, 127.98, 128.74, 129.45, 139.28, 148.93, 150.79, 153.96, 155.42, 155.82, 161.13, 167.10 167.51, 174.35, 191.66.

^{1}H NMR FA-N_3 (DMSO-d_6)

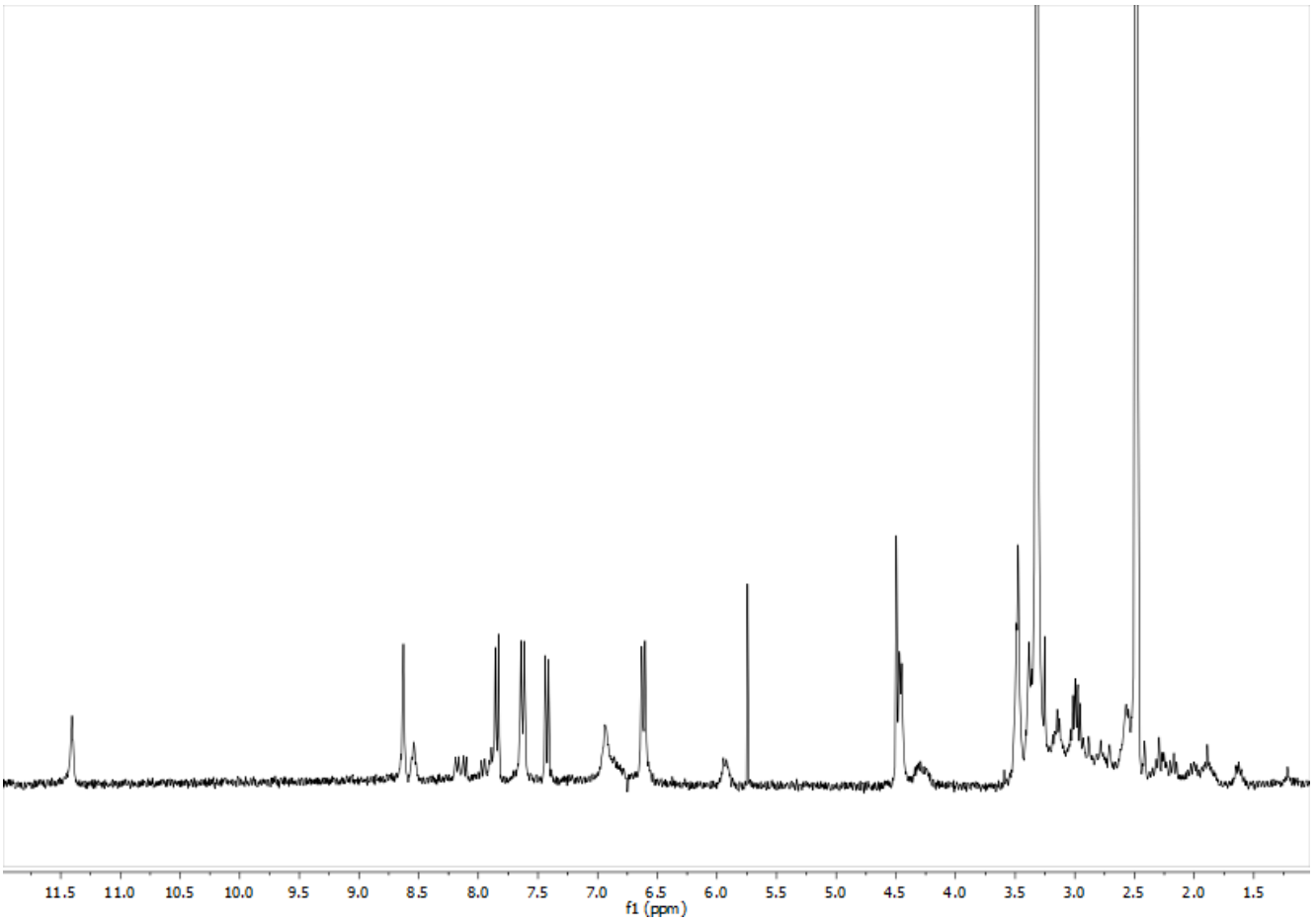

^{13}C NMR FA-N_3 (DMSO-d_6)

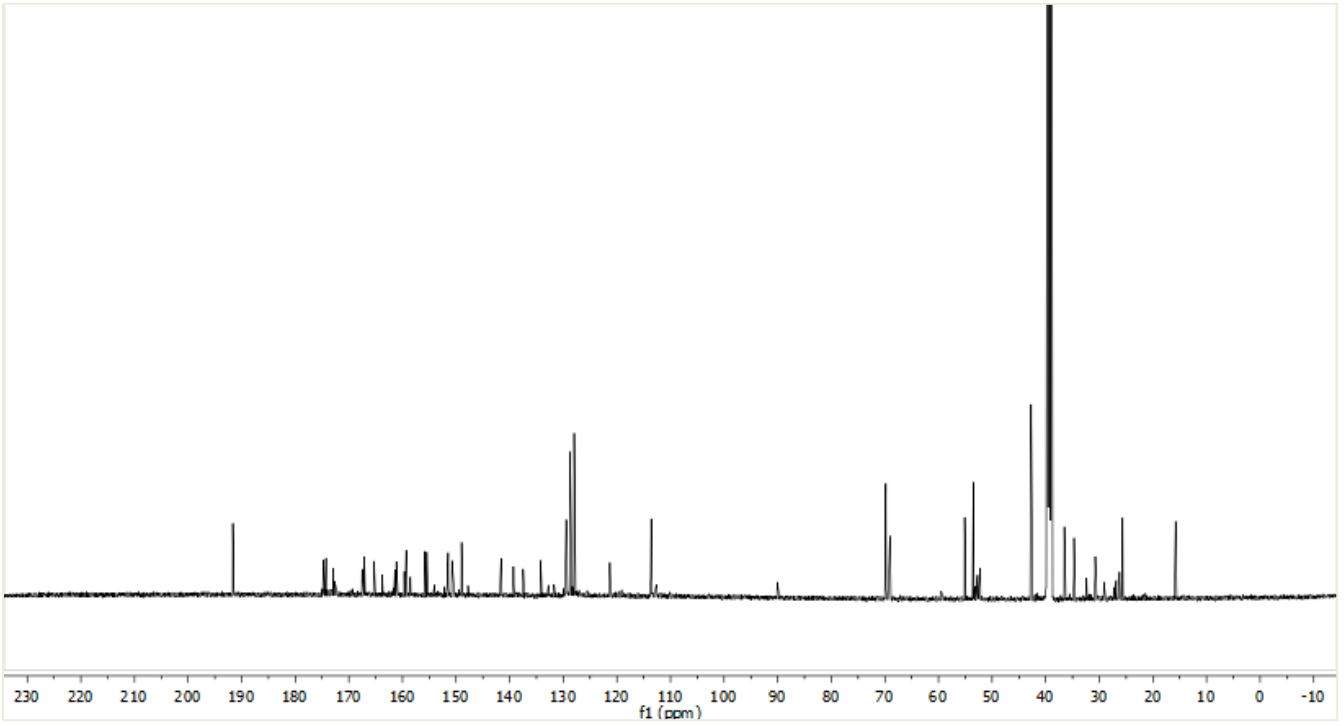

2.6.5 Synthesis of PLA-PEG copolymer

In a round bottom flask, under inert atmosphere, PLA-Prg-Pent (0.02 mmol), mPEG-N_3 (0.02 mmol), $CuSO_4$ (0.04 mmol) and sodium ascorbate (0.08 mmol) were dissolved in 3 mL of anhydrous DMF. The reaction mixture was stirred overnight at room temperature. Water was added to the crude reaction and a precipitate is formed. The suspension was centrifuged, the solid was washed two times with water and finally lyophilized to obtain PLA-PEG copolymer, as a white solid.

^{1}H NMR (500 MHz, $CDCl_3$, δ): 8.0 (s, H triazole), 7.7 (s, H triazole), 7.5 (s, H triazole), 6.6 (br s, NH), 6.5 (br s, NH), 6.4 (br s, NH), 5.2 (m, CH PLA), 4.4 (m, CH_2C]C triazole), 4.0 (m, CH_2NH unreacted alkyne moiety), 3.8–3.6 (s, CH_2CH_2O), 3.3 (s, CH_3O), 3.0 (m, CH_2N triazole), 2.6 (m, CH_{2pent}), 2.5 (m, CH_{2pent} unreacted alkyne moiety), 2.2 (m, C≡CH_{prg} unreacted alkyne moiety), 1.9 (m, C≡CH_{pent} unreacted alkyne moiety), 1.5 (m, CH_3 PLA). From NMR analysis, a content of ≈4 w/w % of PEG grafted on PLA was estimated.

2.6.6 Synthesis of PLA-Flu

In a round bottom flask, under inert atmosphere, PLA-Prg-Pent (0.02 mmol), Flu-N_3 (0.02 mmol), $CuSO_4$ (0.04 mmol) and sodium ascorbate (0.08 mmol) were dissolved in 3 mL of anhydrous DMF. The reaction mixture was stirred overnight at room temperature. Water was added to the crude reaction, to obtain a precipitate. The suspension was centrifuged, the solid was washed with water two times and lyophilized to obtain PLA-Flu, as a pink solid.

^{1}H NMR (500 MHz, $CDCl_3$, δ): 8.0 (s, H triazole), 7.2-7.1 (m, Ar H_{flu}), 6.6 (br s, NH), 6.5 (br s, NH),

6.4 (br s, NH), 5.2 (m, CH PLA), 4.4 (m, CH_2C]C triazole), 4.0 (m, CH_2NH unreacted alkyne moiety),

3.7 (m, NCH_{3flu}), 3.6 (m, CH_2O_{flu}), 3.5 (m, CH_2O_{flu}), 3.2 (m, CH_2N_{flu}), 3.0 (m, CH_2N triazole), 2.7 (m, CH_{2pent}), 2.2 (m, C≡CH_{prg} unreacted alkyne moiety), 1.5 (m, CH_3 PLA).

The amount of dye conjugated on PLA backbone was estimated to be 1.7% by UV–Vis spectroscopy.

2.6.7 Synthesis of PLA-FA

In a round bottom flask, under inert atmosphere, PLA-Prg-Pent (0.02 mmol), FA-N_3 (0.02 mmol), $CuSO_4$ (0.04 mmol) and sodium ascorbate (0.08 mmol) were dissolved in 3 mL of anhydrous DMF. The reaction mixture was stirred overnight at room temperature. Water was added to the crude reaction, to obtain a precipitate. The suspension was centrifuged, the solid was washed with water two times and lyophilized to obtain PLA-FA, as a yellowish solid.

^{1}H NMR (500 MHz, DMSO-d_6, δ): selected peaks 11.41 (bs, 1H), 8.54 (bs, 1H), 8.43 (s, 1H), 7.86 (m, 2H), 7.65 (m, 2H), 7.44 (m, 2H), 6.99 (bs, 1H), 6.76 (m, 2H), 5.16 (m, CH PLA), 4.98 (m, 2H), 4.35 (s, 1H), 4.15 (m, 2H), 3.80-3.90 (m, 8H), 1.94 (m, 2H), 2.07 (m, 2H),1.45 (m, CH_3 PLA).

2.6.7 Preparation of PLA-Flu/Sal NPs

Sal was obtained from its sodium salt as already reported.[19] Briefly, the Sal sodium salt was dissolved in DCM and vigorously stirred for 12 h with aqueous H_2SO_4 (pH 2.0). The organic phase was washed with water, until neutrality, and evaporated under reduced pressure to obtain an oil. The Sal-loaded PLA-Flu NPs with a polymer/drug weight ratio of 10 : 1 was prepared by nanoprecipitation as follows: PLA-Flu (40 mg) and Sal (4 mg) were co-dissolved in 8 ml of acetone. This organic phase was rapidly poured into 16 ml of un aqueous solution at rt under vigorous stirring. The organic solvent was removed by stirring overnight. Nanoparticles were then recovered by centrifugation for 20 min at 15000 rpm, washed two times with distilled water to remove unentrapped drug, and finally lyophilized to yield freeze-dried nanoparticles.

2.6.8 Preparation of PLA-FA/Sal NPs

A modified nanoprecipitation technique was used for the preparation of PLA-FA/Sal NPs due to the poor solubility in acetone. Briefly, 30 mg of PLA-FA and 3 mg of Sal were dissolved in 1 mL of dimethylsulfoxide. The organic solution was added dropwise in 30 mL of ultrapure water under moderate magnetic stirring at room temperature. The suspension was stirred for 3 h, followed by centrifugation (15000 rpm, 20 minutes). The solid was washed three times with deionized water and eventually lyophilized. Similarly, blank PLA-FA NPs were prepared using the same technique, without addition of the drug.

2.6.9 Drug loading

The drug content and the loading efficiency were determined by a suitable GPC method. A weighed amount of Sal-loaded NPs was dissolved in 1 ml of THF, sonicated and centrifuged (9000 rpm); the supernatant was analysed by GPC. The quantitative calibration curve was obtained analysing five mixtures of PLA-FA (or PLA-Flu) at knows content. For each analysis, the intensity ratio between FA (or Flu) and PLA signals was evaluated and correlated with its analytical amount. The drug amount in the Sal-loaded NPs samples was obtained in the same way and the amount of FA (or Flu) was calculated

from the best-fit equation obtained before. The following equations were used to calculate drug content and drug loading efficiency: Drug content (%) = (Drug weight in the NPs/Weight of the drug-loaded NPs) x 100; Drug loading efficiency (%) = (Drug weight in the NPs/Weight of drug used in the formulation) x 100.

2.7 References

1. Billiet, L., Fournier, D., Du Prez, F. Combining “click” chemistry and step-growth polymerization for the generation of highly functionalized polyesters. *J. Polym. Sci. Part A Polym. Chem.* 46, 6552–6564 (2008).
2. Yu, Y., Jiong, Z., Liu, Y., Wei, J., Yukun, L., Wing-Cheung, L., Chong, C. Functional Polylactide-g-Paclitaxel–Poly(ethylene glycol) by Azide–Alkyne Click Chemistry. *Macromolecules* 44, 4793–4800 (2011).
3. Scala, A., Piperno, A., Micale, N., Mineo, P.G., Abbadessa, A., Risoluti, R., Castelli, G., Bruno, F., Vitale, F., Cascio, A., Grassi, G. “Click” on PLGA-PEG and hyaluronic acid: Gaining access to anti-leishmanial pentamidine bioconjugates. *J. Biomed. Mater. Res. Part B Appl. Biomater.* 106, 2778–2785 (2018).
4. Parrish, B., Breitenkamp, R. B., Emrick, T. PEG- and Peptide-Grafted Aliphatic Polyesters by Click Chemistry. *J. Am. Chem. Soc.* 127, 7404–7410 (2005).
5. Scala, A. Piperno, A., Torcasio, S. M., Nicosia, A., Mineo, P. G., Grassi, G. “Clickable” polylactic acids obtained by solvent free intra-chain amidation. *Eur. Polym. J.* 109, 341-346 (2018).
6. Zhang, Q., Ren, H., Baker, G. L. Synthesis and click chemistry of a new class of biodegradable polylactide towards tunable thermo-responsive biomaterials. *Polym. Chem.* 6, 1275–1285 (2015).
7. Yu, Y., Chen, C.-K., Law, W.-C., Mok, J., Zu, J., Prasad, P. N., Cheng, C. Well-Defined Degradable Brush Polymer–Drug Conjugates for Sustained Delivery of Paclitaxel. *Mol. Pharm.* 10, 867–874 (2013).
8. Han, L., Xie, Q., Bao, J., Shan, G., Bao, Y., Pan, P. Click chemistry synthesis, stereocomplex formation, and enhanced thermal properties of well-defined poly(l-lactic acid)-b-poly(d-lactic acid) stereo diblock copolymers. *Polym. Chem.* 8, 1006–1016 (2017).
9. Liénard, R., Zaldua N., Josse T., Winter J., Zubitur M., Mugica A., Iturrospe A., Arbe A., Coulembier O., Müller A.J. Synthesis and Characterization of Double Crystalline Cyclic Diblock Copolymers of Poly(ε-caprolactone) and Poly(l(d)-lactide) (c(PCL-b- PL(D)LA)). *Macromol. Rapid Commun.* 37, 1676–1681 (2016).
10. Lav, T.-X., Lemechko, P., Renard, E., Amiel, C., Langlois, V., Volet, G. Development of a new azido-oxazoline monomer for the preparation of amphiphilic graft copolymers by combination of cationic ring-opening polymerization and click chemistry. *React. Funct. Polym.* 73, 1001–1008 (2013).
11. Le Fer, G., Le Cœur, C., Guigner, J.-M., Amiel, C. & Volet, G. Biocompatible Soft

Nanoparticles with Multiple Morphologies Obtained from Nanoprecipitation of Amphiphilic Graft Copolymers in a Backbone-Selective Solvent. *Langmuir* 33, 2849–2860 (2017).

12. Ranjan, A., Deore, A. S., Yerande, S. G. & Dethe, D. H. Thiol–Yne Coupling of Propargylamine under Solvent-Free Conditions by Bond Anion Relay Chemistry: An Efficient Synthesis of Thiazolidin-2-ylideneamine. *Eur. J. Org. Chem.* 2017, 4130–4139 (2017).
13. Sadeghzadeh, S. M., Zhiani, R., Emrani, S. Ni@Pd nanoparticles supported on ionic liquid-functionalized KCC-1 as robust and recyclable nanocatalysts for cycloaddition of propargylic amines and CO2. *Appl. Organomet. Chem.* 32, e3941 (2018).
14. Zagami, R., Rapozzi V., Piperno A., Scala A., Triolo C., Trapani M., Xodo L.E., Monsù Scolaro L., Mazzaglia A. Folate-Decorated Amphiphilic Cyclodextrins as Cell-Targeted Nanophototherapeutics. *Biomacromol.* 20, 2530–2544 (2019).
15. Lindsey, B. A., Markel, J. E., Kleinerman, E. S. Osteosarcoma Overview. *Rheumatol. Ther.* 4, 25–43 (2017).
16. Durfee, R. A., Mohammed, M., Luu, H. H. Review of Osteosarcoma and Current Management. *Rheumatol. Ther.* 3, 221–243 (2016).
17. Kuşoğlu, A., Biray Avcı, Ç. Cancer stem cells: A brief review of the current status. *Gene* 681, 80–85 (2019).
18. Gupta, P. B., Onder T.T., Jiang G., Tao K., Kuperwasser C., Weinberg R.A., Lander E.S. Identification of Selective Inhibitors of Cancer Stem Cells by High-Throughput Screening. *Cell* 138, 645–659 (2009).
19. Piperno, A., Marrazzo, A., Scala, A., Rescifina, A. Chemistry and biology of salinomycinand its analogues, in: Targets In Heterocyclic Systems, Attanasi, O.A., Merino, P., Spinelli, D., Eds., Società Chimica Italiana, Roma, Italia, 2015, 19, 177–213
20. Zhang, Y., Zhang H., Wang X., Wang J., Zhang X., Zhang Q. The eradication of breast cancer and cancer stem cells using octreotide modified paclitaxel active targeting micelles and salinomycin passive targeting micelles. *Biomaterials* 33, 679–691 (2012).
21. Ni, M., Xiong, M., Zhang, X., Cai, G., Chen, H., Zeng, Q., Yu Z. Poly(lactic-co-glycolic acid) nanoparticles conjugated with CD133 aptamers for targeted salinomycin delivery to CD133+ osteosarcoma cancer stem cells. *Int. J. Nanomed.* 10, 2537–2554 (2015).
22. Duguang, L., Jin H., Xiaowei Q., Peng X., Xiaodong W., Zhennan L., Jianjun Q., Jie Y. The involvement of lncRNAs in the development and progression of pancreatic cancer. *Cancer Biol. Ther.* 18, 927–936 (2017).
23. Fessi, H., Puisieux, F., Devissaguet, J. P., Ammoury, N., Benita, S. Nanocapsule formation by interfacial polymer deposition following solvent displacement. *Int.J.Pharm.* 55, R1–R4 (1989).

CHAPTER 3

Chapter 3

3.1 Star polymers

Branched polymers such as star polymers, dendrimers, and hyperbranched polymers are going to increase interest due to their unique physicochemical properties, which are not accessible in conventional linear analogs[1].

Star polymers possess three dimensional branched architectures, with a structure consisting of multiple variable-length linear chains (*arms*) radiating from a central *core*. Although they might have high molecular weights, they own a good solubility and unique rheological and mechanical properties comparable to the corresponding linear polymers[2].

Furthermore, star polymers combine a spherical and compact shape with a high density of functionalizable end-groups and a *core–shell* structure similar to that of micelles.

Their unique shape and attractive properties, such as low viscosity in dilute solutions, encapsulation capability, internal and peripheral functionality, high arm density, efficient synthesis and enhanced stimuli-responsiveness make them promising tools in various field, including drug and gene delivery[3,4] , tissue engineering[5], coatings[6],etc.

The principal methods employed for the synthesis of star polymer are (1) the *core-first* method (polymerization with a multifunctional initiator) and (2) the *arm-first* method (coupling of linear polymers with a multifunctional terminator)[7]. In the 'core-first' technique, a multifunctionalinitiator with a known number of initiating groups is used to trigger the polymerization of a monomer to produce arms of suitable lenght, while the 'arm-first' technique involves the coupling of linear polymer arms with either multifunctional coupling agents or difunctional monomers (**Figure 1**). The most commonly used method is the *core-first* approach and a perfect star-shaped structure of the final macromolecule is expected only when all functional groups start parallel and steady growth of the linear macromolecular arms.

Synthetic control of the composition and length of the star polymer arms can be assured by controlled polymerization methods, such as atom transfer radical polymerization (ATRP), reversible addition–fragmentation chain-transfer (RAFT) radical polymerization, ring-opening metathesis polymerization (ROMP) and ring-opening polymerization (ROP)[2].

Moreover, the controlled introduction of different types of polymeric arms onto a single core scaffold needs often a combination of synthetic methodologies. As an example, the combination of one of those polymerization techniques with a *click* chemistry reaction (i.e., the Cu^{I}-catalyzed azide-alkyne cycloaddition, CuAAC) has emerged as a powerful tool for the preparation of well-defined

star polymers, because of the mild reaction conditions and high tolerance of functional groups of the *click* reaction[8].

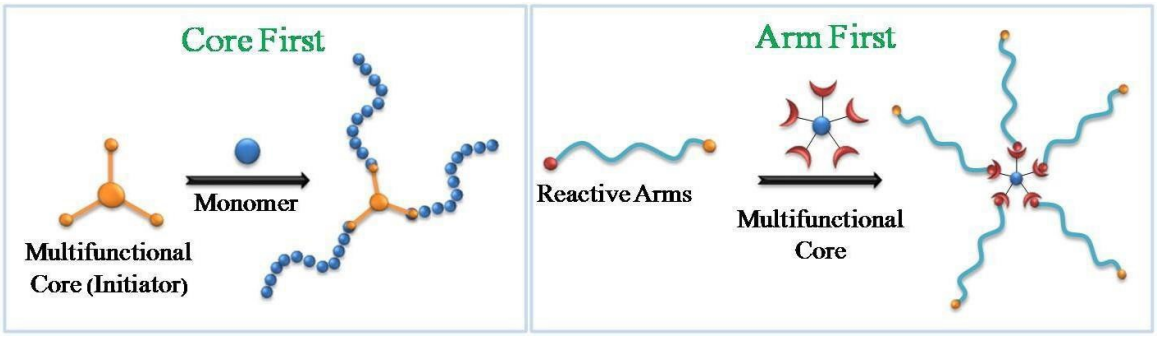

Figure 1. Arm-first and core-first techniques for preparing star polymers

Depending on the chemical compositions of the arms, star polymers can be classified into "*homoarm star polymers*" or "*miktoarm star polymers*". The first one consists of a symmetrical structure in which the arms are all equivalent in length and structure, whereas a miktoarm star molecule contains arms with different chemical compositions and/or molecular weights and/or different end-functionalities (**Figure 2**). As an example, when individual arms are composed of different polymers, *star-block polymers* or *star copolymers* are obtained.

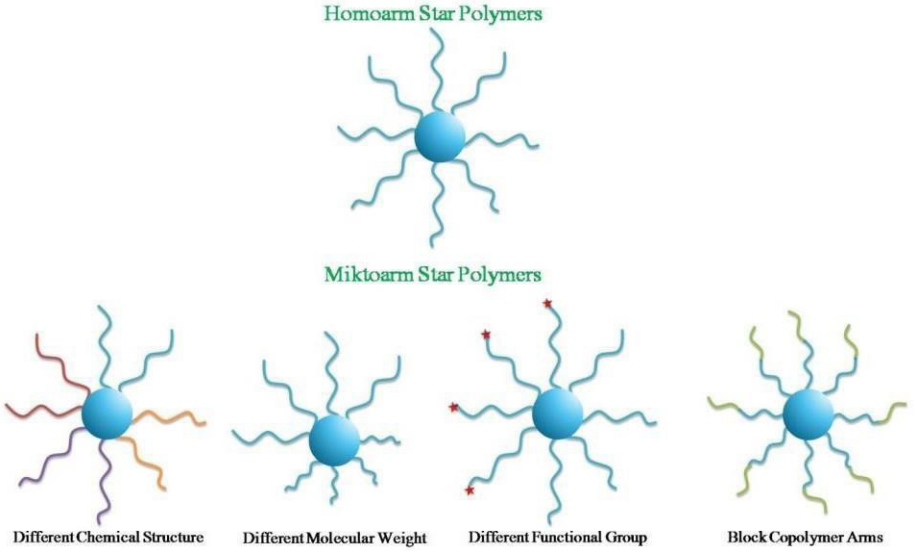

Figure 2. Homoarm star polymers and miktoarm star polymers

The interest in miktoarm star polymers comes from the possibility of combining different type and number of polymeric arms, including also different functionalities into a singlemacromolecule[9]. In particular, amphiphilic miktoarm star copolymers (containing both hydrophobic and hydrophilic moieties onto their arms) are expected to generate nanostructures in water similar to amphiphilic

block copolymers by a self-assembly process in solution promoted by a selective solvent (**Figure 3**)[10].

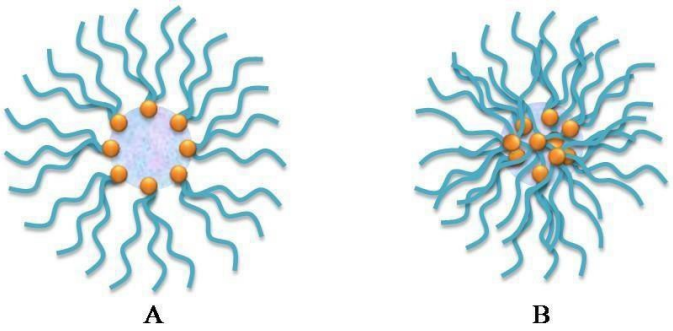

Figure 3. Two possible micellar structures of amphiphilic star copolymers: (A) with strongly segregated arms and (B) with partially intermixed arms[10]

One of the most fascinating properties of block copolymers (either linear or star) with two or more blocks with different solubility (i.e. the hydrophobic PLA and the hydrophilic PEG) is their ability of self-assembling into a variety of ordered nanostructures. The fine tuning of polymer properties, such as the relative block length and the solution conditions allows polymeric micelles or micellar-like nanoparticles to be prepared[11], although differences in the micellization properties are observed with respect to linear diblock copolymers as a result of the topological constraints of the star copolymers[12,13,14]. In fact, unimolecular micelles or multimolecular micellar aggregates may form (**Figure 4**), depending on the number of arms and on the block length and architecture, as pointed out by molecular simulations performed on model amphiphilic block copolymers[15,16,17,18].

Benifiting from the different core/shell properties of amphiphilic star copolymers, phase separation easily occurs in aqueous medium, which drives unimolecular micelle formation. Moreover, the formation of large multimolecular micelles (multi-micelle aggregates) can occur by the secondary aggregation of unimolecular micelles, in high concentration (**Figure 4**)[19].

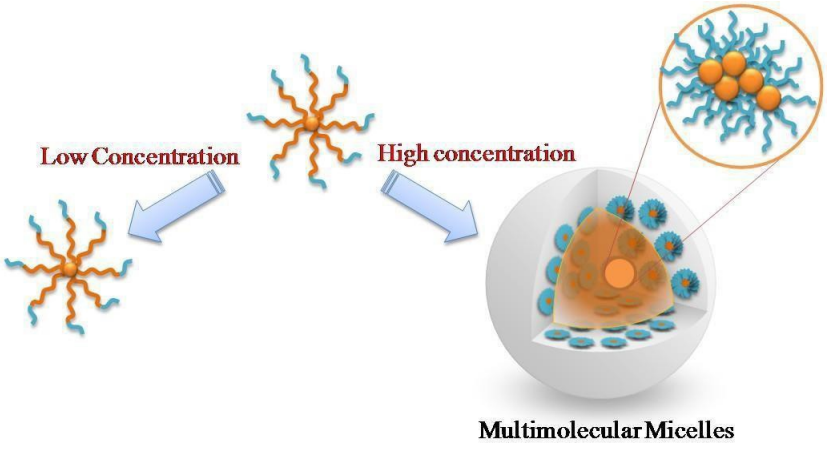

Figure 4. Unimolecular and multimolecular micelles

Thus, a careful control over the length of the block segments is decisive to prevent the aggregation of the star polymers and to afford unimolecular nanocarriers with controlled sizes in aqueous media. Unimolecular micelles possess a very high and intrinsic stability upon dilution due to the covalently reinforced core-shell structure of the amphiphilic copolymer which makes them stable towards high dilution or other condition changes. Moreover, the dense outer shell prevents the core segments from aggregating and avoids protein adsorption[20]. Owing to this ultra-stability, unimolecular micelles accommodating guest biomolecules within their core are promising platform for bio-application, especially in imaging and diagnosis[21]. One of the main advantages of unimolecular micelles compared to the conventional ones is that the latter might disassemble when subjected to high dilution in the bloodstream, leading to burst effect of the encapsulated drug and potential toxic effects (**Figure 5**)[21]. In fact, differently from conventional polymeric micelles, which are thermodynamic aggregates of amphiphiles above a certain concentration threshold (Critical Micelle Concentration, CMC), unimolecular micelles are stable upon high dilutions, and could be formed below CMC values typically expected for the hydrophilic/lipophilic balance of amphiphilic polymer[22]

Figure 5. Left: Unimolecular micelles in aqueous solution are single-molecule architectures constituted by a hydrophobic core (blue) and a hydrophilic shell (green) covalently linked to a central backbone (blue). Right: Conventional polymeric micelles in aqueous solution are an aggregation of amphiphiles having hydrophobic (red) and hydrophilic (green) moieties. At concentration below the CMC, they disassemble into free polymeric chains.

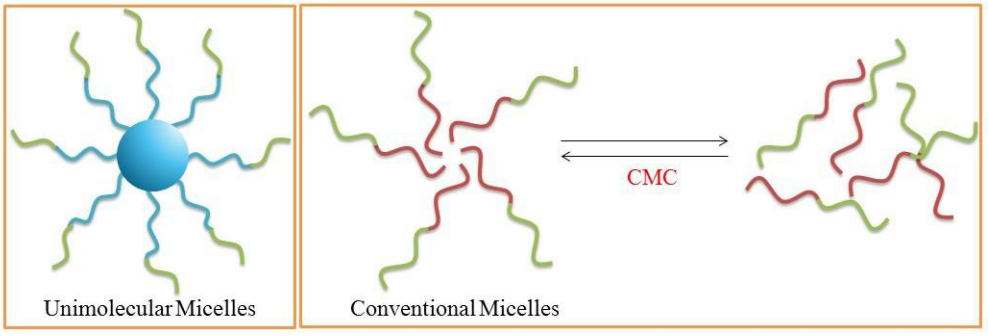

3.2 Star PLA-PEG copolymers

One of the most important class of star polymers is built from aliphatic polyesters, obtained by ring-opening polymerization (ROP) of cyclic esters with multi-functional alcohols, as initiators, in a core-first approach[23]. Although star polymers were first reported in 1948, the first star PLA was prepared in 1989[24], and, currently, the research in this area and the market have going to increase interest due to the unique properties of star PLA compared to their linear analogue. When built into a star structure, PLA shows a lower melting temperature (T_m), glass transition temperature (T_g), and

crystallization temperature (T_c) than the linear PLA of a similar molar mass. Additionally, star PLA exhibits lower hydrodynamic volume and a viscosity that is proportional to the number of end groups. These features provide exciting opportunities for developing new functional polymers with desirable properties for applications in emerging nanotechnologies[23].

Depending on the polyalcohol used as ROP initiator (e.g. glycerol, erythritol, pentaerythritol, xylitol, dipentaerythritol, etc, **Figure 6**), multi-armed star PLA can be obtained (e.g. three-, four-, five, or six-armed)

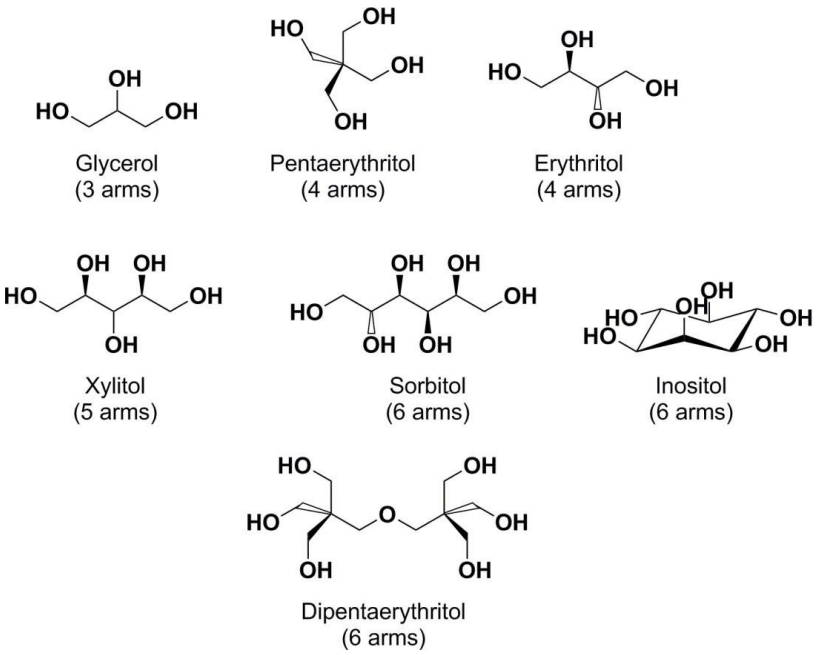

Figure 6. Polyalcohols in star PLA synthesis

The end-groups of star PLA can be properly functionalized to generate multifunctional polymeric star-shaped architectures with specific features and applicability. Furthermore, star polymers display superior stimuli-responsiveness because of the possibility to introduce diverse valuable functionalities at the end of the star arms[25]. Stimuli-responsive moieties able to automatically undergo conformational/chemical changes upon external signals (e.g., changes in temperature or pH, irradiation with light, exposure to alternating electric or magnetic fields) are ideal for drug delivery applications, in which the spatial-temporal release of the drug is crucial[26].

Hydrophilic polymer arms are usually chosen as star polymers' shell in biological application because of their good solubility in aqueous medium and biocompatibility. Among them, polyethylene glycol (PEG) is the most effective material to prolong the circulation time of nanoparticles by reducing non-specific protein adsorption in blood. In fact, as well known, besides ensuring water solubility, the PEG shell may endow the star polymer enhanced stability, longer plasma half-life, and reduced *in vivo* immunogenicity[27]. Furthermore, the versatile end-group chemistry of the PEG-arms

allows the proper functionalization, i.e. with targeting ligand or fluorescent probes, to afford star polymers with targeting and imaging capabilities[28].

3.3 Synthesis of three-arm star PLA-PEG-RGD

In collaboration with the University of Mons (UMONS, Belgium), under the supervision of Prof. Olivier Coulembier, the synthesis of a novel three-arm star PLA-PEG copolymer was developed in a *core-first* approach. During the time spent at UMONS, the work has been focused on the synthesis and characterization of the amphiphilic star copolymer which was eventually decorated with the cyclo-RGDyK peptide (**Figure 7B**), as an integrin targeting ligand. The final product was intended to the targeted cancer therapy, after micellization and incorporation of a suitable anticancer drug (i.e., Doxorubicin).

Arginine-glycine-aspartic acid peptide (Arg-Gly-Asp or RGD peptide, **Figure 7A**) is a cell recognition motif, specifically recognized by the $\alpha_v\beta_3$ integrin receptor, which is highly expressed in tumor cells and strongly involved in the regulation of tumor angiogenesis. RGD-based strategies, including RGD antagonists, RGD-conjugates, and RGD-decorated nanoparticles,[29] are promising approach for targeting tumor cells for both cancer therapy and diagnosis. A great number of RGD peptides and cyclopeptides are reported in literature[30] for the targeted delivery of therapeutics. To date, PLA-PEO micelles grafted with RGD peptide have been designed for the targeted delivery of paclitaxel, showing a higher tumor uptake compared to untargeted PLA-PEO micelles and a good therapeutic efficacy in mice.[31]

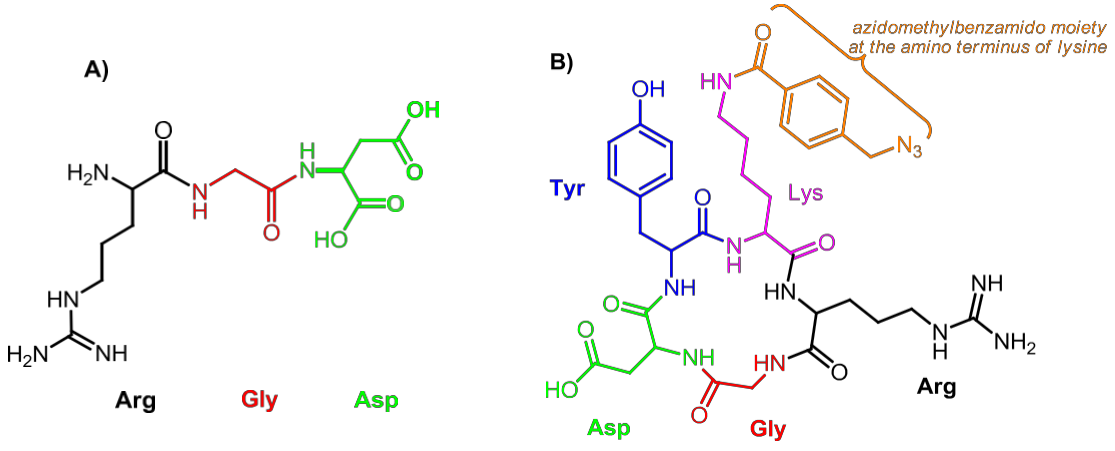

Figure 7. A) Tripeptide Arg-Gly-Asp (RGD peptide); B) its cyclic derivative cyclo-RGDyK peptide (Gly-Arg-Asp-Tyr-Lys) bearing an azidomethylbenzamido moiety at the amino terminus of the lysine

The synthetic strategy for the preparation of the novel three-arm star PLA-PEG copolymer decorated with RGD peptide, summarized in Scheme 1, was articulated as follows:

a) synthesis of the three-arm star PLA end-functionalized with alkyne moieties (**6**) (hydrophobic domain); *b)* synthesis of the hydrophilic mono-azide PEG (**9**); *c)* CuAAC *click* coupling leading to the three-arm star PLA-PEG copolymer (**10**), further derivatized with alkyne end-groups to yield (**11**); *d)* final CuAAC *click* coupling of (**11**) with the azide-functionalized cyclic RGDyK peptide (RGD-N_3, **12**). The final three-arm star PLA-PEG-RGD (**13**) and all the intermediates were fully characterized by ^{1}H NMR spectroscopy, SEC and MALDI-ToF analyses.

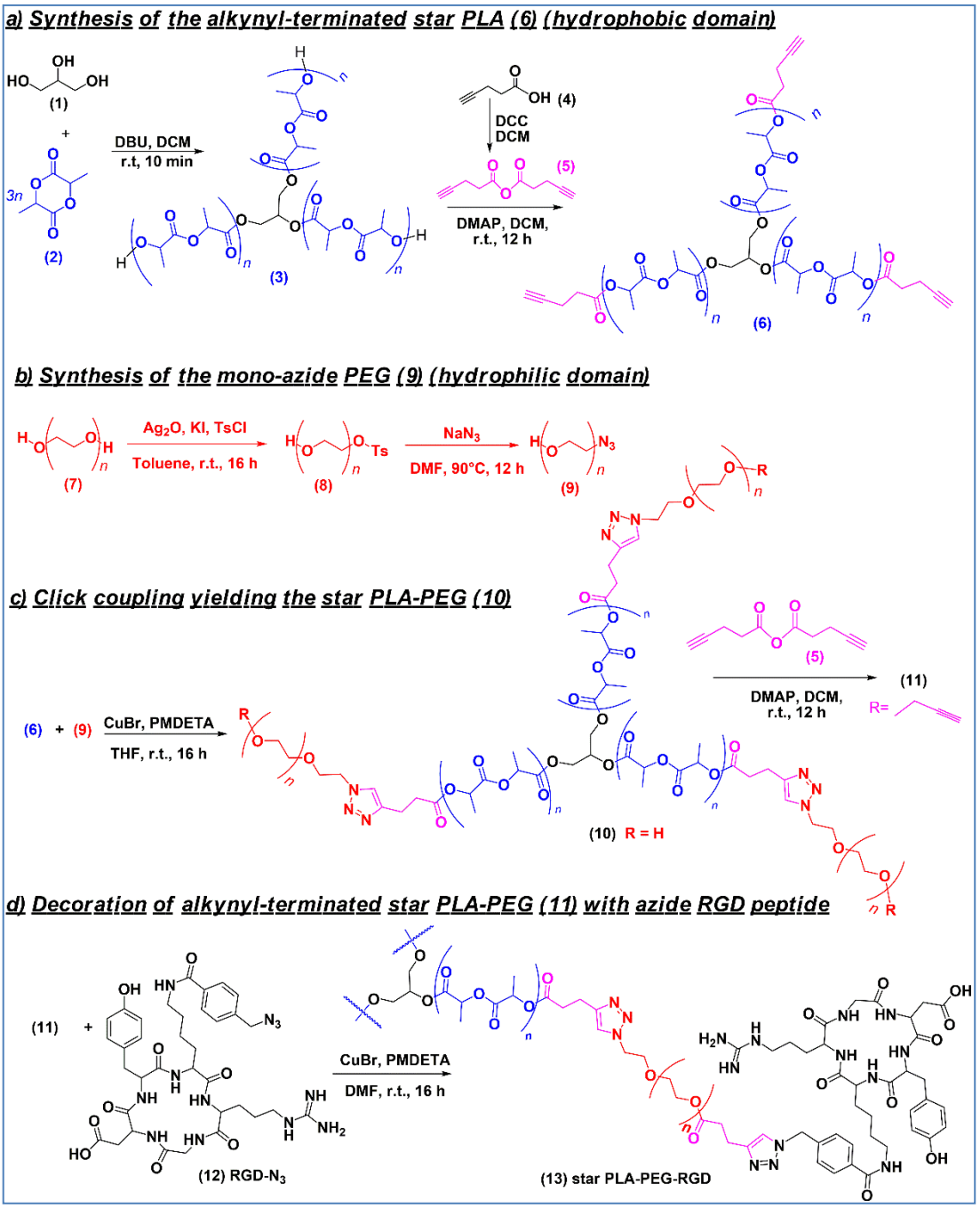

Scheme 1. Multi-step synthesis of the novel three-arm star PLA-PEG-RGD

Since the control over the molecular weight, the chemical composition and the number of the arms is of paramount importance to the synthesis of star-shaped polymers and has a significant effect on polymer properties (e.g. crystallinity, degradation rate, micellization), first of all we decided to synthesize a star PLA-PEG copolymer with a final molecular weight of 20000 g/mol. Moreover, a hydrophobic: hydrophilic ratio of 14000:6000 g/mol was set, that might allow the *self- assembly* of the final PLA- PEG-RGD in aqueous solution.

The synthesis was carried out in a *core-first* approach. The first step consisted in a ROP ofL-lactide (**2**) using glycerol (**1**) as the multifunctional initiator and 1,8-diazabicyclo(5.4.0)undec-7-ene (DBU) as a catalyst (**Scheme 2**). During the ROP, the arms are directly grown from the initiating core.

To calculate the amount of alcoholic initiator and catalyst, the Polymerization Degree (DP) was calculated, starting from the desired molecular weight of the final product star PLA, as follow:

$$DP = \frac{Mn}{m} = \frac{14.000\ g/mol}{144{,}13\ g/mol} = 97$$

Where *Mn* represents the final desired molecular weight (*Mn*=14000 g/mol) and *m* represents the molecular weight of the L-lactide monomeric unit (*m* = 144.13 g/mol).
Then, the DP was used to calculate the quantity of alcoholic initiator (I), following the formula:

$$[I] = \frac{[M]}{[DP]}$$

]Where *M* represent the amount of final desired product expressed in moles. As an example, for 1 g of desired product, the amount of initiator (moles) is calculated as follow:

$$[I] = \frac{\frac{1\ g}{144{,}13\ \frac{g}{mol}}}{97} = 6 \cdot 10^{-3}\ mol$$

The synthetic pathway for the preparation of the three-arm star PLA (**3**) is illustrated in Scheme 2. Glycerol and DBU were used as ring-opening polymerization initiator and catalyst, respectively, affording PLA samples with terminal hydroxyl functionality. The ROP was carried out in dichloromethane (DCM) at room temperature (r.t.).

An initial [lactide (L-LA)]$_0$/[initiator]$_0$/[DBU]$_0$ ratio of 97/1/2 ([L-LA]$_0$ = 1 M) has been selected to obtain a star PLA **(3)** with a molecular weight of 14.000 g/mol. In such experimental conditions, the polymerization was extremely fast, yielding quantitative monomer conversion in 10 minutes.

After 10 minutes, the DBU catalyst was quenched with an excess of benzoic acid and the product star PLA (**3**) was purified by precipitation into cold methanol, followed by centrifugation and filtration to ensure product purity and to avoid instability over the time, due to any traces of benzoic

acid/DBU salt[32].

The described method led to a very pure product, with an almost quantitative yield (98%), in a very fast and single step reaction, with easy removal of the catalyst.

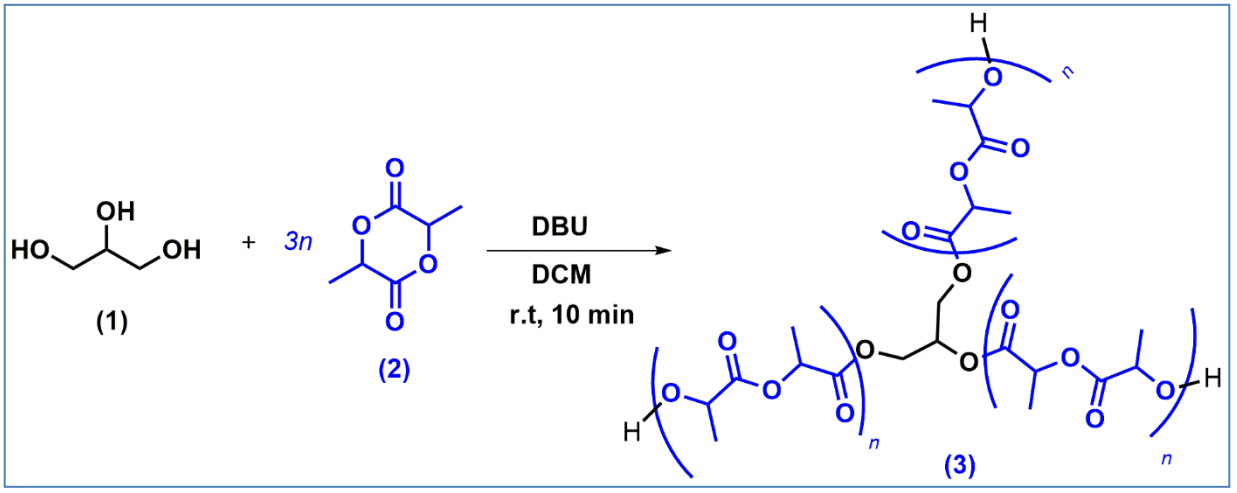

Scheme 2. ROP reaction of L-lactide (2) on glycerol (1) to obtain three arm star PLA (3).

^{1}H NMR spectroscopy (**Figure 8A**) confirmed the structure of the desired product (**3**).

The DP can be determined experimentally by comparing the relative intensity of the signal at δ 4.15-4.40 ppm (attributed to the glycerol protons (5H) and the methine protons of the PLA end-groups (3H), totally 8 H) to that of the repeating lactidyl methine protons at δ 5.15 ppm whose integral resulted 196.7. Dividing that value by two (the monomer L-Lactide has two methine protons), a DP of 98 is obtained in close agreement to the theoretical value of 97.

No trace of benzoic acid or DBU were observed, confirming the purity of (**3**). Moreover,

SEC analysis confirmed the homogeneity of the polymer, with $Đ_M = 1.12$ and $\overline{M}^{SEC,app} = 21.019$ g/mol (**Figure 8B**).

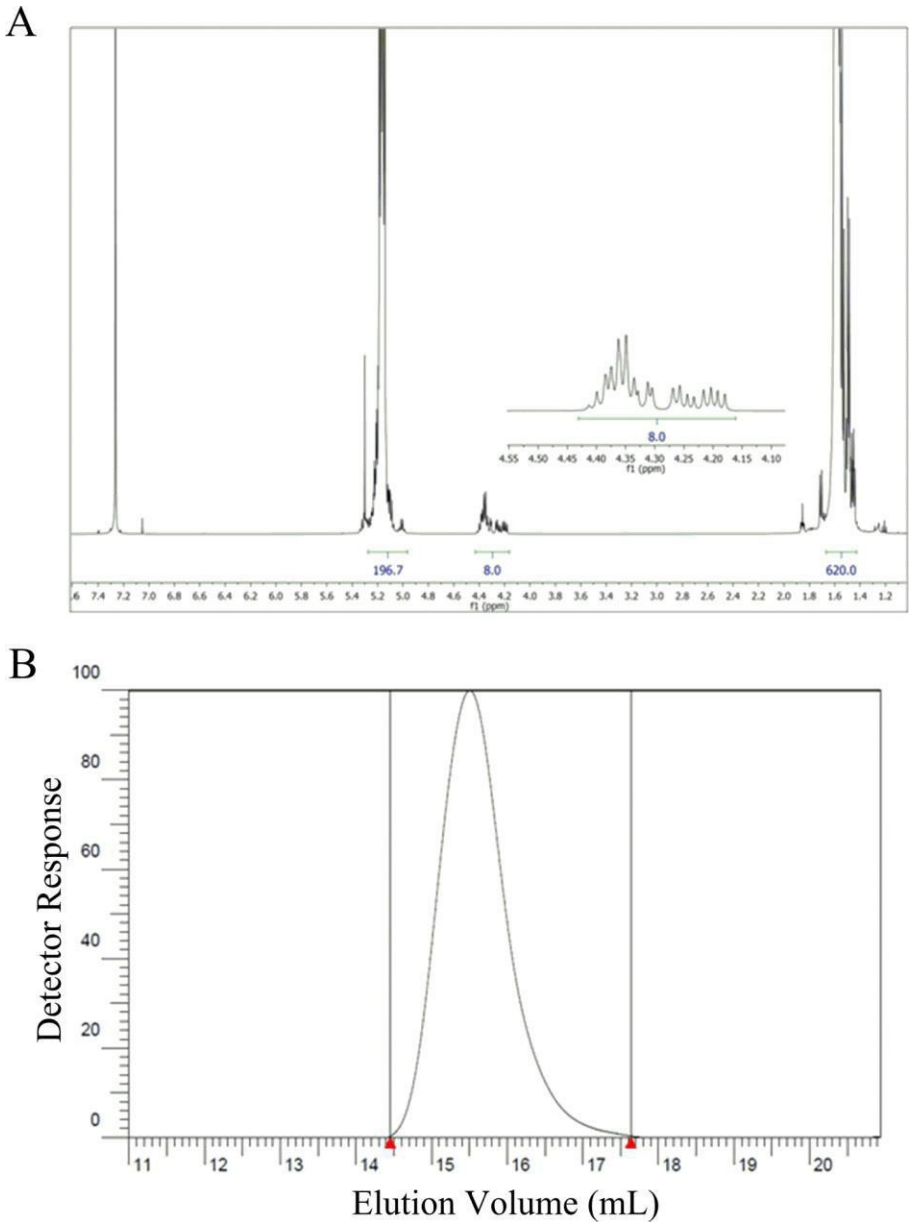

Figure 8. ^{1}H NMR (A) and SEC (B) analysis of star PLA (3)

In the hereabove DP calculation, we assumed that all three alcohol functions of the glycerol did initiate the polymerization of the LA monomer. To confirm that hypothesis, a kinetic study was performed, comparing the polymeric chain elongation on glycerol with that on a monofunctional alcoholic initiator, i.e. benzyl alcohol (BnOH), for the same total DP. The ROP of L-lactide from benzyl alcohol was then realized using an initial $[L\text{-}LA]_0/[initiator]_0/[DBU]_0$ ratio of 97/1/1 ($[L\text{-}LA]_0$ = 0.4 M). Samples were then withdrawn every 2 minutes for 14 minutes (t_0, t_2, t_4, t_6, t_8, t_{10}, t_{12}, t_{14}) for SEC analyses.

As represented by the Figure 9, whichever the initiator used, experimental Mn ($M_{n,SEC}$) are all aligned on the same straight-line attesting the good correspondence between both DP.

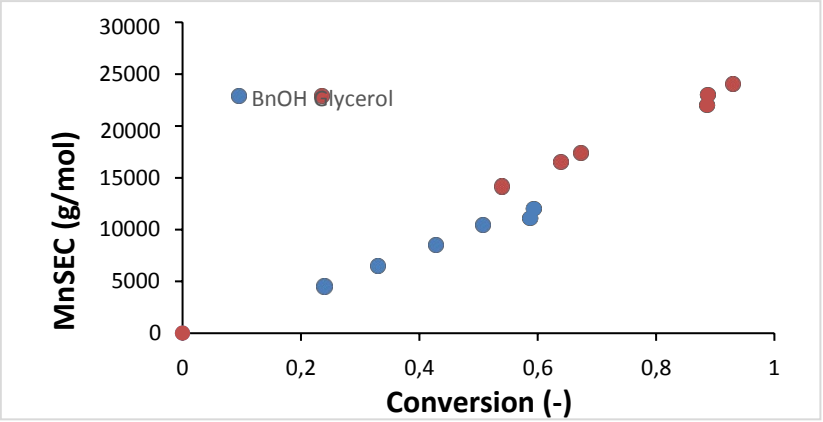

Figure 9. Dependence of molar mass (Mn SEC) of poly(L-lactide) measured by SEC on calculated conversions. Conditions of polymerization: $[L\text{-}LA]_0/[ROH]_0/[DBU]_0$ = 97:1:2 (with ROH=glycerol); 97:1:1 (with ROH=BnOH); blue dots: ROH = BnOH, orange dots: ROH = glycerol.

To confirm the initiation from all three O-H groups of the glycerol, we then compared the kinetics of ROP from glycerol to that of BnOH in the presence of DBU (Figure 10). The kinetics are consistent with the rate law: $-d[LA]/dt = k_{obs}[LA]$ for $k_{obs} = k_1[ROH][DBU]$, where [ROH] = glycerol (containing 3 OH groups) or BnOH (containing 1 OH group). These studies reveal that the rate constant for monomer consumption (k_1) is approximately three times higher when LA is polymerized from glycerol ($k_{1\text{-}3OH}$) compared to when LA is polymerized from BnOH ($k_{1\text{-}OH}$), $k_{1\text{-}3OH}/\ k_{1\text{-}OH}$ = 2.73, consistent with the tripling of the number of propagating –OH end groups when polymerization is initiated from the glycerol initiator.

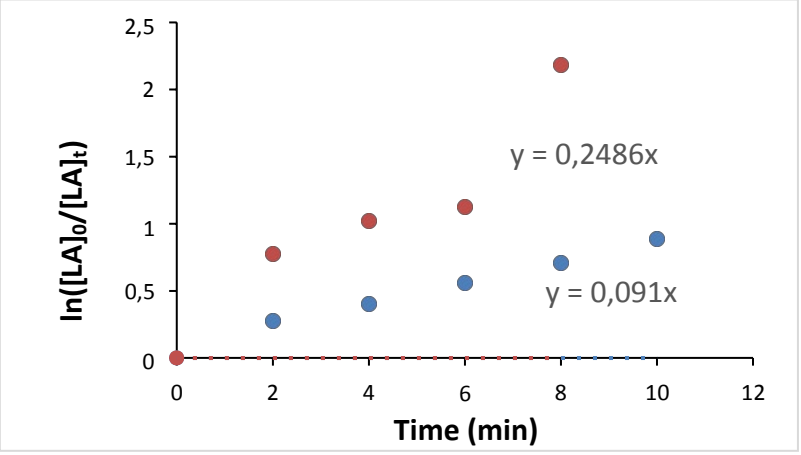

Figure 10. Comparison of rates of LA polymerization with glycerol (orange dots) and BnOH (blue dots) catalyzed by DBU.

In a following step, the hydroxyl end-groups of the star PLA (**3**) have been functionalized with pentynoic anhydride (**5**), prepared from the commercially available pentynoic acid (**4**) using 1,3-

dicyclohexylcarbodiimide (DCC) as dehydrating agent. The reaction was carried out in the presence of DMAP in order to obtain a *clickable* alkynyl-terminated star PLA (**6**) (**Scheme 3**).

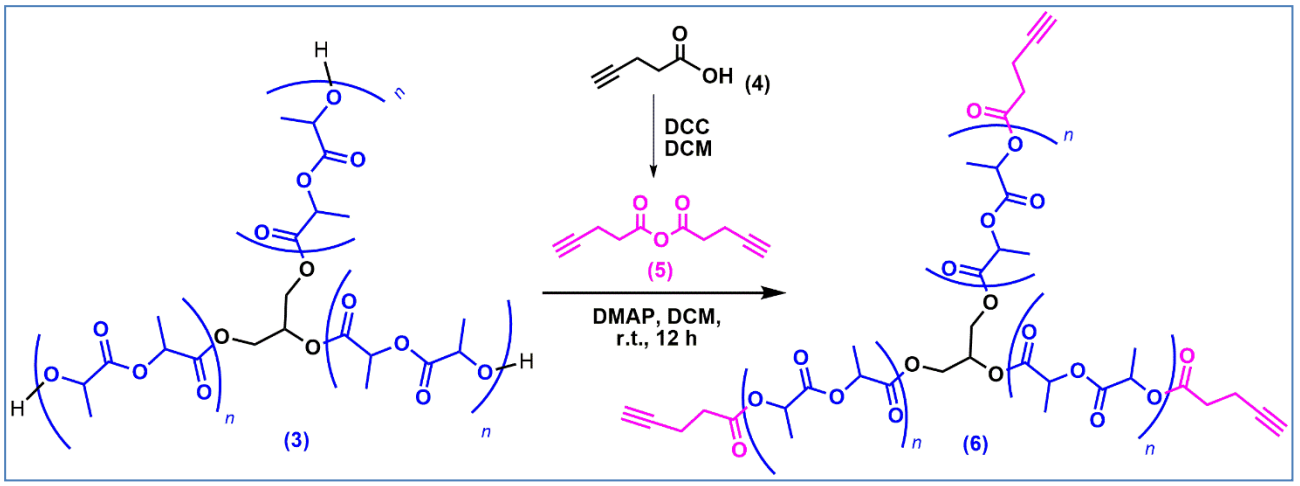

Scheme 3. Esterification of star PLA (3) with pentynoic anhydride (5)

^{1}H NMR analysis (**Figure 11**) confirmed the structure of (**6**) by the disappearance of the resonance at δ 4.36 ppm, attesting for the quantitative esterification of the terminal hydroxyl groups, together with the appearance of a novel set of signals attributed to the pentynoic end-group protons at δ 2.65, 2.52, 1.98 ppm (inset Figure 11). The SEC analysis showed a $Đ_M$ = 1.13 and an $M_{n,SEC,app}$ = 21.207 g/mol.

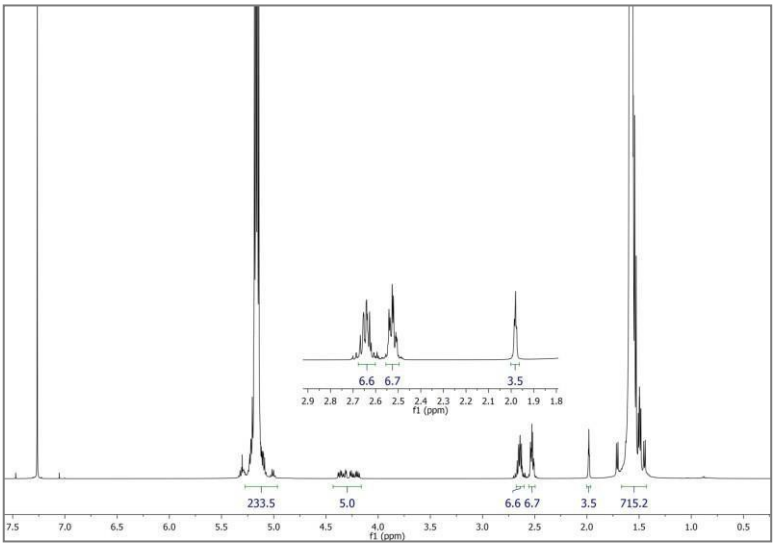

Figure 11. ^{1}H NMR spectrum of (6) recorded in $CDCl_3$ at r.t.

For the preparation of the hydrophilic domain of the final product, a mono-azide PEG was synthesized starting from commercially available PEG diol (Mw 2000 g/mol) in a two-step process (**Scheme 4**).[33]

Briefly, one of the two hydroxyl end-groups of PEG (**7**) was mono-tosylated in the presence of Ag_2O and KI (1.5:0.2 ratio to avoid the formation of di-tosylated product) affording mono-tosyl PEG (**8**), which was characterized by SEC-UV_{254} and ^1H NMR analysis. The mono-tosyl PEG (**8**) was converted in mono-azide PEG (**9**) by reaction with sodium azide in anhydrous DMF at 90° C, followed by washing with distilled water and brine.

^1H NMR analysis (**Figure 12A**) confirmed the structure of (**9**) by the typical signal at δ3.39 ppm relative to the azidomethylene protons. Peaks integration pointed out that the sample is a 1:1 mixture of mono-azide PEG (**9**) and unreacted PEG diol (**7**). The latter was removed in the next synthetic step and related work up (see Experimental).

Furthermore, the MALDI-ToF analysis (**Figure 12B-C**) excluded the presence of the undesired di-azide derivative and confirmed the azidation due to the presence of a small population showing 28 mass units less than the main population corresponding to the elimination of a nitrogen molecule during characterization typical for azide-containing polymers.[34]

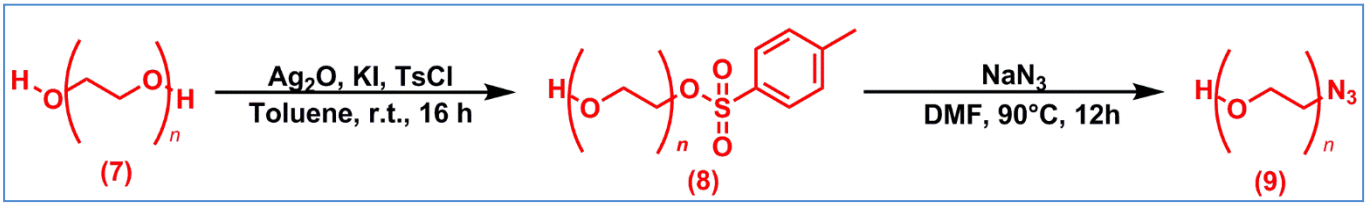

Scheme 4. Two-step synthetic pathway to prepare mono-azide PEG (9) starting from commercial PEG diol (7).

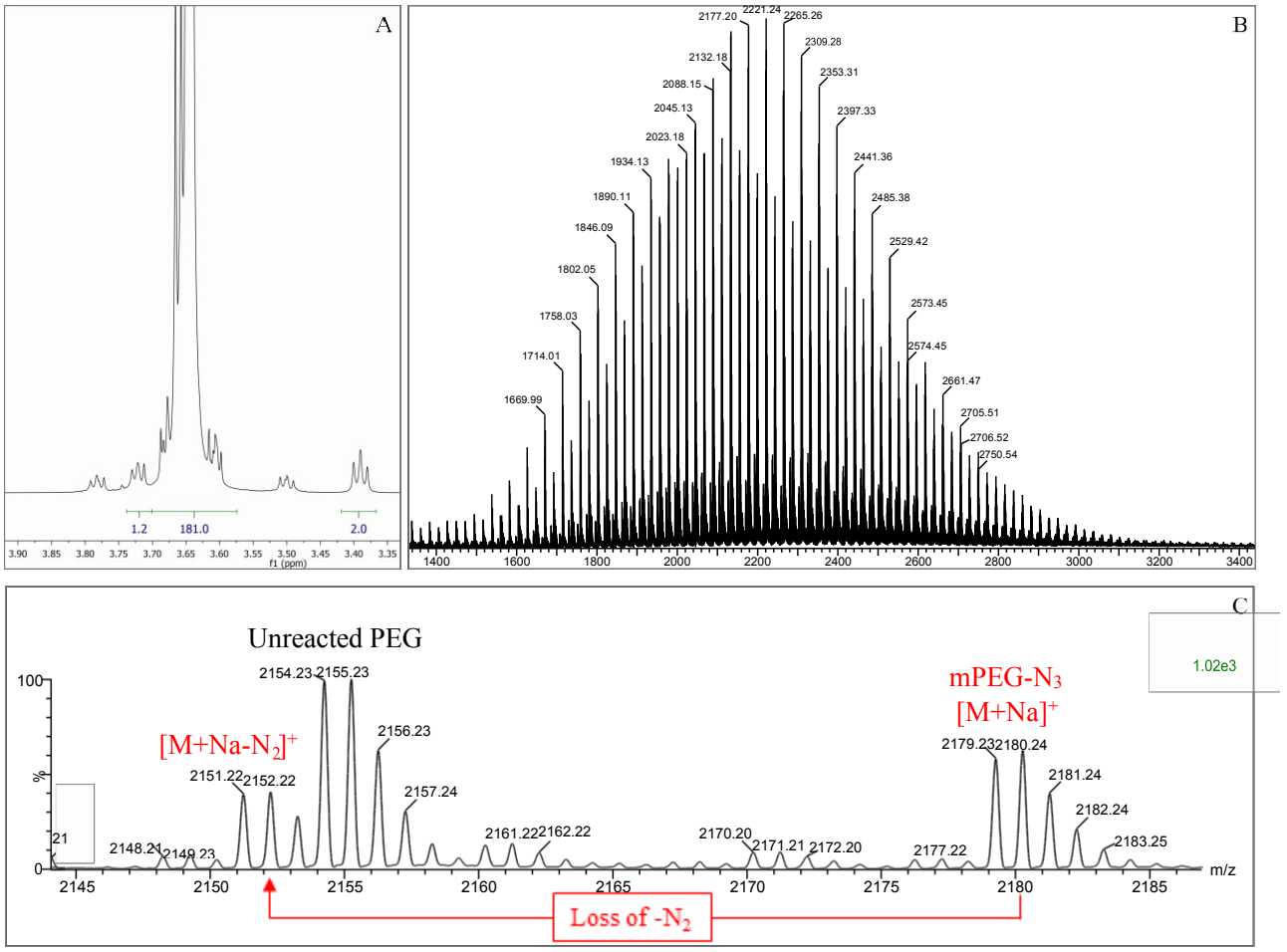

Figure 12. Mono-azide functionalization of PEG confirmed by ^{1}H NMR (A) and MALDI-ToF analysis (B, C).

Hydrophobic and hydrophilic domains, namely the alkynyl-terminated star PLA (**6**) and the mono-azide PEG (**9**) were coupled in a 1:3 ratio by CuAAC *click* chemistry reaction to obtain the amphiphilic three-arm star PLA-PEG copolymer (**10**) (**Scheme 5**).

The CuAAC reaction was performed in anhydrous tetrahydrofuran in the presence of CuBr and N,N,N′,N″,N″-pentamethyldiethylenetriamine (PMDETA) as catalyst and ligand, respectively. The workup by washing with water allowed the purification of the functionalized polymer, which was obtained in a very good yield (96%).

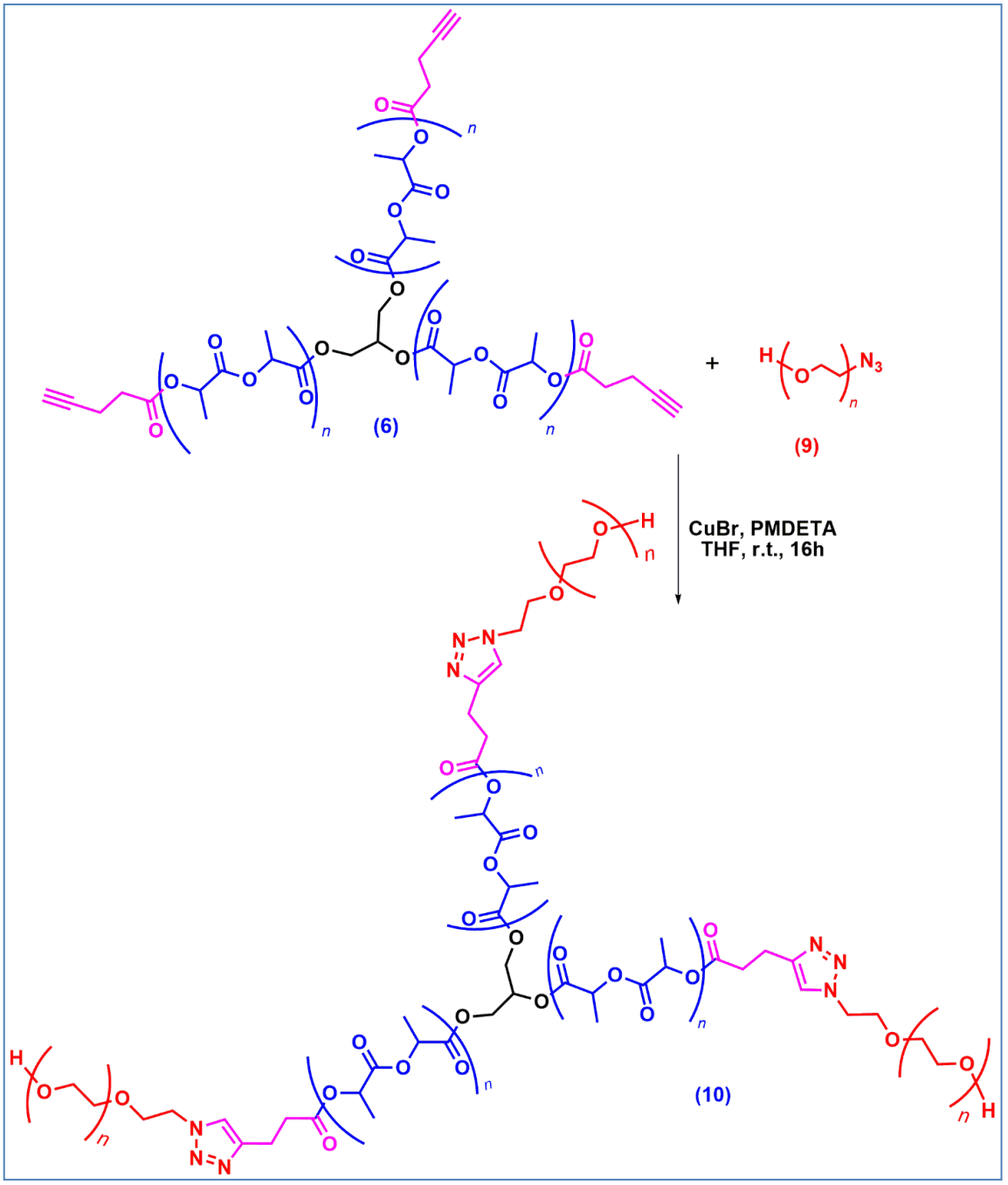

Scheme 5. Click chemistry reaction of alkynyl-terminated star PLA (6) and mono-azide PEG (9).

SEC analysis (**Figure 13**) confirmed the coupling reaction with the shift of the curve related to the star PLA-PEG (dashed line) compared to the alkynyl-terminated star PLA precursor (solid line). Furthermore ^{1}H NMR analysis confirmed the formation of the expected triazole linkage, connecting the hydrophilic and the hydrophobic polymeric portions, by the typical signal at δ 7.58 ppm corresponding to the triazole H-5 proton (black circle, **Figure 14**). In addition, both shifts of the azido-methylene protons resonance (from δ 3.39 to 3.06 ppm, blue circles), and the pentynoic-

methylene protons signal (from δ 2.52 to 4.49 ppm, orange circles), together with the disappearance of the alkyne proton signal at δ 1.98 ppm were observed (black dashed circle, **Figure 14**).

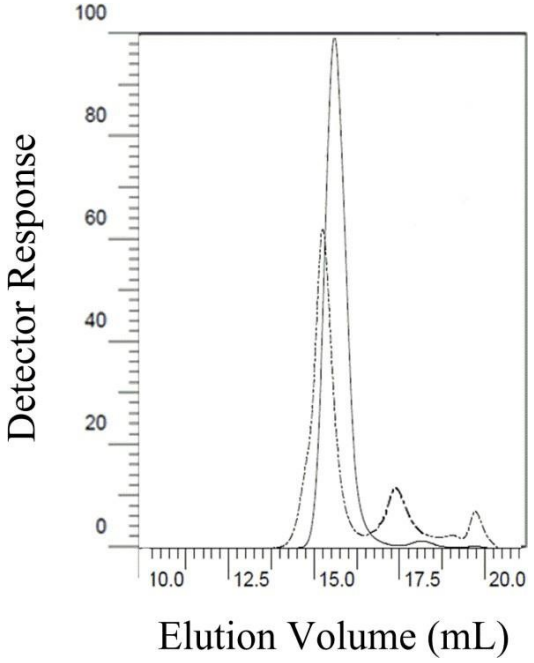

Figure 13. SEC chromatograms of star PLA-PEG (10, dashed line) compared to alkynyl-terminated star PLA precursor (6, solid line).

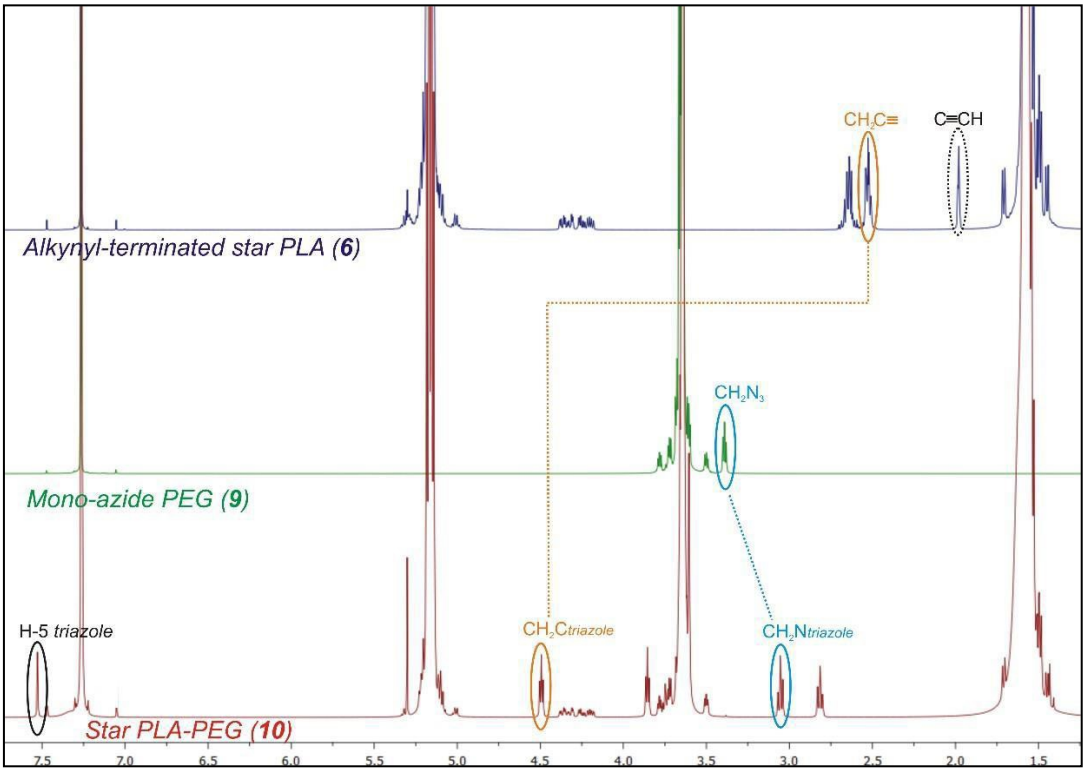

Figure 14. ^{1}H NMR spectra of three-arm star PLA-PEG (10, red trace), mono-azide PEG (9, green trace), alkynyl-terminated star PLA (6, blue trace). All the spectra were recorded in $CDCl_3$ at r.t.

The final synthetic step did consist on the esterification of the hydroxyl end-groups of (**10**) with pentynoic anhydride in presence of DMAP, followed by CuAAC *click* coupling of the alkynyl-terminated star PLA-PEG (**11**) with azide-RGD peptide (**12**) to afford the desired three-arm star PLA-PEG-RGD (**13**) (**Scheme 6**).

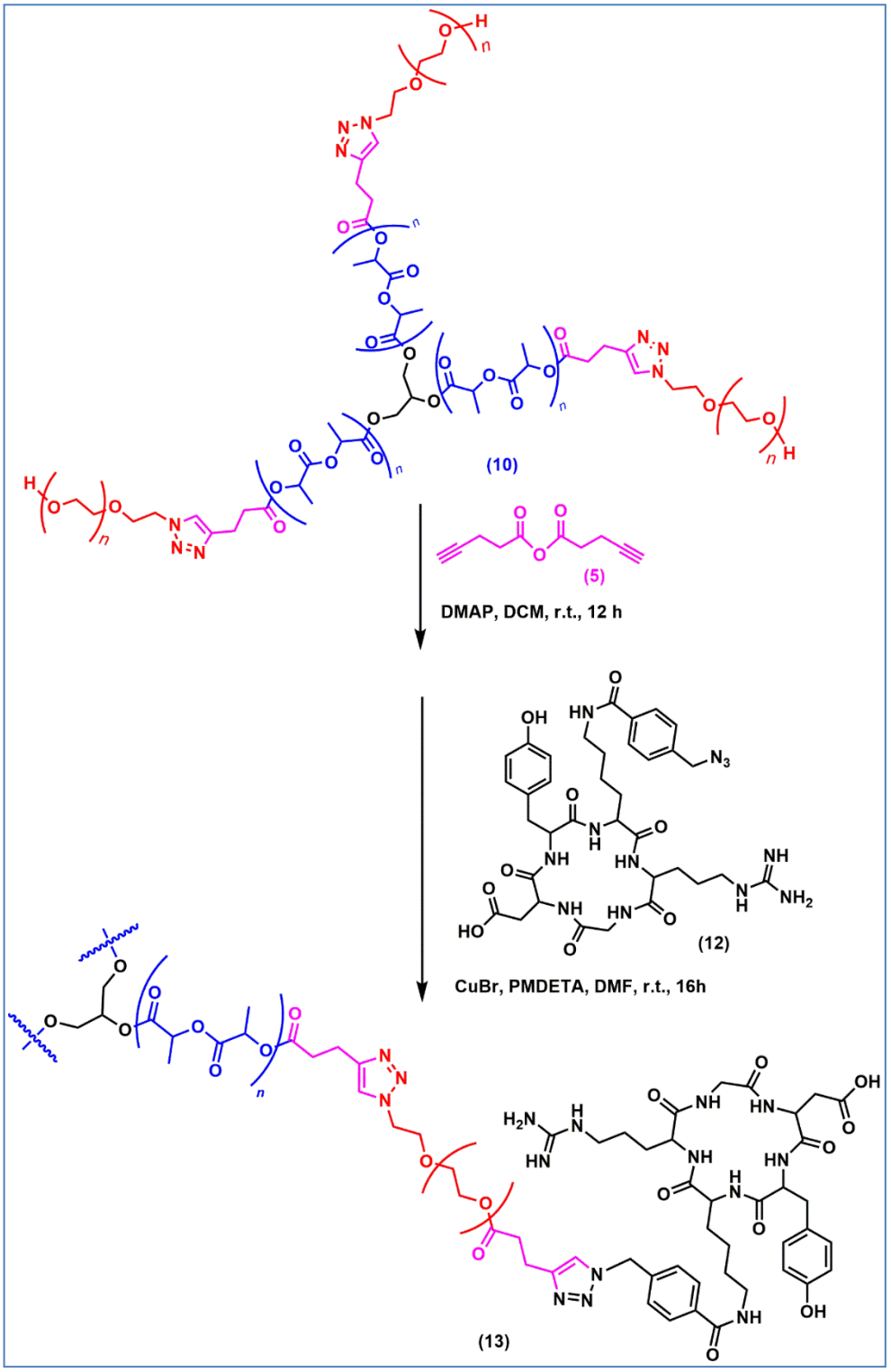

Scheme 6. Esterification of star PLA-PEG (10) with pentynoic anhydride and subsequent *click* coupling of the alkynyl-end groups with azide-RGD peptide (12) affording PLA-PEG-RGD (13).

The final CuAAC reaction of alkynyl-terminated star PLA-PEG (**11**) with azide-RGD peptide (**12**) was performed in anhydrous dimethylformamide, due to the poor solubility of the azide-RGD in tetrahydrofuran. The reaction was carried out in the presence of CuBr and PMDETA, using a 2:1 ratio of azide: alkyne. After 16 h, the solvent was removed under vacuum, and the product PLA-PEG- RGD (**13**) was washed with deionized water and dried under vacuum at 40°C.

^{1}H NMR spectrum of PLA-PEG-RGD (**13**) was registered in N,N-dimethylformamide-d_7 showing characteristic aromatic signals (δ 7.96, 7.43, 7.02, 6.72 ppm) ascribable to aromatic portions of RGD moiety together with several broad peaks likely ascribable to NH-protons (from δ 8.74 to δ 7.61 ppm) (Experimental).

Preliminary SEC analysis of PLA-PEG-RGD in THF (**Figure 15A**), carried out by connecting in parallel a differential refractometer detector and a UV–visible spectrophotometer set at the λ_{max} of RGD (280 nm), indicated the successful grafting of RGD on the polymer backbone.

The presence of two signals (also observed in preliminary DLS measurements, **Figure 15B**) might suggest the formation of reverse micelles during the SEC analysis in THF. We could suppose that the presence of some water in THF (even the small percent present in each organic solvent) promoted the formation of reverse micelles.

This behavior was confirmed by preliminary DLS measurements (**Figure 15B**), showing a bimodal size distribution in the same solvent, with the presence of two species having a D_h of about 10 and 100 nm; the small one might be related to the unimolecular micelles, whereas the large one should come from the self-assembled multi-micelle aggregates.

Moreover, since the UV response is proportional to the concentration in RGD peptide (Beer-Lambert Law), the UV response appeared well more important for the bigger micelles composed by more PLA-PEG-RGD, as compared to the unimolecular micelles.

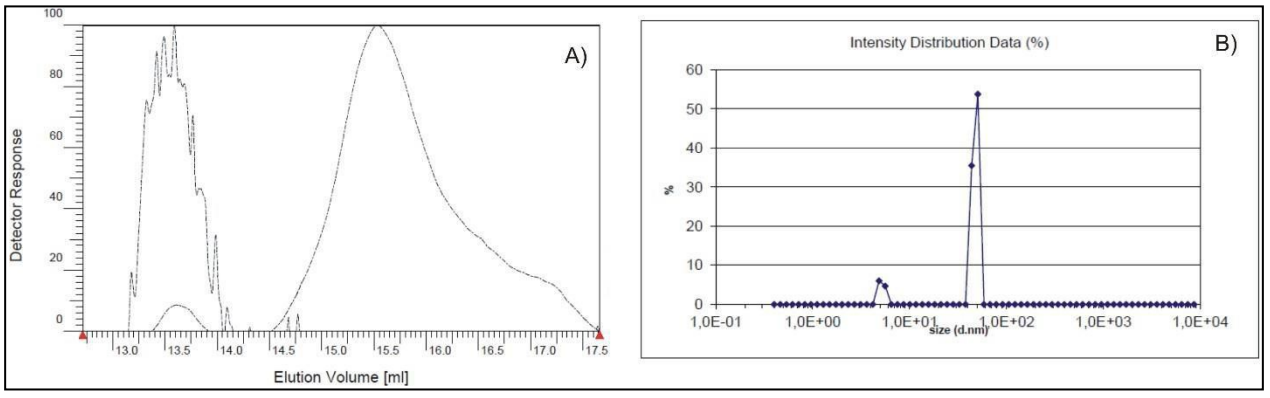

Figure 15. Preliminary SEC analysis (A) and DLS measurements (B) of PLA-PEG-RGD in THF.

These preliminary results suggested that our PLA-PEG-RGD star polymer with a well-designed hydrophobic/hydrophilic ratio, is able to self-assemble into micelles. A deeper investigation of the self-assembly behavior is currently under investigation.

Moreover, the anticancer drug Doxorubicin (Dox) will be incorporated in the inner micelle core (**Figure 16**) and the biological properties of the drug-loaded delivery system will be eventually investigated.

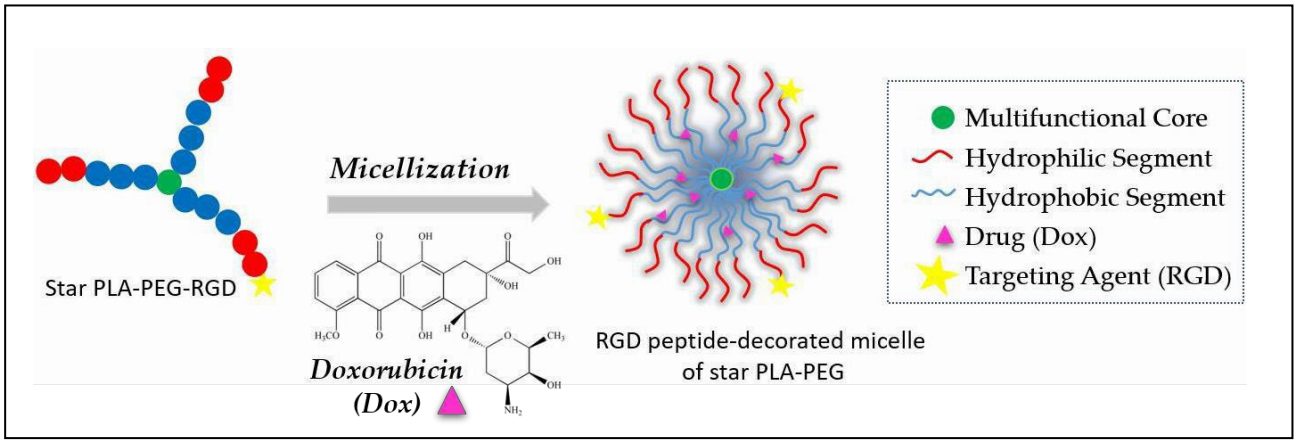

Figure 16. Micellar nanoformulation of the star PLA-PEG-RGD incorporating the anticancer drug Doxorubicin

3.4 Experimental

3.4.1 Materials and methods

L-Lactide, 1,8-diazabicyclo[5.4.0]undec-7-ene (DBU), glycerol, benzoic acid, 4-pentynoic acid, sodium bicarbonate ($NaHCO_3$), sodium bisulfate ($NaHSO_4$), sodium sulfate anhydrous (Na_2SO_4), 1,3-dicyclohexyl-carbo-diimide (DCC), silver oxide (Ag_2O), tosyl chloride (TsCl), potassium iodide (KI), polyethyleneglycol (PEG, MW=2000), sodium azide (NaN_3), copper bromide (CuBr), *N*,*N*,*N*′,*N*″,*N*″-pentamethyldiethylenetriamine (PMDETA), 4-dimethylaminopyridine (DMAP), dichloromethane (DCM), anhydrous dimethylformamide (DMF), anhydrous toluene, anhydrous tetrahydrofuran (THF) and other solvents and reagents were purchased from Sigma-Aldrich. Azide- RGD peptide was purchased from Scintomics.

NMR spectra were recorded at room temperature using a Varian 300 and a Varian 500 MHz spectrometers. Chemical shifts (d) were expressed in ppm using tetramethylsilane (TMS) as an internal reference.

Size exclusion chromatography (SEC) was performed in THF at 30°C using a Polymer Laboratories liquid chromatograph equipped with a PL-DG802 degasser, an isocratic HPLC pump LC 1120 (flow rate = 1ml/min), a triple detector: refractive index (ERMA 7517), capillary viscometry and light scattering RALS (Viscotek T-60) (Polymer Laboratories GPC-RI/CV / RALS), an automatic injector (Polymer Laboratories GPC-RI/UV) and four columns: a PL gel 10 μm guard column and three PL gel Mixed-B 10μm columns. PS standards were used for calibration.

3.4.2 Synthesis of star PLA (3)

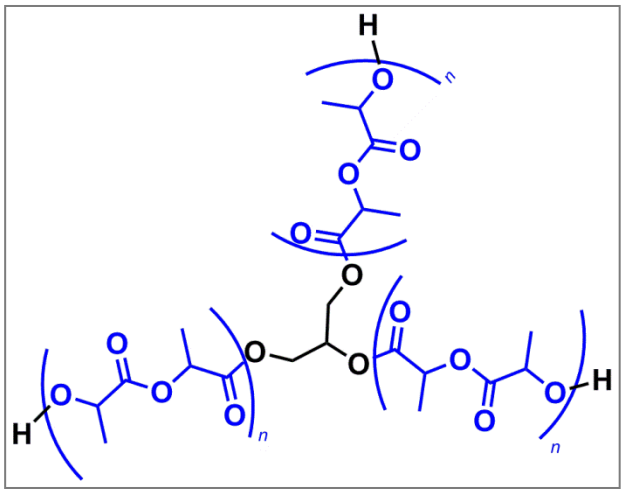

An initial [lactide (L-LA)]$_0$/[initiator]$_0$/[DBU]$_0$ ratio of 97/1/2 ([L-LA]$_0$=1 M) has been selected to obtain a star PLA **(3)** with a molecular weight of 14.000 g/mol. In a glove box under nitrogen pressure, glycerol **(1)** (6.6 mg, $3.98 \cdot 10^{-5}$ mol, 1 equiv) and DBU (21.77 mg, $7.96 \cdot 10^{-5}$ mol, 2 equiv) were solubilized in 2 mL of anhydrous DCM into a glass vial. L-Lactide **(2)** (1 g, $6.9 \cdot 10^{-3}$ mol, 97 polymerization degree) was solubilized in 5 mL of anhydrous DCM into another glass vial and then added to the first solution. The reaction was left to stir 12 minutes, and then benzoic acid (20.96 mg, $9.55 \cdot 10^{-5}$ mol, 2,4 equiv) dissolved in 0.2 mL of anhydrous DCM was added to stop the polymerization. The vial was taken out of glove box, the solution was transferred into a round bottom flask to reduce the volume under vacuum. The solution was precipitated into cold technical methanol, centrifuged and dried for 5 h into a vacuum oven at 60°C to give 980 mg (98% yield) of star PLA **(3)** as a white powder.

^{1}H NMR (500 MHz, $CDCl_3$, δ): 1.57 (m, 3H, $[CH_3]_n$), 4.22 (m, 5H, $-CH_2CHCH_2$), 4.36 (m, 1H, CH-OH), 5.15 (m, 1H, $[CH]_n$). Polymerization Degree$^{1H\ NMR}$ = 97, $M_n^{1H\ NMR}$ = 14.000 g/mol, SEC: $M_n^{SEC,app}$ = 21.019 g/mol, $Đ_M$ = 1.12.

3.4.3 Synthesis of pentynoic anhydride ***(5)***

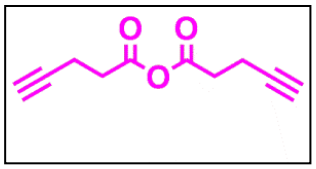

Pentynoic acid **(4)** (2 g, $20.4 \cdot 10^{-3}$ mol, 2 equiv) and DCC (2.1 g, $10.2 \cdot 10^{-3}$ mol, 1 equiv) were solubilized in 20 mL of DCM into a round bottom flask. The solution was left to stir for 12 h, then was filtered on filter paper and the solid was washed two times with 20 mL of DCM. The organic phase was evaporated under vacuum to obtain an oil, that was precipitated into 10 mL of n-hexane to form two liquid phases; the bottom part was recovered with a syringe and then dried under vacuum to obtain 940 mg (94% yield) of pentynoic anhydride **(5)** as a brown oil. ^{1}H NMR (500 MHz, $CDCl_3$, δ): 2.67 (t, J = 7.2 Hz, 2H, $\underline{CH_2}CH_2C{\equiv}CH$), 2.47 (dt, J = 7.2 Hz, J = 2.6 Hz, 2H, $CH_2\underline{CH_2}C{\equiv}CH$), 1.97 (t, 1H, J = 2.6 Hz, C≡CH); ^{13}C NMR (500 MHz, $CDCl_3$, δ): 167.2 (C=O), 81.5 (C≡), 69.7 (≡CH), 34.2 (CH_2), 13.7 (CH_2).

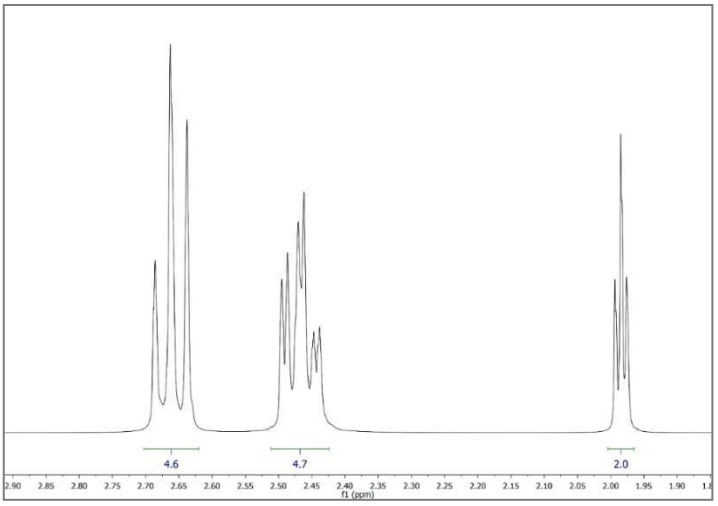

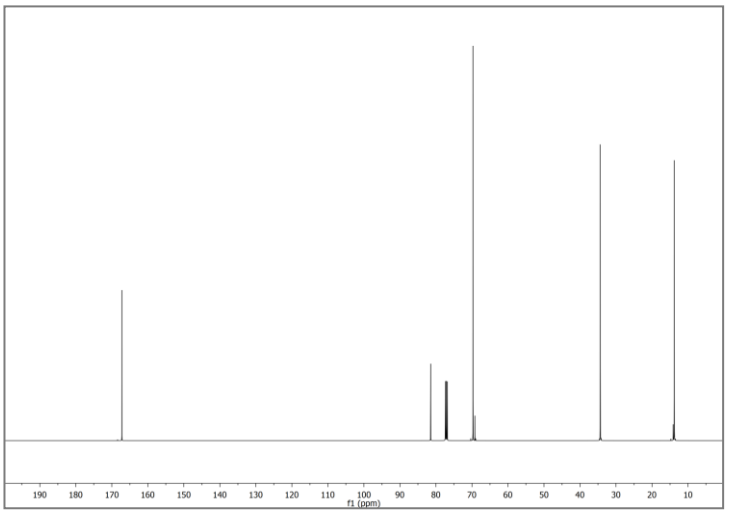

3.4.4 Synthesis of alkynyl-terminated star PLA ***(6)***

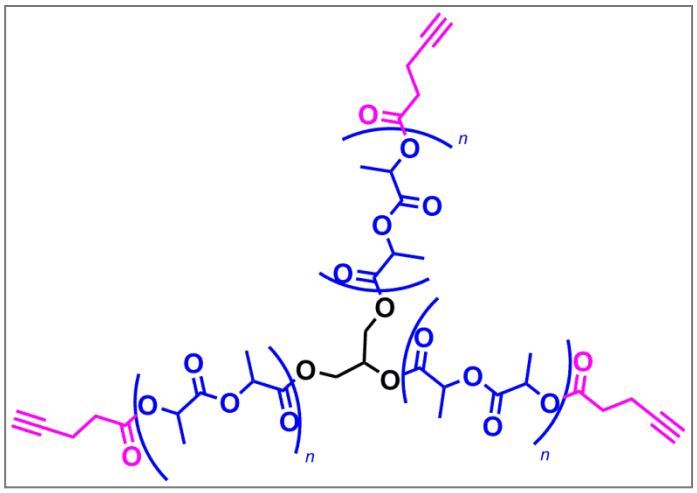

Star PLA **(3)** (980 mg, $7 \cdot 10^{-5}$ mol, 1 equiv), DMAP (34 mg, $2.77 \cdot 10^{-4}$ mol, 4 equiv) and pentynoic anhydride **(5)** (50 mg, $2.77 \cdot 10^{-4}$ mol, 4 equiv) were solubilized in 30 mL of DCM into a round bottom flask and left stirring for 12 h at room temperature. The solution was washed three times with a saturated solution of $NaHCO_3$ and three times with a saturated solution of $NaHSO_4$. Organic phases were collected, dried over Na_2SO_4, filtered and concentrated under vacuum. The solution was precipitated into cold technical methanol, centrifuged and dried for 5 h into a vacuum oven at 60°C to obtain 900 mg (92% yield) of alkynyl-terminated star PLA **(6)** as a white powder.

^{1}H NMR (500 MHz, $CDCl_3$, δ): 1.57 (m, 3H, -[CH_3]$_n$-), 2.65 (m, 2H, $\underline{CH_2}CH_2C{\equiv}CH$), 2.52 (m, 2H, $CH_2\underline{CH_2}C{\equiv}CH$), 1.98 (t, 1H, J = 2.5 Hz, C≡CH), 4.22 (m, 5H, -CH_2CHCH_2-), 5.15 (m, 1H, -[CH]$_n$-). Polymerization Degree$^{1H\ NMR}$ = 97, $M^{1H\ NMR}$ = 14.294 g/mol, $SEC\text{-}M^{SEC,app}$ = 21.207 g/mol, $Đ_M$ = 1.13.

3.4.5 Synthesis of mono-tosyl PEG ***(8)***

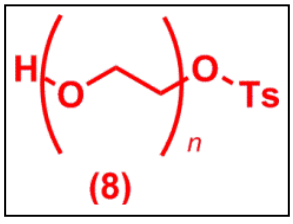

In a glove box under nitrogen pressure PEG diol **(7)** (500 mg, $2.5 \cdot 10^{-4}$ mol, 1 equiv) was dissolved in 6.75 mL of dry toluene in a glass vial and vigorously stirred till complete dissolution. Then Ag_2O (87 mg, $3.75 \cdot 10^{-4}$ mol, 1.5 equiv) and KI (8.3 mg, $5 \cdot 10^{-5}$ mol, 0.2 equiv) were added, and after 15 minutes

of vigorous stirring TsCl (50 mg, $2.63 \cdot 10^{-4}$ mol, 1.05 equiv) was added. The reaction was stirred for 16 h in the glove box. The solution was taken out of the glove box, filtered on paper filter and dried under vacuum to obtain 287 mg of a colorless oil. ^{1}H NMR and MALDI-ToF analyses demonstrated that it is a mixture of mono-tosyl PEG **(8)** and unreacted PEG diol **(7)** (ratio 1:1), that was directly used in the next synthetic step, without further purification.

^{1}H NMR (500 MHz, $CDCl_3$, δ): 2.44 (s, 3H, CH_3), 3.64 (m, 4H, -$[CH_2CH_2O]_n$-), 4.15 (t, 2H, J=5 Hz, CH_2OTs), 7.33 (d, 2H, J= 8.5 Hz, Ar H), 7.79 (d, 2H, J= 8.5 Hz, Ar H).

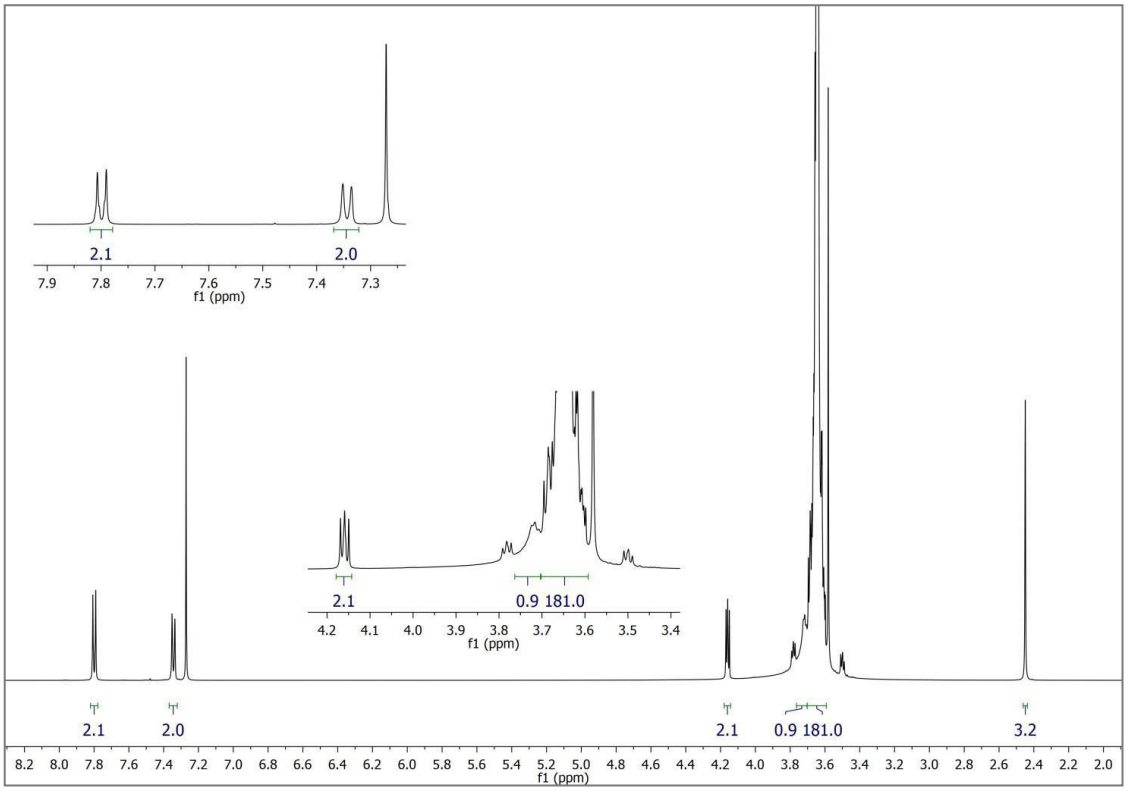

3.4.5 Synthesis of mono-azide PEG ***(9)***

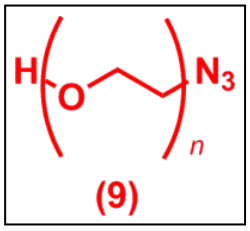

In a glove box under nitrogen pressure mono-tosyl PEG **(8)** (287 mg, $1.33 \cdot 10^{-4}$ mol, 1 equiv) and NaN_3 (22 mg, $3.33 \cdot 10^{-4}$ mol, 5 equiv) were dissolved into 5 mL of anhydrous DMF into a round bottom flask. Then the flask was taken out from the glove box and stirred for 12 h into an oil bath at 90°C. Afterwards, DMF was evaporated under vacuum and the crude product was dissolved in DCM

and washed two times with brine and two times with deionized water. Organic phases were collected, dried over Na_2SO_4 and evaporated under vacuum to obtain 120 mg of a white solid. ^1H NMR and MALDI-ToF analyses demonstrated that it is a mixture of mono-azide PEG **(9)** and unreacted PEG diol **(7)** (ratio 1:1).

^1H NMR (500 MHz, $CDCl_3$, δ): 3.39 (t, 2H, J= 5 Hz, $-CH_2N_3$), 3.64 (m, 4H, $-[CH_2CH_2O]_n$).

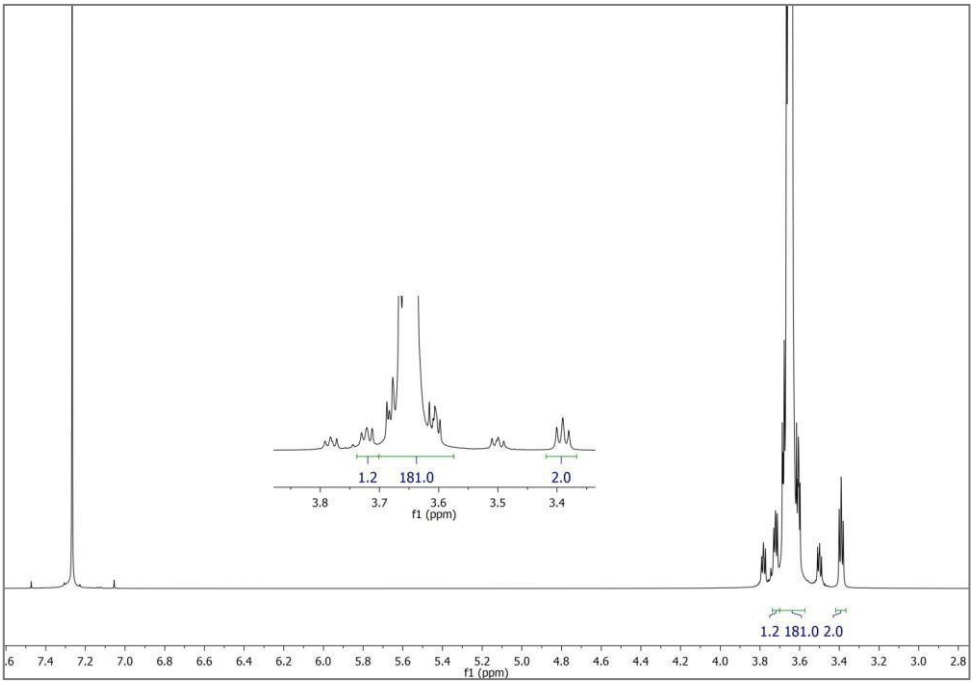

3.4.6 Synthesis of star PLA-PEG (10)

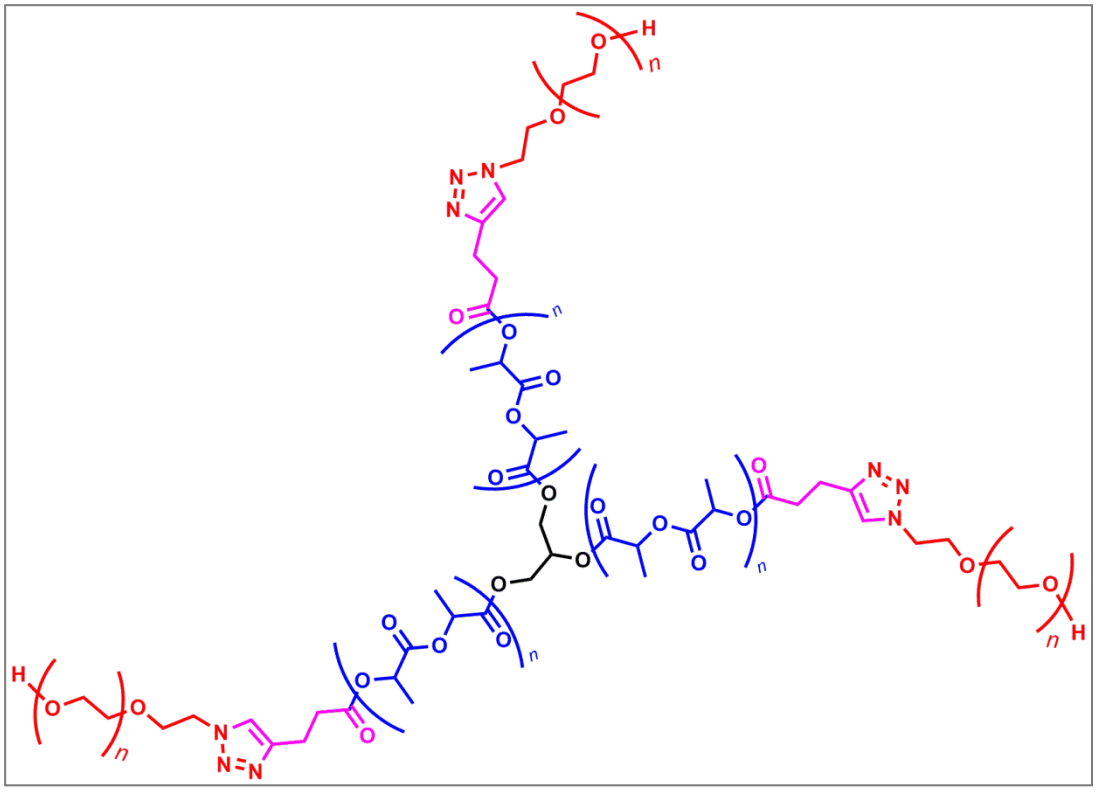

Alkynyl-terminated star PLA **(6)** (650 mg, $4.56 \cdot 10^{-5}$ mol, 1 equiv) and compound **(9)** (555 mg, $1.37 \cdot 10^{-4}$ mol, 3 equiv of which 1.5 equiv consisted of mono-azide PEG and 1.5 equiv of unreacted PEG-diol) were dissolved in 2 mL of anhydrous THF into a glass vial. Then CuBr (0.65 mg, $4.56 \cdot 10^{-6}$ mol, 0.1 equiv) and PMDETA (0.79 mg, $4.56 \cdot 10^{-6}$ mol, 0.1 equiv) were added to the reaction mixture. The solution was stirred at room temperature for 16 h. The vial was taken out of glove box and the solvent was evaporated under vacuum. The residue was washed three times with 5 mL of deionized water to remove the unreacted PEG-diol and centrifuged at 2800 rpm for 50 minutes at 10°C. The solid was dried at 40°C in a vacuum oven for 4h leading to 891 mg (yield 96%) of star PLA-PEG **(10)**.

^{1}H NMR (500 MHz, $CDCl_3$, δ): 1.57 (d, 3H, -[CH_3]$_n$-), 2.82 (t, 2H, J= 5 Hz, $\underline{CH_2}CH_2C_{triazole}$), 3.06 (t, 2H, J= 7.5 Hz, $CH_2N_{triazole}$), 3.64 (m, 4H, -[CH_2CH_2O]$_n$-), 4.22 (m, 5H, -CH_2CHCH_2-), 4.49 (t, 2H, J= 5 Hz, $CH_2\underline{CH_2}C_{triazole}$), 5.15 (m, 1H, -[CH]$_n$-), 7.53 (s, 1H, $CH_{triazole}$). $M^{SEC,app}$ = 32.212 g/mol, $Đ_M$ = 1.14.

3.4.7 Synthesis of alkynyl-terminated star PLA-PEG ***(11)***

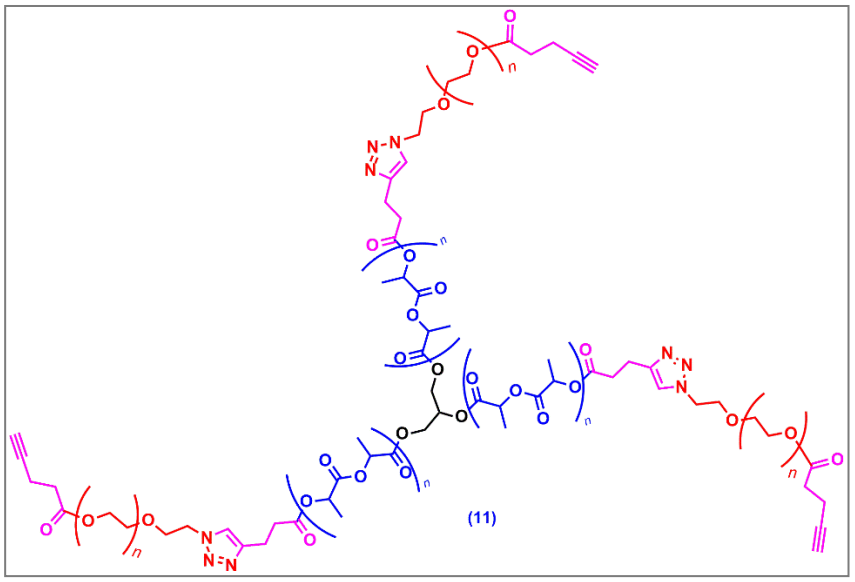

Star PLA-PEG **(10)** (891 mg, $4.38 \cdot 10^{-5}$ mol, 1 equiv), DMAP (21 mg, $1.73 \cdot 10^{-4}$ mol, 4 equiv) and pentynoic anhydride **(5)** (31 mg, $1.73 \cdot 10^{-4}$ mol, 4 equiv) were solubilized in 30 mL of DCM into a round bottom flask and the mixture was stirred for 12 h at room temperature. The solution was washed three times with deionized water. Organic phases were collected, dried over Na_2SO_4, filtered and dried under vacuum to obtain 788 mg (88% yield) of alkynyl-terminated star PLA-PEG **(11)** as a white powder. ^{1}H NMR (500 MHz, $CDCl_3$, δ): 1.57 (d, 3H, -[CH_3]$_n$-), 1.98 (t, 1H, J= 2.7 Hz, C≡CH), 2.52 (dt, 2H, J= 2.7, J= 6.5 Hz, $CH_2\underline{CH_2}C{\equiv}CH$), 2.67 (t, 2H, J= 6.5 Hz, $\underline{CH_2}CH_2C{\equiv}CH$), 2.82 (t, 2H, J= 5 Hz, $\underline{CH_2}CH_2C_{triazole}$), 3.06 (t, 2H, J= 7.5 Hz, $CH_2N_{triazole}$), 3.64 (m, 4H, -[CH_2CH_2O]$_n$-), 4.22 (m, 5H, -CH_2CHCH_2-), 4.27 (t, 2H, J= 5 Hz, $OCH_2\underline{CH_2}OCO$), 4.49 (t, 2H, J= 5 Hz, $CH_2\underline{CH_2}C_{triazole}$), 5.15 (m, 1H, -[CH]$_n$), 7.53 (s, 1H, $CH_{triazole}$). $M_n^{SEC,app}$ = 34.203 g/mol, $Đ_M$ = 1.16.

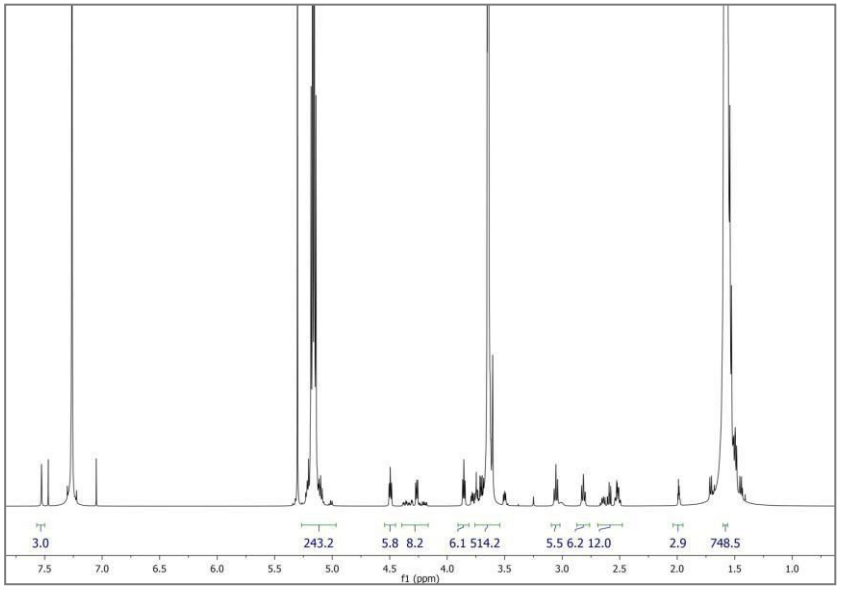

3.4.8 Synthesis of star PLA-PEG-RGD (13)

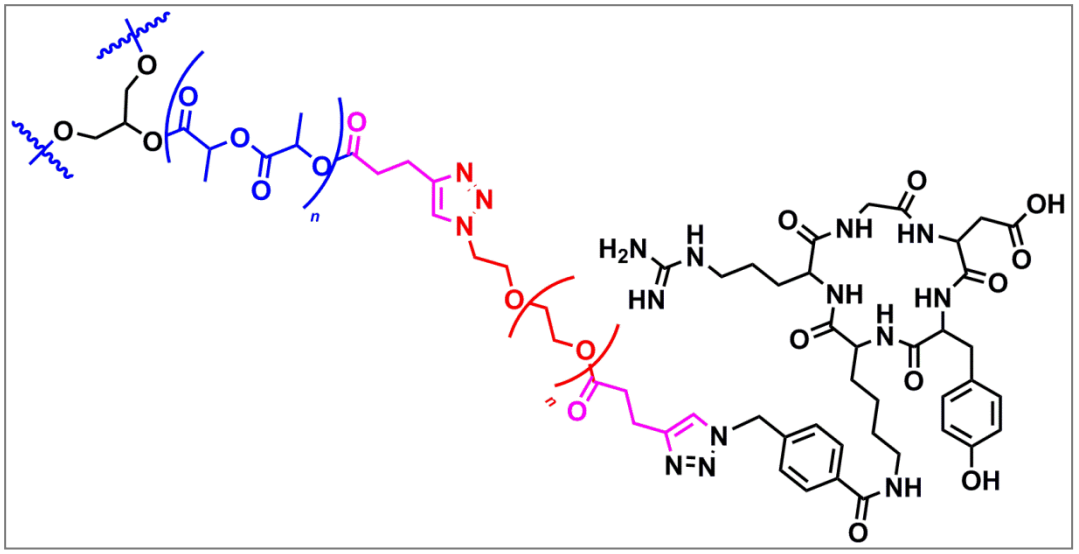

In a glove box, under nitrogen pressure, alkynyl-terminated star PLA-PEG **(11)** (137 mg, $6.18 \cdot 10^{-6}$ mol, 1 equiv) and azide-RGD peptide **(12)** (10 mg, $1.23 \cdot 10^{-5}$ mol, 2 equiv) were dissolved into 2 mL of anhydrous DMF into a glass vial. Then CuBr (0.1 mg, $6.18 \cdot 10^{-7}$ mol, 0.1 equiv) and PMDETA (0.1 mg, $6.18 \cdot 10^{-7}$ mol, 0.1 equiv) were added to the reaction mixture. The solution was left under stirring at room temperature for 16 h. The solvent was evaporated under vacuum and then the solid residue was washed two times with deionized water and centrifuged at 2800 rpm for 50 minutes at 10°C. Water residues were removed in a vacuum oven at 40°C for 2 h to obtain 80 mg (54% yield) of star PLA-PEG-RGD **(13)**, as a brown solid.

^{1}H NMR (500 MHz, d_7-DMF, δ): selected peaks 1.53 (d, 3H, -[CH_3]$_n$-), 1.98 (t, 1H, J= 2.7 Hz C≡CH), 2.52 (m, 2H, $CH_2\underline{CH_2}C{\equiv}CH$), 2.65 (m, 2H, $\underline{CH_2}CH_2C{\equiv}CH$), 2.82 (t, 2H, J= 5 Hz, $\underline{CH_2}CH_2C_{triazole}$), 2.99 (m, 2H, $CH_2N_{triazole}$), 3.58 (m, 4H, -[CH_2CH_2O]$_n$-), 4.19 (m, 2H, CH_2), 4.22 (t, 2H, J= 5 Hz, $OCH_2\underline{CH_2}OCO$), 4.38 (m, 5H, -CH_2CHCH_2-), 4.56 (t, 2H, J= 5 Hz, $CH_2\underline{CH_2}C_{triazole}$), 5.28 (m, 1H, -[CH]$_n$), 6.65 (br s, 1H, NH), 6.72 (d, 2H, Ar H, J=8 Hz), 7.02 (d, 2H, Ar H, J=8 Hz), 7.39 (s, 1H, $CH_{triazole}$), 7.43 (d, 2H, Ar H, J=8 Hz), 7.60 (br s, 1H, NH), 7.78 (br s, 1H, NH), 7.97 (d, 2H, ArH, J=8 Hz), 8.39 (br s, 1H, NH), 8.55 (br s, 1H, NH), 8.74 (br s, 1H, NH).

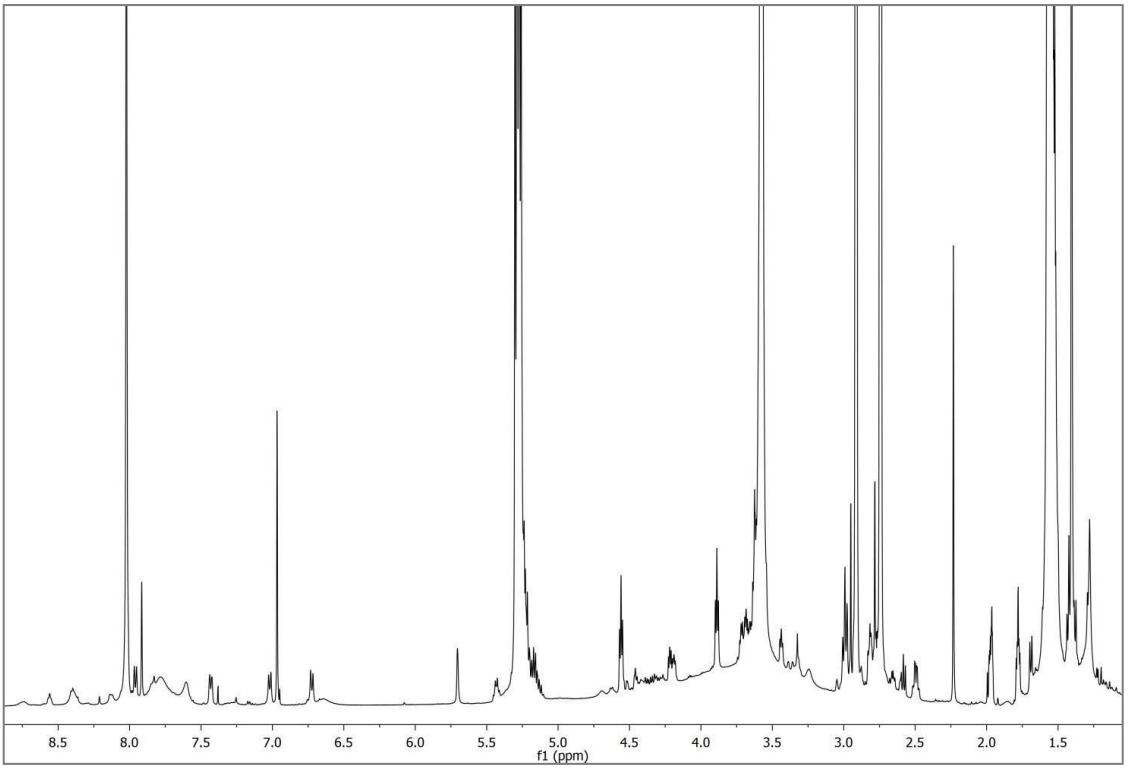
8.5
8.0
7.5
7.0
6.5
6.0
5.5
5.0
4.5
4.0
3.5
3.0
2.5
2.0
1.5
f1 (ppm)

3.5 References

1. Shrivastava, A. Polymerization, in: *Plastics Design Library*, Andrew, W., Ed., Oxford, United Kingdom, 2018, 2, 17-48.
2. Ren, J. M., McKenzie, T. G., Fu, Q., Wong, E. H., Xu, J., An, Z., Shanmugam, S., Davis, T. P., Boyer, C., Qiao, G. G., Star Polymers, *Chem. Rev.* 116, 6743–6836 (2016).
3. Long L. X., Zhao J., Li K., He L. G., Qian X. M., Liu C. Y., Wang, L.-M., Yang, X.-Q., Sun, J., Ren, Y., Khang, C.-S., Yan, X.-B., Synthesis of star-branched PLA-b-PMPC copolymer micelles as long blood circulation vectors to enhance tumor-targeted delivery of hydrophobic drugs in vivo. *Mater. Chem. Phys.* 180, 184–194 (2016).
4. Wu, T., Cai, Y., Zhao, X., Ngai, C. X., Chu, B., Hsiao, B., Hadjiargyrou, M., Grubbs, R. B., Synthesis and characterization of poly(ethylene oxide)/polylactide/polylysine tri-arm star copolymers for gene delivery. *J. Polym. Sci. Part A Polym. Chem.* 56, 635–644 (2018).
5. Liu, X., Jin, X., Ma, P. X. Nanofibrous hollow microspheres self-assembled from star-shaped polymers as injectable cell carriers for knee repair. *Nat. Mater.* 10, 398–406 (2011).
6. Kim, B.-S., Gao, H., Argun, A. A., Matyjaszewski, K., Hammond, P. T. All-Star Polymer Multilayers as pH-Responsive Nanofilms. *Macromolecules* 42, 368–375 (2009).
7. Coulembier, O., Degée, P., Cammas-Marion, S., Guérin, P., Dubois, P. New Amphiphilic Poly[(R,S)-β-malic acid-b-ε-caprolactone] Diblock Copolymers by Combining Anionic and Coordination−Insertion Ring-Opening Polymerization. *Macromolecules* 35, 9896–9903 (2002).
8. Khanna, K., Varshney, S., Kakkar, A. Designing Miktoarm Polymers Using a Combination of "Click" Reactions in Sequence with Ring-Opening Polymerization. *Macromolecules* 43, 5688–5698 (2010).
9. Khanna, K., Varshney, S., Kakkar, A. Miktoarm star polymers: advances in synthesis, self-assembly, and applications. *Polym. Chem.* 1, 1171–1185 (2010).
10. Hadjichristidis, N., Pitsikalis, M., Iatrou, H. *Polymers with star-related structures, in Macromolecular Engineering*. *Precise Synthesis, Materials Properties, Applications, Wiley Inc., New York* (2007).
11. Calucci, L., Forte, C., Buwalda, S. J., Dijkstra, P. J., Feijen, J. Self-Aggregation of Gel Forming PEG-PLA Star Block Copolymers in Water. *Langmuir* 26, 12890–12896 (2010).
12. Jie, P., Venkatraman, S. S., Min, F., Freddy, B. Y. C., Huat, G. L. Micelle-like nanoparticles of star-branched PEO–PLA copolymers as chemotherapeutic carrier. *J. Control. Release* 110,

20–33 (2005).

13. Salaam, L. E., Dean, D., Bray, T. L. In vitro degradation behavior of biodegradable 4-star micelles. *Polymer (Guildf).* 47, 310–318 (2006).
14. Hiemstra, C., Zhong, Z., Dijkstra, P. J., Feijen, J. Stereocomplex Mediated Gelation of PEG-(PLA)2 and PEG-(PLA)8 Block Copolymers. *Macromol. Symp.* 224, 119–132 (2005).
15. Sheng, Y.-J., Nung, C.-H., Tsao, H.-K. Morphologies of Star-Block Copolymers in Dilute Solutions. *J. Phys. Chem. B* 110, 21643–21650 (2006).
16. Chou, S.-H., Tsao, H.-K., Sheng, Y.-J. Morphologies of multicompartment micelles formed by triblock copolymers. *J. Chem. Phys.* 125, 194903 (2006).
17. Chou, S.-H., Tsao, H.-K., Sheng, Y.-J. Atypical micellization of star-block copolymer solutions. *J. Chem. Phys.* 129, 224902 (2008).
18. Lin, C.-M., Chen, Y.-Z., Sheng, Y.-J., Tsao, H.-K. Effects of macromolecular architecture on the micellization behavior of complex block copolymers. *React. Funct. Polym.* 69, 539–545 (2009).
19. Hong, H., Mai, Y., Zhou, Y., Yan, D., Cui, J. Self-Assembly of Large Multimolecular Micelles from Hyperbranched Star Copolymers. *Macromol. Rapid Commun.* 28, 591–596 (2007).
20. Fan, X., Li, Z., Loh, X. J. Recent development of unimolecular micelles as functional materials and applications. *Polym. Chem.* 7, 5898–5919 (2016).
21. Jin, X., Sun, P., Tong, G., Zhu, X. Star polymer-based unimolecular micelles and their application in bio-imaging and diagnosis. *Biomaterials* 178, 738–750 (2018).
22. Ordanini, S., Cellesi, F. Complex Polymeric Architectures Self-Assembling in Unimolecular Micelles: Preparation, Characterization and Drug Nanoencapsulation. *Pharmaceutics* 10, (2018).
23. Cameron, D. J. A., Shaver, M. P. Aliphatic polyester polymer stars: synthesis, properties and applications in biomedicine and nanotechnology. *Chem. Soc. Rev.* 40, 1761–1776 (2011).
24. Zhu, K. J., Bihai, S., Shilin, Y. "Super microcapsules" (SMC). I. Preparation and characterization of star polymethylene oxide (PEO)-polylactide (PLA) copolymers. *J. Polym. Sci. Part A Polym. Chem.* 27, 2151–2159 (1989).
25. Wu, W., Wang, W., Li, J. Star polymers: Advances in biomedical applications. *Prog. Polym. Sci.* 46, 55–85 (2015).
26. Yang, D.-P., Oo, M. N. N. L.,Deen, G. R., Li, Z., Loh, X. J. Nano-Star-Shaped Polymers for Drug Delivery Applications. *Macromolecular Rapid Communications* 38, (2017).
27. Lin, W., Ma, G., Ji, G., Zhang, J., Wang, J., Sun, H., Chen, S. Biocompatible long-circulating star carboxybetaine polymers. *J. Mater. Chem. B* 3, 440–448 (2015).

28. Li, X., Qian, Y., Liu, T., Hu, X., Zhang, G., You, Y., Liu, S. Amphiphilic multiarm star block copolymer-based multifunctional unimolecular micelles for cancer targeted drug delivery and MR imaging. *Biomaterials* 32, 6595–6605 (2011).
29. Danhier, F., Le Breton, A., Préat, V. RGD-Based Strategies To Target Alpha(v) Beta(3) Integrin in Cancer Therapy and Diagnosis. *Mol. Pharm.* 9, 2961–2973 (2012).
30. Hersel, U., Dahmen, C., Kessler, H. RGD modified polymers: biomaterials for stimulated cell adhesion and beyond. *Biomaterials* 24, 4385–4415 (2003).
31. Ergun, C., Liu, H., Webster, T. J., Olcay, E., Yilmaz, S., Sahin, F. C. Increased osteoblast adhesion on nanoparticulate calcium phosphates with higher Ca/P ratios. *J. Biomed. Mater. Res. Part A* 85A, 236–241 (2008).
32. Coulembier, O., Moins, S., Raquez, J.-M., Meyer, F., Mespouille, L., Duquesne, E., Dubois, P. Thermal degradation of poly(l-lactide): Accelerating effect of residual DBU-based organic catalysts. *Polym. Degrad. Stab.* 96, 739–744 (2011).
33. Mahou, R.,Wandrey, C. Versatile Route to Synthesize Heterobifunctional Poly(ethylene glycol) of Variable Functionality for Subsequent Pegylation. *Polymers* 4, (2012).
34. Boopathi, S. K., Hadjichristidis, N., Gnanou, Y., Feng, X. Direct access to poly(glycidyl azide) and its copolymers through anionic (co-)polymerization of glycidyl azide. *Nat. Commun.* 10, 293 (2019).

CONCLUSIONS

In this PhD thesis, reproducible and efficient procedures for the multimodal functionalization of polylactide (PLA) have been reported and discussed. The main scope of the work was the development of reliable and mild synthetic procedures for access to a variety of functionalized PLA derivatives suitable for nanoparticles preparation.

Specifically, a new method for the grafting of propargylamide units has been proposed and the subsequent CuAAC coupling of the *"clickable"* alkyne-terminated PLA with selected azido-derivatives (methoxypolyethylene glycol azide, azide-fluor 545, azide-folate) has been investigated. The newly synthesized PLA derivatives (PLA-PEG, PLA-Flu and PLA-FA) have been formulated in nanoparticles loaded with Salinomycin, by nanoprecipitation technique.

Furthermore, in collaboration with the University of Mons (UMONS, Belgium), the synthesis of a novel three-arm star PLA-PEG copolymer was developed, in a *core-first* approach, and the amphiphilic star copolymer was eventually decorated with RGD peptide as an integrin-targeting ligand specifically recognized by integrin receptors over-expressed in tumor cells. The final product PLA-PEG-RGD was intended to the targeted cancer therapy, after micellization and incorporation of a suitable anticancer drug (i.e., Doxorubicin).

The drug-loaded PLA-based nanoparticles are going to be tested in antitumoral assays at ISTEC (Institute of Science and Technology for Ceramics) belonging to the CNR Department of Chemical Science and Materials Technology (Faenza (RA), Italy).

The present PhD thesis confirm the great potential of the azide-alkyne copper(I)-catalyzed Huisgen 1,3-dipolar cycloaddition, one of the most widely exploited *click* chemistry protocols, for the multimodal functionalization of PLA-based materials.

The major drawback could concern the use of catalyst copper (I), that tends to stick to the formed triazole, making challenging the purification of the products. Moreover, during nanoparticles preparation, traces of copper (I) could remain attached on the surface or encapsulated as impurities, even after extensive purification (i.e., centrifugation or dialysis). The copper-induced toxicity may have an impact in the biological applications of the newly synthesized materials, whereby the exploitation of *"copper-free click chemistry"* could open new perspectives for biopolymer functionalization. Specifically, the use of strained or electron-deficient alkynes (e.g. the cyclooctyne moiety and its derivatives) makes straightforward the purification step, avoiding possible traces of copper salts not eliminated. Such benign copper-free conditions are recently emerged as an environmentally friendly alternative for the orthogonal functionalization of

polymeric nanostructures. In perspective, copper-free *click* reactions could be exploited to attach stimuli-responsive moieties on PLA backbone or to synthesize hyperbranched or dendrimeric PLA structures.

Publications:

Scala, A. Piperno, A., Torcasio, S. M., Nicosia, A., Mineo, P. G., Grassi, G. *"Clickable" polylactic acids obtained by solvent free intra-chain amidation*. Eur. Polym. J. 109, 341-346 (2018).

Piperno, A. Mazzaglia, A. Scala, A. Pennisi, R. Zagami, R. Neri, G. Torcasio, S. M. Rosmini, C. Mineo, P. Potara, M. Focsan, M. Astilean, S. Zhou, G. Sciortino, M. T. *Casting Light on Intracellular Tracking of a New Functional Graphene-based microRNA Delivery System by FLIM and Raman Imaging* ACS Applied Materials & Interfaces, Submitted

Communications at congresses:

1. S. M. Torcasio, A. Piperno, P.G. Mineo, O. Coulembier and A. Scala
Engineering of polylactic acids for biomedical applications
Convegno Congiunto delle Sezioni Sicilia e Calabria della SCI, Palermo, 1-2 Marzo 2019, Oral Communication OC11.

2. S. M. Torcasio, A. Piperno, P.G. Mineo, O. Coulembier and A. Scala
Functionalized PLA-Based Nanoparticles for Biological Applications
XLIV "A. Corbella" International Summer School on Organic Synthesis ISOS 2019, Gargnano, 9-13 Giugno 2019, Oral Communication OC22.

3. S. M. Torcasio, A. Piperno, P.G. Mineo, O. Coulembier and A. Scala
Multifunctional Polylactides for Biological Applications
II Convention DOCTOCHEM UNIME, Messina, 1 Luglio 2019, Oral Communication L16.

4. S. M. Torcasio, O. Coulembier, P.G. Mineo, A. Piperno and A. Scala
Multifunctional nanostratured PLA-based materials for biological investigations
XV Convegno Nazionale AIMAT & XII Convegno INSTM sulla Scienza e Tecnologia dei Materiali, Ischia Porto, 21-24 Luglio 2019, Oral Communication O_1_27.

5. A. Scala, A. Piperno, S. M. Torcasio, P.G. Mineo, O. Coulembier
Engineered Polylactide-based Nanoparticles as Multifunctional Drug Delivery Systems
XXXIX Convegno Nazionale della Divisione di Chimica Organica, CDCO Torino 2019, 8-12 settembre 2019, OC-57.

6. A. Cordaro, S. M. Torcasio, A. Scala, A. Piperno, G. Grassi, R. Zagami, A. Mazzaglia, P. G. Mineo, R. Pennisi, M. Musarra Pizzo, M. T. Sciortino.
MicroRNA Nanocarrier Based on Graphene Engineered with Cationic Cyclodextrins.
Congresso congiunto delle sezioni Sicilia e Calabria 2018, Catania, 9-10 febbraio 2018, Poster, PO27.

7. S. M. Torcasio, A. Piperno, N. Micale, P.G. Mineo, G. Grassi, and A. Scala
Preparation of PLA-based nanoparticles loaded with Salynomicin and Folic Acid
Workshop Società Chimica Italiana delle sezioni Sicilia e Calabria 2016-17, Messina 9-10 Febbraio 2017, Poster P-34.

Member of the *Organizing Committee* of the II Convention DOCTOCHEM UNIME, Messina, 1 Luglio 2019.

ACKNOWLEDGEMENTS

'A time for each action, and a direction for everything'

I would like to thank all the people that in those years of PhD helped me not only in carrying out my research activity, but also helped me personally to be in focus, at peace and relaxed to correctly expend my energies in work.

Many thanks to my supervisor, professor Angela Scala, who always pushed me to do my best, even at distance. Beside the guide on technical work, suggestions and tips for me was important to learn your motivation and strength in carrying on the research activity, also in these years where the University of Messina was in renovation and so the work conditions weren't optimal. I admired your enthusiasm and endurance and I will try to remember those qualities also when will be harder for me to do that.

Many thanks to professor Nicola Micale, that after those years I consider like a friend. Thanks to support me at distance with your life experiences, to be there to hear me and share your point of view and advices on life happenings, travels, blessing and sorrows of life and in general large part of personal sphere that I couldn't face up in the same way without sharing with you. Thank to convey to me your patience and resilience, and more, to help me understand when apply the patience and when the strength and to focus on important things of life. Thanks to put me in focus again, your example it was important for me and I will take always in my heart and mind.

Thanks to all the research group that allowed me to carry on my research activity: professor Anna Piperno and professor Massimo Cordaro thanks for your support and suggestions on my technical work in the lab, for the interesting conversations on science and for your help.

The renovation in University of Messina was a good opportunity to share knowledge and leisure moments with other PhD students. Many thanks to Annalaura and Andrea, inseparable lab companions, I will miss you so much when I will be again on the desk, our sharing on chemistry and all our crazy way to find solution, the mutual support in facing new experiences abroad, pieces of life and friendship. Specifically thanks Annalaura to hear me, this was really important for me even if I was was far.

Many thanks to Donatella, Anna, Rosy to have shared the room with me and to have made the thesis writing funnier and lighter.

I was lucky to have the possibility to travel abroad during my PhD thesis, so thanks to professor Olivier Coulembier that in first instance worked because my presence in SMPC lab were

possible and made me feel welcomed. I really appreciate that you always encouraged me to do new things, to experiment and to give a try to my ideas, to don't be scary to do wrong because if needed you were there with tips and suggestions. I really hope to be for people that ask help for me like you were for me: helping to walk on their own legs with me being there if needed.

I would like to thank also professor Jean Marie Raquez for welcoming me in the lab, to share with me ideas on my work and for the humor that he shared with us Italians in the lab, making lighter some tiresome journeys.

Thanks to professor Philippe Dubois to allow me to work in the lab and to be really attentive to my work. I really appreciate your kindness, charism and strength, you motivated me even by far.

A super big thanks to 'the gang' of the lab, my friends Sebastien, Alexandre, Noemi, Gabriela, Xavier, Jean-Emile, Romain, Dalila, Johnathan, Rosica, Mounch, Jeremy, Samira. Without you the abroad experience couldn't been the same. Many thanks to my girls to always be patient with me and share life in the lab and outside: Rana, Chiara, Meriam, Valentina and Paloma, you really be with me in all the life moment of this experience.

Many thanks to friends that remained in Italy and support me by far, Andrea, Silvana, Ivana, Claudia, Davide, Gabriella, Mimma e Sergio. You will always be welcomed, in any part of the world I will be! I wait for you to come and visit!

Thanks Bertrand (Bertino) to be with me in this year. Your love helped me to grow, and I have no words to express how this is important for me, for the person that I am and for the person that I want to be.

Finally many thanks to my family that teached me to endure, that 'no one will be saved alone' and that relationships are the most important thing in life, that you can love someone even if you have different life visions and that despite all, at the end of the day, this is what truly remains.

Thanks to everyone, by the bottom of my hearth.

Finally, but essentially to say for who I am, I am really thankful to Jesus, to give me a life that I never could image, and that is more and more that I can image and to have take the lead when I was too broken to drive, teach me how to rest, how to have faith in Him, and how to go on, through errors, through high and downs, also and especially when I understood nothing and I had just to follow the wind on my veils; to the future that you will give me, to the eternity and the fact that despite me being me, with my flaws and smallness, you love me and I thank you because feel it. Thanks to always send me people that are expression of your love, and thanks to open my eyes and make me see You in them. I pray that also they will see You in me.

Psalm 127

If the Lord is not helping the builders, then the building of a house is to no purpose: if the Lord does not keep the town, the watchman keeps his watch for nothing.
It is of no use for you to get up early, and to go late to your rest, with the bread of sorrow for your food; for the Lord gives to his loved ones in sleep.